

**Model Predictive Control of Non-Isothermal Dispersive Chemical
Tubular Reactors with Recycle Flow**

by

Syedhamidreza Khatibi

A thesis submitted in partial fulfillment of the requirements for the degree of

Master of Science

in

Process Control

Department of Chemical and Materials Engineering

University of Alberta

Abstract

Tubular reactors have widespread applications in petrochemical, biochemical and pharmaceutical unit operations. The design of a control law, which accounts for stabilization of the concentration and the temperature of the chemical component during the reaction in an isothermal/non-isothermal tubular reactor with axial dispersion, is still challenging issue in process engineering. The mathematical models for this kind of chemical unit operation is represented by distributed parameter systems (DPS) models. The major issue of DPS models is that they take the form of partial differential equations (PDEs) or a mixed set of PDEs and ordinary differential equations (ODEs). The complexity of DPS models lies in spatial approximation in order to obtain finite-dimensional models amenable for corresponding controllers/observers.

Moreover, in process engineering, recycle-loop are typically used around the reactor to reduce the hot-spot temperature while maintaining the component conversion at the desired level. Unfortunately, a recycle-loop may bring the system instability, thereby introducing a controller, which also accounts for instability and physical limitations of the process is essential.

This work provides a model predictive control as well as observer design for dispersive chemical tubular reactors with recycle flow. The discrete version of the DPS is constructed by energy preserving Cayley-Tustin transformation. Along the same vein, the DPS is kept without any model reduction or spatial approximation.

First, we explore a model predictive control and a discrete observer design for a coupled axial dispersion reactor and continuous stirred tank reactor (CSTR) given by

a cascade ODE-PDE system (a case study for polymerization process) in which the regulator design accounts for stability and physical limitations of the process implemented by input/state constraints.

Next, the proposed design is extended to a non-isothermal tubular reactor with recycle flow described by a class of convection-diffusion-reaction PDEs with a non-linear reaction term (a case study for chemical and bio-processing). Based on the different mass and heat Peclet values the system can exhibit multiple equilibria that can be stable or unstable. The objective is to design a model predictive controller and discrete observer for the linearized system around the unstable steady state profile. The controller can provide state stabilization, constraints satisfaction and input disturbance rejection. Finally, the performance of the both controllers are assessed via numerical simulations.

Preface

Chapter 2 of this work has been published as S. Khatibi, G. O. Cassol, S. Dubljevic, “Linear Model Predictive Control for a Coupled CSTR and Axial Dispersion Tubular Reactor with Recycle”, *Mathematics* (2020), and portions of this chapter have been published as S. Khatibi, G. O. Cassol, S. Dubljevic, “Linear Model Predictive Control for a Cascade ODE-PDE System”, *Proceedings of the American Control Conference* (2020). Chapter 3 of this thesis has been submitted for publication as S. Khatibi, G. O. Cassol, S. Dubljevic, “Model Predictive Control of Non-Isothermal Axial Dispersion Tubular Reactors with Recycle”, *Computers & Chemical Engineering*.

For all the above contributions, I was responsible for numerical simulations and manuscript composition. G. O. Cassol was involved in methodology and manuscript editing and Dr. S. Dubljevic was the supervisory author and was involved with concept formation and manuscript review.

To my beloved parents ...

Acknowledgements

I wish to express my gratitude to my research supervisor at the University of Alberta, Dr. Stevan Dubljevic, for conceiving my project and challenging me to pursue my MSc degree with the best quality. His support in finding the right direction throughout my academic trajectory is always appreciated. My Special thanks also go to the committee members, who kindly evaluated this thesis and provided insightful suggestions and comments.

I would also like to thank my colleagues at distributed parameter systems lab for their helpful advices over two years of my study at the University of Alberta.

I would also like to acknowledge the financial support for this research program provided by Natural Sciences and Engineering Research Council (NSREC) of Canada.

Most important of all, I would like to express my deep appreciation to my parents for their continuous and unparalleled love and unconditional support. I would not have been able to start and finish my work without their encouragement, prayer and love. They selflessly encouraged me to explore new directions in life and seek my own destiny. Their faith in my capabilities has always been the source of strength. I am also grateful to my older brother, Seyedalireza, who always helped me not to feel homesick being far away from home.

Contents

List of Tables	x
List of Figures	xi
1 Introduction	1
1.1 Motivation	1
1.2 Control of distributed parameter systems	2
1.3 Semigroup theory	4
1.4 Scope and outline	5
References	6
2 Model Predictive Control for a Coupled CSTR and Axial Disper-	
 sion Tubular Reactor with Recycle	9
2.1 Introduction	9
2.2 Case study: Polymerization process	12
2.2.1 System Representation	12
2.2.2 Open-Loop Stability	14
2.3 Discrete Representation	15
2.3.1 Discrete Operators	15
2.3.2 Discrete Adjoint Operators	18
2.4 Luenberger Observer Design	20
2.5 Model Predictive Control for Linear Coupled ODE-PDE System . . .	21
2.5.1 Optimization Problem	21
2.5.2 Terminal State Penalty Operator	23
2.5.3 Stability Constraint	24

2.6	Simulation Results	25
2.6.1	Observer Design and Open-Loop Response	26
2.6.2	MPC Implementation	28
2.7	Summary	29
	References	31
3	Model Predictive Control of Non-Isothermal Axial Dispersion Tubular Reactors with Recycle	34
3.1	Introduction	34
3.2	Case study: Biochemical reactors	37
3.2.1	Model formulation	37
3.2.2	Steady state solutions	39
3.3	Linearized model	40
3.3.1	System linearization	40
3.3.2	Infinite-dimensional system representation	42
3.4	Linear system stability analysis ($Pe_T \neq Pe_m$)	43
3.4.1	Eigenvalues and eigenfunctions of the operator A	43
3.4.2	Eigenfunctions of the operator A^*	44
3.5	Cayley-Tustin time discretization	46
3.5.1	Discrete time representation	46
3.5.2	Resolvents and discrete operators	47
3.5.3	Resolvents of the adjoints and corresponding discrete operators	48
3.6	Observer design for a coupled parabolic PDEs	49
3.6.1	Design for continuous-time observer	49
3.6.2	Design for discrete-time observer	50
3.7	Model predictive control for unstable coupled parabolic PDEs	51
3.7.1	Optimization problem	51
3.7.2	Input disturbance rejection	54
3.8	Simulation results	54
3.9	Summary	61
	References	63

4 Conclusion and Recommendations	67
4.1 Conclusion	67
4.2 Future work	68
Bibliography	69
A Discrete adjoint operators	75
A.1 A_d^*	75
A.2 B_d^*	77
B Sample code	78
C Adjoint operator and boundary conditions	93
D Resolvent operators	95
D.1 Resolvent of the tubular reactor with recycle	95
D.2 Resolvent of adjoint operators	96
E Terminal cost operator	98
F Stability of the discrete observer error	99

List of Tables

2.1	Parameter values used in numerical simulation	25
3.1	Parameters of the chemical tubular reactor system used to model Eq.(3.1)	38
3.2	Values of the parameters used in numerical simulations	55

List of Figures

1.1	An illustrative example of a coupled LPS-DPS configuration.	4
2.1	CSTR-tubular reactor system with recycle stream.	12
2.2	Eigenvalues distribution for unstable coupled ODE-PDE system when there is no diffusion within the tubular reactor	15
2.3	Effects of diffusivity within the dispersive reactor on the eigenvalues placement for unstable coupled ODE-PDE system	16
2.4	Shifting the unstable eigenvalue of the observer for different values of the observer gain.	21
2.5	Representation of the closed loop.	23
2.6	Evolution of the discrete error dynamics with the value $L_c = 5$ for observer gain.	26
2.7	(a) The estimated state profile evolution ($x_I(\zeta, k)$) through dispersive tubular reactor constructed on the basis of discrete-time coupled ODE-PDE system in an open-loop condition; (b) Dynamics reconstruction of the scalar variable within the CSTR in an open-loop condition. . .	27
2.8	a), b) and c) demonstrate the comparison between input profiles under model predictive control law: with and without input/state constraints, with constraints and with disturbance for $20 \leq t \leq 25$; d), e) and f) denote reconstructed dynamics of the scalar variable within the CSTR under model predictive law: with and without input/state constraints, with constraints and with disturbance for $20 \leq t \leq 25$. . .	28
2.9	Evolution of the stabilized spatial profile for the tubular reactor with all constraints.	29

3.1	Schematic view of a non-isothermal axial dispersion tubular reactor with recycle	37
3.2	Multiple equilibrium profiles of obtained for a non-isothermal tubular reactor with recycle.	40
3.3	Comparison of the eigenvalue distribution with different setting for Peclet numbers.	45
3.4	Scheme of the model predictive controller used for the non-isothermal axial dispersion tubular reactor with recycle	52
3.5	Transition of the unstable eigenvalue to stable one by increasing the values for L	56
3.6	Discrete error dynamics given by Eq.(3.47) for $L = 24$	56
3.7	The evolution of the estimated state profiles though the axial dispersion tubular in an open-loop condition.	57
3.8	Dynamics reconstruction of the stabilized spatial profiles for the axial dispersion tubular reactor constructed on the basis of a discrete time coupled parabolic PDEs system.	58
3.9	Comparison between the inputs with square wave disturbance, controlled inputs and concentration profiles under model predictive controller subjected to all constraints (solid-lines) or only stability constraint (dotted lines). . .	60
3.10	Comparison of the system output (solid lines) and observer output (dashed lines) with and without measurement noise in the non-isothermal tubular reactor under the model predictive control and using the Luenberger observer in Eq.(3.44).	61

1

Introduction

1.1 Motivation

A substantial proportion of unit operations in petrochemical and biochemical processes take place in distributed parameter systems (DPS). The mathematical models of the mentioned controlled systems depend on both temporal and spatial variables. On the contrary, the systems in which the variables do not rely on spatial parameters (e.g., well-mixed reactors) are known as lumped parameter systems (LPS).

Due to widespread applications of DPS and economic benefits of controlling these systems precisely, developing controllers with consideration of the accurate model is of great importance. The objective of this thesis is focused on designing the advanced controllers for class of distributed parameter systems and coupled LPS-DPS unit operations with special emphasis on axial dispersion tubular reactors. The methodology of designing controller in this work is based on the model predictive controller (MPC) for DPS setting (see Alessio and Bemporad 2009 for a survey). The optimization-based algorithm yields a sequence of optimal control actions and the first move is applied on the system (Muske and Rawlings, 1993). The MPC for DPS must preserve the nature of infinite dimensional setting while providing naturally constraints satisfaction emerging form physical limitations.

Another interesting research direction in this thesis, particularly for chemical processes, is the application of recycle flow in biochemical and polymerization process presented by DPS and coupled LPS-DPS models, respectively. When chemical reactor is considered with recycle of energy/mass, the model analysis and subsequent controller design become more challenging and require careful consideration since recycle is known to induce instability in apparently stable reactor operations. Hence, in the proposed regulator design, stability constraint has been taken into account. To address the issue of having access to all the state variables, the output discrete observer is also provided for the both systems: class of parabolic PDEs and a coupled cascade ODE-PDE system. In the pursuing sections, the available contributions of distributed parameter systems with the outline of the thesis will be summarized.

1.2 Control of distributed parameter systems

As mentioned earlier, the most conventional approach for designing controller for DPS is by using lumping techniques to approximate the PDE models. In other words, it consists of some idealization of the process originating from spatial uniformity. Methods such as finite difference can be utilized for spatial discretization; however, such the mentioned simplifications cannot accurately capture the dynamical properties and/or may leads to high dimensionality of the controller generated by sets of ODEs. Moreover, the observability/controllability of the systems will rely on the location and number of discretization points (Christofides, 2001). Another approach for regulator design of DPS is based on developing the control theory for DPS then employing discretization on the resulting controller (late lumping). The outstanding privilege of this method is that the proposed controller accounts for the nature of the original model of the system. Over the years, research direction particularly for DPS is oriented to introduce novel algorithms dealing with infinite dimensional nature of the systems.

Some researchers explored control of systems described by PDEs by robust control, dynamic optimization and output feedback regulator design (Armaou and Christofides, 2002). A more precise way, originated from the study of the dynamic properties in

the frequency domain, is analyzing the nature of the infinite-dimensional part of the system and then designing the controllers for PDE (Ray, 1981). There are also other approaches relied on analytic formulation using semigroup theory and PDE backstepping control methodologies (Curtain and Zwart, 1995; Krstic, 2008).

The theory of optimal control for DPS began in late 1960s. Notable research has been carried out to solve the well-known Riccati equation, which is developed to apply optimal control for particular class of PDEs (see Aksikas et al. 2009; Aksikas et al. 2007). Along the same vein, MPC controllers are introduced as an algorithm in which the control action is found by solving finite horizon open-loop objective function at each sampling time (Muske and Rawlings, 1993). Several contributions have been concentrated on developing MPC strategies of DPS (Dubljevic et al., 2006), boundary actuation (Dubljevic and Christofides, 2006a) and predictive output feedback control of PDEs (Dubljevic and Christofides, 2006b). As the implementation of MPC applications in digital computer controllers, the discrete version of the overall system is generally obtained by conversion of the models or controllers into a discrete time setting using methods such as explicit or implicit Euler, Runge-Kutta and etc.. The main disadvantages of these methods is that the accuracy of the discretization can be deteriorated by increasing the sampling period. It has been demonstrated that the Cayley-Tustin method conserves the characteristics and intrinsic energy of the linear distributed parameter system (V.Havu and Malinen, 2007) rather than the traditional numerical time discretization.

On the other hand, the mathematical models in most complex processes are in the mixed form of distributed and lumped parameter systems (LPS) (Oh and Pantelides, 1996) as can be seen in chemical reactions, pharmaceutical plants, coupled electromagnetic and coupled mechanical systems (see Fig.1.1). Several researchers have studied coupled LPS-DPS systems (Hasan et al. 2016; Tang and Xie 2011 to cite a few). There are two types of possible interaction between PDEs and ODEs: First is by in-domain coupling where the parameters of the DPS are coupled to the LPS. This can be seen in catalytic reactions, for instance, where the deactivation in the catalyst is described by the number of ODEs (Mohammadi et al., 2015). The second type of interaction is called cascaded ODE-PDE where the boundary conditions for the DPS are coupled to the LPS (e.g., Susto and Krstic 2010). Motivated by all above, we

will develop MPC controllers for two different setting of chemical engineering plants represented by class of parabolic PDEs and a coupled ODE-PDE system.

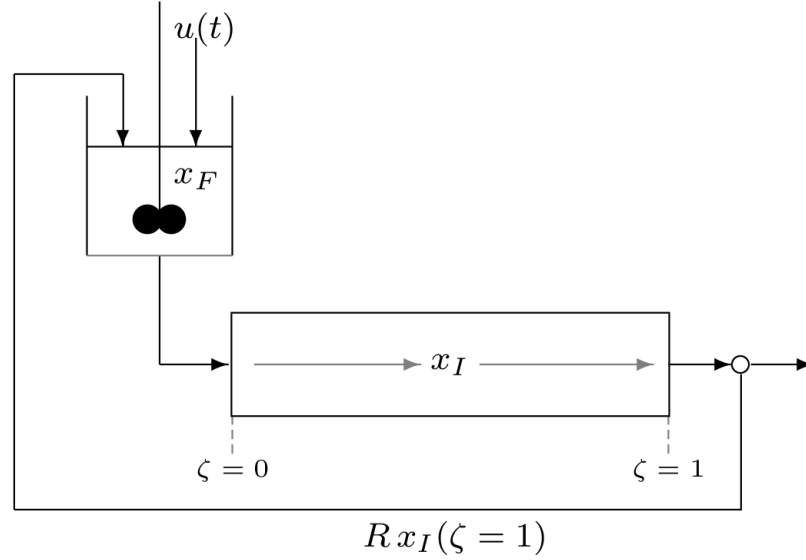


Figure 1.1: An illustrative example of a coupled LPS-DPS configuration.

1.3 Semigroup theory

Let us start with the linear representation of the finite dimensional system (A, B, C, D) defined on finite dimensional spaces X , U and Y :

$$\dot{x} = Ax(t) + Bu(t), \quad y(t) = Cx(t) + Du(t) \quad (1.1)$$

where $A \in \mathcal{L}(X)$, $B \in \mathcal{L}(U, X)$, $C \in \mathcal{L}(X, Y)$ and $D \in \mathcal{L}(U, Y)$ are well-defined bounded linear maps between finite dimensional spaces. Then, the following well known expression of the finite dimensional system can be written as:

$$x(t) = e^{At}x(0) + \int_0^t e^{A(t-\tau)}Bu(\tau)d\tau \quad (1.2)$$

Hence, with the input vector $u(t) \in L_2([0, \tau]; U)$, one can obtain $x(t) \in L_2([0, \tau]; X)$ and $y(t) \in L_2([0, \tau]; Y)$. Accordingly, the corresponding transfer function is given by:

$$G(s) = C(SI - A)^{-1}B + D \quad (1.3)$$

As can be seen, we always study matrix exponential functions as the solution of the control problem in finite-dimensional spaces. Thus, it is natural to ask whether by analogy with the finite dimensional case, can we reach a solution for infinite-dimensional spaces. The answer is given by the C_0 -semigroup operator described as the exponential function of an operator which is no longer bounded (Curtain and Zwart, 1995).

The concept of the semigroup theory is relied on the the system with zero input. The corresponding abstract standard version of the infinite dimensional setting can be represented by the following state space equation:

$$\dot{x}(\zeta, t) = Ax(\zeta, t) \quad (1.4)$$

$x(\zeta, t) \in H$ and H is a real Hilbert space. The following properties are hold for a strongly continuous semigroup infinitesimal generator T constructed by the operator A from \mathbb{R}^+ to H (Curtain and Zwart, 1995):

- $T(t+s) = T(t)T(s)$ for $t, s \geq 0$ (time invariance property)

- $T(0) = I$

- $\|T(t)x_0 - x_0\| \rightarrow 0$ as $t \rightarrow 0^+$ for $\forall x_0 \in H$

Therefore, the operator $A : D(A) \subset H \rightarrow H$ is a generator of a C_0 -semigroup on H such that

$$x(\zeta, t) = T(t)x_0 \quad (1.5)$$

1.4 Scope and outline

As mentioned earlier, we are interested to propose the model predictive controller for the more complicated systems.

Chapter 2 addresses a novel output model predictive controller design for a representative model of continuous stirred-tank reactor (CSTR) and axial dispersion reactor with recycle. The underlying model takes the form of ODE-PDE in series and it is operated at an unstable point. The model predictive controller (MPC) design is explored to achieve optimal closed-loop system stabilization and to account

for naturally present input and state constraints. The discrete representation of the system is obtained by application of the structure properties (stability, controllability and observability) preserving Cayley-Tustin discretization to the coupled system. The design of a discrete Luenberger observer is also considered to accomplish the output feedback MPC realization. Finally, the simulations demonstrate the performance of the controller, indicating proper stabilization and constraints satisfaction in the closed loop.

In Chapter 3 the MPC design is extended to a class of nonlinear parabolic PDEs (convection-diffusion-reaction PDEs). The emphasis placed on biochemical reactors as a case study for non-isothermal dispersive chemical tubular reactors with recycle. The model accounts for energy and mass transport in recycle stream. The dynamical system is considered with different Peclet numbers which prevent analytic solutions for eigenvalues and eigenfunctions of the system. The linearization of the system and corresponding multiple steady state will be addressed. Then, based on the unstable equilibria, the MPC will be designed to tackle with instability and physical limitations of the system. Furthermore, the new quadratic form of the optimization problem will be developed for class of convection-diffusion-reaction PDEs providing rejecting disturbances arising from reactor operations. Finally, the controller performance is assessed via simulation studies, implying proper state stabilization and constraints satisfaction with input disturbance rejection.

Chapter 4 is the conclusion of the work and summarizes the contributions of the thesis with possibilities for future research directions.

References

- Aksikas, I., Fuxman, A., Forbes, J. F., and Winkin, J. J. (2009). Lq control design of a class of hyperbolic pde systems: Application to fixed-bed reactor. *Automatica*, 45(6):1542 – 1548.
- Aksikas, I., Winkin, J. J., and Dochain, D. (2007). Optimal lq-feedback regulation of a nonisothermal plug flow reactor model by spectral factorization. *IEEE Transactions*

- on Automatic Control*, 52(7):1179–1193.
- Alessio, A. and Bemporad, A. (2009). *A Survey on Explicit Model Predictive Control*, volume 384. Springer Berlin Heidelberg.
- Armaou, A. and Christofides, P. (2002). Dynamic optimization of dissipative pde systems using nonlinear order reduction. *Chemical Engineering Science*, 57(24):5083–5114.
- Christofides, P. (2001). *Nonlinear and robust control of PDE systems. Methods and applications to transport-reaction processes*.
- Curtain, R. F. and Zwart, H. (1995). *An introduction to Infinite-Dimensional Linear Systems Theory*. New York: Springer-Verlag.
- Dubljevic, S. and Christofides, P. D. (2006a). Predictive control of parabolic pdes with boundary control actuation. *Chemical Engineering Science*, 61(18):6239 – 6248.
- Dubljevic, S. and Christofides, P. D. (2006b). Predictive output feedback control of parabolic partial differential equations (pdes). *Industrial & Engineering Chemistry Research*, 45(25):8421–8429.
- Dubljevic, S., El-Farra, N. H., Mhaskar, P., and Christofides, P. D. (2006). Predictive control of parabolic pdes with state and control constraints. *International Journal of Robust and Nonlinear Control*, 16(16):749–772.
- Hasan, A., Aamo, O. M., and Krstic, M. (2016). Boundary observer design for hyperbolic pde–ode cascade systems. *Automatica*, 68:75 – 86.
- Krstic, M. (2008). *Boundary Control of Pdes: A Course on Backstepping Designs*. Society for Industrial and Applied Mathematics, USA.
- Mohammadi, L., Aksikas, I., Dubljevic, S., and Forbes, J. F. (2015). Optimal boundary control of coupled parabolic PDE – ODE systems using infinite-dimensional representation. *Journal of Process Control*, 33:102–111.

- Muske, K. R. and Rawlings, J. B. (1993). Model predictive control with linear models. *AIChE Journal*, 39(2):262–287.
- Oh, M. and Pantelides, C. (1996). A Modelling and Simulation Language for Combined Lumped and Distributed Parameter Systems. *Computers and Chemical Engineering*.
- Ray, W. (1981). *Advanced process control*. New York McGraw-Hill.
- Susto, G. A. and Krstic, M. (2010). Control of pde–ode cascades with neumann interconnections. *Journal of the Franklin Institute*, 347(1):284 – 314.
- Tang, S. and Xie, C. (2011). State and output feedback boundary control for a coupled pde–ode system. *Systems & Control Letters*, 60(8):540 – 545.
- V.Havu and Malinen, J. (2007). The cayley transform as a time discretization scheme. *Numerical Functional Analysis and Optimization*, 28(7-8):825–851.

2

Model Predictive Control for a Coupled CSTR and Axial Dispersion Tubular Reactor with Recycle

2.1 Introduction

The modeling of many chemical engineering process plants relies on the description given by either transport-reaction mathematical models, which belong to the class of distributed parameter systems (DPS), or by lumped parameter system models, which represent idealization of the process units where some assumptions of spatial uniformity (mainly due to the mixing) can take place (Ray, 1981). The transport-reaction processes are modeled as distributed parameter systems and take the form of partial differential equations (PDEs) which are given by parabolic or hyperbolic PDEs.

To apply control methods on PDEs, one approach is the traditional method, which uses lumping techniques to convert the PDEs to a set of ordinary differential equations (ODEs) (Muske and Rawlings, 1993; Rawlings, 2000; Eaton and Rawlings, 1992; Richalet et al., 1978; Shang et al., 2004). Due to the high numbers of modes required in this approach, especially when it comes to the parabolic PDE models, this type of simplification leads to the high dimensionality of the ensuing controller. Furthermore,

neglecting the nature of the infinite dimensionality in the original setting might result in instability of the closed-loop system. There are several contributions focused on the synthesis of low-order controllers, which address the issue of having the spatially varying nature in transport-reactions systems. These contributions include the analysis of dynamic properties in the frequency domain, nonlinear, and robust controllers for different classes of dissipative PDEs and Lyapunov-based control methodologies (e.g., Ray 1981; Armaou and Christofides 2002; Krstic and Smyshlyaev 2008).

Along the line of modeling, most complex processes are in the mixed form of distributed and lumped parameter systems (LPS), and the latter are generally modeled by ODEs (Oh and Pantelides, 1996). The interconnected coupling of DPS and LPS is a challenging task, but in essence is the proper way to address a variety of process units in real world plants. There are two types of possible interactions between PDEs and ODEs. The first is an in-domain coupling, where the parameters of the DPS are coupled to the LPS (e.g., Mohammadi et al. 2015; Moghadam et al. 2013). The second type of interaction is called cascaded ODE-PDE, where the boundary conditions for the DPS are coupled to the LPS (Susto and Krstic, 2010). There are numerous research efforts focused on this type of interaction in the control literature, for instance, the observer design of coupled ODE-PDE cascade systems (Hasan et al., 2016), feedback boundary control for coupled ODE-PDE system (Tang and Xie, 2011) and backstepping boundary control for coupled ODE-PDE (Krstic and A.Smyshlyaev, 2008; Meglio et al., 2018).

Although the aforementioned contributions consider the stabilization of the ODE-PDE coupled system, they never address either input or state constraints, which are naturally present in the process plants. If constraints are present in the system, one can use a model predictive control (MPC) methodology to take into account these limitations in the process control realization. Basically, within the optimal control framework, the popularity of the so-called online receding horizon control comes from its capability to handle the constraints, particularly for the manipulated input and state variables (Mayne et al., 2000). Motivated by this, some researchers investigated the properties of MPC controllers, such as the stability of the closed-loop system, constraints validation and system performance (Chen and Allgöwer, 1998; García et al., 1989; Ito and Kunisch, 2002). In addition, some works considered a class of the Riesz

spectral systems with separable spectrums and successfully designed MPC algorithms with constraints (Dubljevic et al., 2006; Liu et al., 2014; Dubljevic and Christofides, 2006). There are also some other relevant studies regarding nonlinear MPC for DPS, such as data-based modeling or the techniques based on model reduction by using repeatedly online linearization (Bonis et al., 2012; Ai and San, 2013).

Computer applications in various engineering areas require a modern controller realization, which is implemented in the discrete setting. Hence, in order to turn the models/controllers into a discrete setting, mostly traditional numerical methods, such as explicit and implicit Euler (Kazantzis and Kravaris, 1999), are used for time discretization. However, from the linear system theory, this may impact the stability of the system when there is an increase in sampling period, mapping a stable continuous system into an unstable discrete one (Åström and Wittenmark, 1990). The mentioned issue becomes more serious when DPS are analyzed, as these are represented by infinite-dimensional state-spaces. It has been demonstrated that the Crank-Nicolson midpoint integration rule method (Cayley-Tustin) preserves the system characteristics and intrinsic energy (i.e., Hamiltonian preserving) of the linear distributed parameter system (V.Havu and Malinen, 2007). Motivated by this, in this contribution, the conversion of the continuous linear infinite-dimensional system representation to the linear discrete-time infinite-dimensional one, is done by the application of the Cayley-Tustin discretization (Hairer et al., 2006).

In this work, the extension of the standard finite-dimensional MPC for linear systems (Mayne, 2014; Rawlings et al., 2017) is considered. The optimal constrained finite-dimensional controller is applied to the lumped parameter system coupled to a distributed parameter system, and ensures the input and state constraints satisfaction within the framework of finite-dimensional quadratic optimization problem (Scockaert et al., 1999). The relevant process engineering model includes a continuous stirred-tank reactor (CSTR), and the output of this reactor is coupled to an axial dispersion mono-tubular reactor that has a recycle stream. The system of coupled equations includes a parabolic PDE with algebraic boundary conditions (representing the tubular reactor), while the ODE refers to the CSTR model dynamics. The discrete Luenberger observer is designed to account for the system output and its stability is based on the design in the continuous-time setting. The reconstructed system states are then

used in the MPC, providing optimal stabilization of the ODE-PDE cascade with the inclusion of state and input constraints.

The manuscript is organized as follows. In Section 2.2.1, the coupled ODE-PDE system is introduced in the appropriate abstract Hilbert space. Then, in addition to the stability analysis of the system in Section 2.2.2, the discretization scheme is accomplished by the Cayley-Tustin method in Section 2.3. It is followed by the observer design for the coupled ODE-PDE system in Section 2.4. Finally, in Section 2.5, considering an unstable operating condition, the feasible optimization problem is realized with input, state, and stability constraints, and it is followed by the simulation studies, which show the performance of the optimization-based controller design.

2.2 Case study: Polymerization process

2.2.1 System Representation

Consider the following coupled CSTR-tubular reactor configuration as the combination of a lumped and parabolic distributed parameter system. This setting is used for some chemical processes (see, e.g., Fogler 2005). It is also applied for polymerization process (see, Chen 1994). The process can be represented as follows (Fig. 2.1):

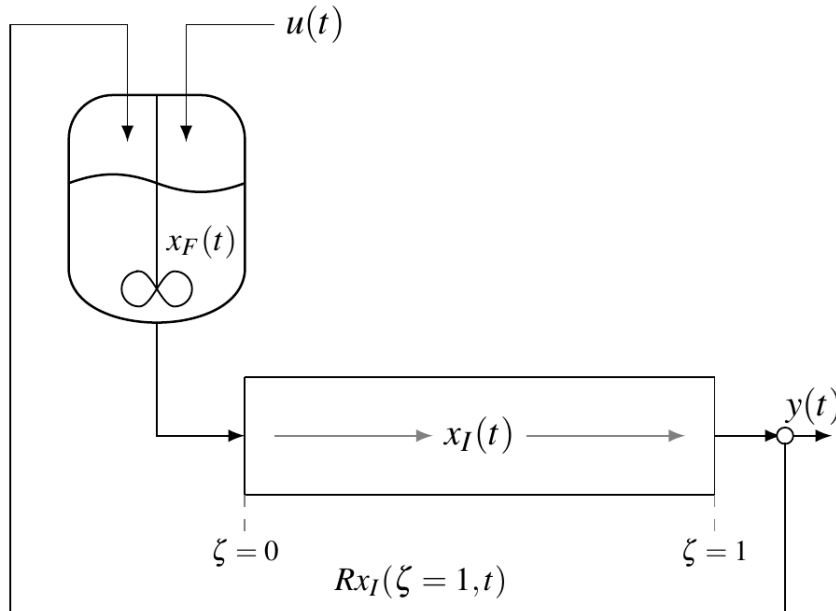


Figure 2.1: CSTR-tubular reactor system with recycle stream.

The mentioned process can be described by the following coupled ODE-PDE system of equations on domain $\{t \in \mathfrak{R}^+, \zeta \in [0, 1]\}$ with algebraic coupled boundaries and initial condition:

$$\begin{aligned}
\frac{dx_F(t)}{dt} &= a_1 x_F(t) + a_2 u(t) + R x_I(1, t) \\
\frac{\partial x_I(\zeta, t)}{\partial t} &= D \frac{\partial^2 x_I(\zeta, t)}{\partial \zeta^2} - v \frac{\partial x_I(\zeta, t)}{\partial \zeta} + \psi x_I(\zeta, t) + f(\zeta) d(t) \\
x_F(0) &= x_I(\zeta, 0) = 1 \\
x_I(0, t) &= x_F(t) \\
\left. \frac{\partial x_I(\zeta, t)}{\partial \zeta} \right|_{\zeta=1} &= 0 \\
y(t) &= x_I(1, t)
\end{aligned} \tag{2.1}$$

where the second order linear parabolic PDE corresponds to convection-diffusion reactor. The transport of a property $x_I(\zeta, t) \in L^2(0, 1) - L^2(0, 1)$ is a Hilbert space—through the tubular reactor, given with the inner product $\langle \cdot, \cdot \rangle$, $(L^2(\Omega; Z), \langle h, f \rangle = \int_{\Omega} \langle h(z), f(z) \rangle_Z dz)$, the ODE indicates the dynamics of the variable $x_F \in \mathfrak{R}$ within the CSTR. $\zeta \in [0, 1]$ is the position and $t \geq 0$ is the time variable. $\psi \in \mathfrak{R}$ and $a_1 \in \mathfrak{R}$ are the constant values responsible for the consumption or generation of $x_I(\zeta, t)$ and $x_F(t)$, respectively. $R \in \mathfrak{R}^+$ refers to the recycle factor in the system and is considered to be a bounded parameter ($0 \leq R \leq 1$). $v \in \mathfrak{R}^+$, $D \in \mathfrak{R}^+$ are the constant transport velocity and diffusion-constant, respectively. $a_2 \in \mathfrak{R}$ is a constant number, and $u(t) \in \mathfrak{R}$ represents the system input. $f(\zeta)$ and $d(t)$ represent a known disturbance which may present in the tubular reactor and can express changes in unit operations, such as temperature. $d(t)$ is considered to be a step function and $f(\zeta)$ is given as follows:

$$f(\zeta) = \begin{cases} 0 & 0 \leq \zeta < y_I \\ k_I & y_I \leq \zeta \leq 1 \end{cases} \tag{2.2}$$

where y_I and k_I are constant values. Here, the linear coupled finite-infinite-dimensional system can be rewritten by the following state-space equations:

$$\begin{aligned}
\dot{x}(t) &= Ax(t) + Bu(t) + Md(t) \\
y(t) &= Cx(\zeta, t)
\end{aligned} \tag{2.3}$$

x is state representing both finite and infinite part of the process $\left(x = \begin{bmatrix} x_F \\ x_I \end{bmatrix} \right)$. For the sake of simplicity in the paper, index F refers to finite part of the system (ODE), while index I indicates the infinite part (PDE). A is defined as a linear operator $\mathfrak{L}(X)$ (where X is a real space $\mathfrak{R} \oplus L^2(0, 1)$), such that $D(A) = \{x \in X : x_F \in \mathfrak{R}, x_I(\zeta) \in L^2(0, 1) \mid x_I(\zeta), \frac{dx}{d\zeta} \text{ are absolutely continuous, } x_I(0) = x_F \text{ and } \frac{dx(\zeta=0)}{d\zeta} = 0\}$. $B = \begin{bmatrix} a_2 \\ 0 \end{bmatrix}$ is the

linear input operator $\mathfrak{L}(\mathfrak{R}, X)$, $M = \begin{bmatrix} 0 \\ f(\zeta) \end{bmatrix}$ is the linear disturbance input operator and $C = \begin{bmatrix} 0 & \int_0^1 \delta(\zeta - 1)(\cdot) d\zeta \end{bmatrix}$ is the linear output operator.

2.2.2 Open-Loop Stability

The generality of the ensuing design can be established by performing the stability analysis of the target system given by Equation (2.1). The eigenvalue problem for the open-loop ($u(t) = 0$) unstable coupled ODE-PDE system is defined as below:

$$A\Phi = \lambda\Phi \quad (2.4)$$

where:

$$A = \begin{bmatrix} A_F = a_1 & R(\cdot)_I \Big|_{\zeta=1} \\ 0 & A_I = -v \frac{\partial(\cdot)_I}{\partial \zeta} + D \frac{\partial^2(\cdot)_I}{\partial \zeta^2} + \psi(\cdot)_I \end{bmatrix}, \Phi(\zeta) = \begin{bmatrix} \Phi_F \\ \Phi_I(\zeta) \end{bmatrix} \quad (2.5)$$

λ and Φ are the eigenvalues and eigenfunctions, respectively. The boundary conditions are given by

$$\Phi_I(\zeta = 0) = \Phi_F, \frac{d\Phi_I(\zeta)}{d\zeta} \Big|_{\zeta=1} = 0. \quad (2.6)$$

After some simple manipulation and using the boundary conditions defined by Equation (2.6) in Equation (2.4), one gets the following:

$$\frac{d^2\Phi_I}{d\zeta^2} - \frac{v}{D} \frac{d\Phi_I}{d\zeta} - \frac{(\lambda - \psi)}{D} \Phi_I = 0 \quad (2.7a)$$

$$\Phi_I(\zeta = 0) = \Phi_F = -\frac{R\Phi_I(\zeta = 1)}{a_1 - \lambda}, \frac{d\Phi_I}{d\zeta} \Big|_{\zeta=1} = 0 \quad (2.7b)$$

λ and $\Phi_I(\zeta)$ are found numerically from Equation (2.7a). The solution of Equation (2.4) with the set of parameters $R = 0.55$, $v = 1.8$ and consumption of the desired component in both CSTR and dispersive tubular reactor ($\psi = -1$ and $a_1 = -0.25$), shows that most eigenvalues have negative real parts and there is only one unstable eigenvalue in the system (see Figs. 2.2 and 2.3). To explore the effects of diffusion (D) on eigenvalues placement, several values for diffusion were considered. By analyzing Fig. 2.3, with the same conditions, one can notice that as diffusivity increases, the distribution will shift from complex eigenvalues to the real ones.

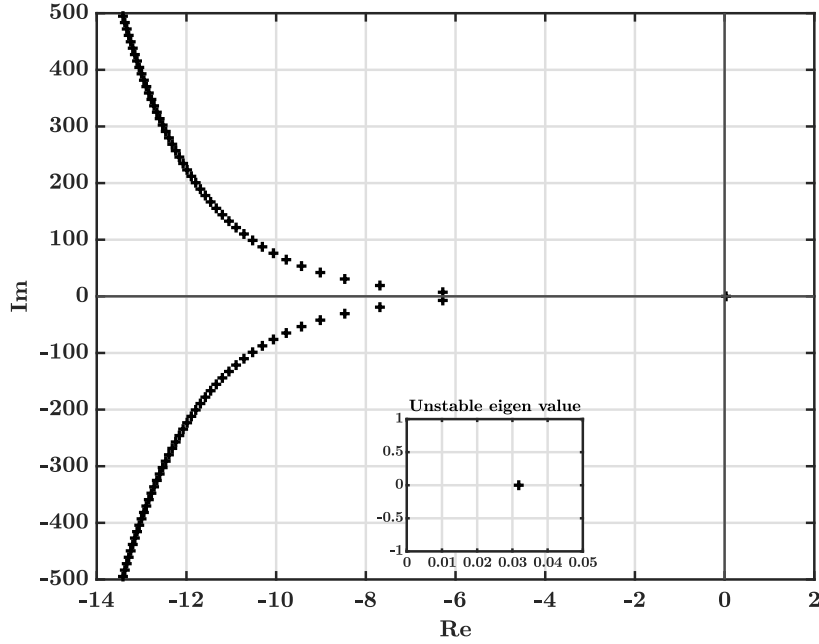


Figure 2.2: Eigenvalues distribution for unstable coupled ODE-PDE system when there is no diffusion within the tubular reactor

In this particular chemical engineering system, with the boundary conditions mentioned above, the instability of the coupled ODE-PDE system present with the value assigned for R . As will be discussed in Section 2.5 by canceling the unstable mode under model predictive control, the stabilization of the system is addressed.

2.3 Discrete Representation

2.3.1 Discrete Operators

In this section, the Cayley-Tustin time discretization is applied, which maps the mentioned coupled ODE-PDE system from continuous-time to a discrete one, preserving all energy properties with the feature of no spatial discretization. The discrete version of Equation (2.3) with sampling time Δt can be represented as follows:

$$\begin{aligned} x_{k+1} &= A_d x_k + B_d u_k + M_d d_k \\ y_k &= C_d x_k + D_d u_k + N_d d_k \end{aligned} \quad (2.8)$$

$\delta = 2/\Delta t$ and $(A_d, B_d, C_d, D_d, M_d, N_d)$ are the linear discrete operators defined by:

$$\begin{bmatrix} A_d & B_d & M_d \\ C_d & D_d & N_d \end{bmatrix} = \begin{bmatrix} -I + 2\delta [\delta - A]^{-1} & \sqrt{2\delta} [\delta - A]^{-1} B & \sqrt{2\delta} [\delta - A]^{-1} M \\ \sqrt{2\delta} C [\delta - A]^{-1} & C [\delta - A]^{-1} B & C [\delta - A]^{-1} M \end{bmatrix} \quad (2.9)$$

where $\delta = 2/\Delta t$, and $[\delta - A]^{-1} = R(\delta, A)$ is given as the resolvent operator of A

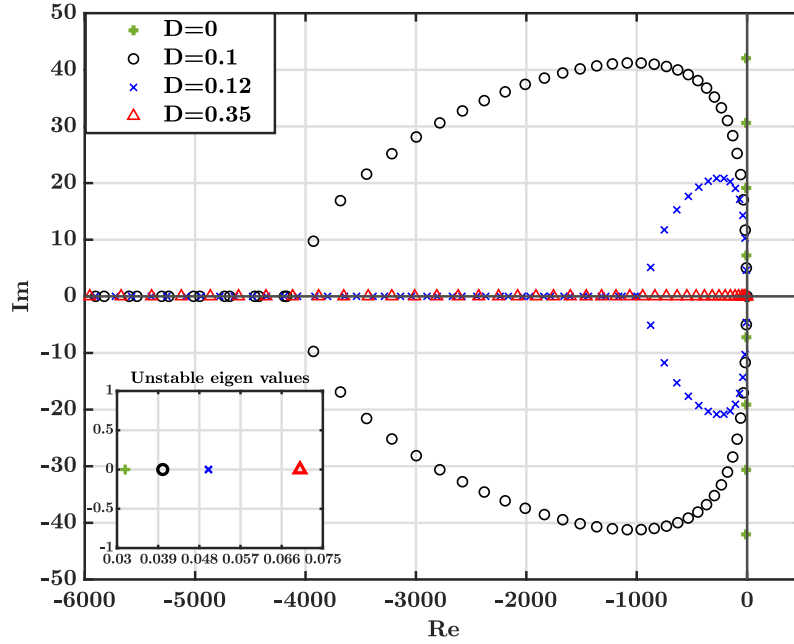


Figure 2.3: Effects of diffusivity within the dispersive reactor on the eigenvalues placement for unstable coupled ODE-PDE system

in Equation (2.5). It should be mentioned that the discrete operators are found by replacing s with δ in $R(s, A)$. In order to find the resolvent operator, one may easily apply Laplace transform to the set of Equations (2.1):

$$\underbrace{\frac{\partial}{\partial \zeta} \begin{bmatrix} x_I(\zeta, s) \\ \frac{\partial x_I(\zeta, s)}{\partial \zeta} \end{bmatrix}}_{X(\zeta, s)} = \underbrace{\begin{bmatrix} 0 & 1 \\ \frac{s - \psi}{D} & \frac{v}{D} \end{bmatrix}}_P \begin{bmatrix} x_I(\zeta, s) \\ \frac{\partial x_I(\zeta, s)}{\partial \zeta} \end{bmatrix} + \underbrace{\begin{bmatrix} 0 \\ -\frac{x_I(\zeta, 0)}{D} \end{bmatrix}}_H \quad (2.10)$$

Since P is a constant matrix, one can calculate $e^{P\zeta}$ with the Laplace inverse transform ($L^{-1}\{[sI - P]^{-1}\}$). Therefore, the solution of the mentioned system ($X(\zeta, s) = e^{P\zeta} X(0, s) + \int_0^\zeta e^{P(\zeta-\eta)} H d\eta$) can be expressed as follows:

$$\begin{bmatrix} x_I(\zeta, s) \\ \frac{\partial x_I(\zeta, s)}{\partial \zeta} \end{bmatrix} = \begin{bmatrix} e_1(\zeta) & e_2(\zeta) \\ e_3(\zeta) & e_4(\zeta) \end{bmatrix} \begin{bmatrix} x_I(0, s) \\ \frac{\partial x_I(0, s)}{\partial \zeta} \end{bmatrix} + \begin{bmatrix} b_1(\zeta) \\ b_2(\zeta) \end{bmatrix}. \quad (2.11)$$

After applying the boundary conditions ($x_I(\zeta = 0, s) = x_F(s)$, $\frac{\partial x_I(\zeta=1, s)=0}{\partial \zeta}$) to Equation (2.11), the discrete operators are obtained and have the following form:

$$A_d(\cdot) = - \begin{bmatrix} (\cdot)_F \\ (\cdot)_I \end{bmatrix} + 2\delta \begin{bmatrix} R_{FF} & R_{FI} \\ R_{IF} & R_{II} \end{bmatrix} \begin{bmatrix} (\cdot)_F \\ (\cdot)_I \end{bmatrix} \quad (2.12)$$

$$B_d = \sqrt{2\delta} \begin{bmatrix} R_{FF}B \\ R_{IF}B \end{bmatrix}; M_d = \sqrt{2\delta} \begin{bmatrix} R_{FI}f(\zeta) \\ R_{II}f(\zeta) \end{bmatrix} \quad (2.13)$$

$$C_d = \sqrt{2\delta} \begin{bmatrix} R_{IF}|_{\zeta=1} & R_{II}|_{\zeta=1} \end{bmatrix} \begin{bmatrix} (\cdot)_F \\ (\cdot)_I \end{bmatrix} \quad (2.14)$$

$$D_d = [R_{IF}B]|_{\zeta=1}; N_d = [R_{II}f(\zeta)]|_{\zeta=1} \quad (2.15)$$

with the following components:

$$\begin{aligned} R_{FF}(\cdot)_F &= \left(\frac{\frac{(\cdot)_F}{R}}{\frac{\delta - a_1}{R} - f_3^{(1)}} \right), R_{FI}(\cdot)_I = \left(\frac{b_1^{(1)} - \frac{e_2^{(1)}b_2^{(1)}}{e_4^{(1)}}}{\frac{\delta - a_1}{R} - f_3^{(1)}} \right) \\ R_{IF}(\cdot)_F(\zeta) &= f_3(\zeta) \left(\frac{\frac{(\cdot)_F}{R}}{\frac{\delta - a_1}{R} - f_3^{(1)}} \right) \\ R_{II}(\cdot)_I(\zeta) &= f_3(\zeta) \left(\frac{b_1^{(1)} - \frac{e_2^{(1)}b_2^{(1)}}{e_4^{(1)}}}{\frac{\delta - a_1}{R} - f_3^{(1)}} \right) - \frac{e_2^{(1)}b_2^{(1)}}{e_4^{(1)}} + b_1 \\ R_{FF}B &= f_3(\zeta) \left(\frac{\frac{a_2}{R}}{\frac{\delta - a_1}{R} - f_3^{(1)}} \right) + \frac{a_2}{\delta - a_1} \\ R_{IF}B(\zeta) &= f_3(\zeta) \left(\frac{\frac{a_2}{R}}{\frac{\delta - a_1}{R} - f_3^{(1)}} \right), R_{FI}f(\zeta) = \left(\frac{k_1^{(1)} - \frac{e_2^{(1)}k_2^{(1)}}{e_4^{(1)}}}{\frac{\delta - a_1}{R} - f_3^{(1)}} \right) \\ R_{II}f(\zeta) &= f_3(\zeta) \left(\frac{k_1^{(1)} - \frac{e_2^{(1)}k_2^{(1)}}{e_4^{(1)}}}{\frac{\delta - a_1}{R} - f_3^{(1)}} \right) - \frac{e_2^{(1)}k_2^{(1)}}{e_4^{(1)}} + k_1 \end{aligned} \quad (2.16)$$

in above equations $e_1(\zeta), e_2(\zeta), e_3(\zeta), e_4(\zeta), b_1(\zeta), b_2(\zeta), k_1(\zeta), k_2(\zeta)$ and $f_3(\zeta)$ are defined by the following expressions:

$$\begin{aligned}
e_1(\zeta) &= e^{\frac{m\zeta}{2}} \left(\cosh\left(\frac{h\zeta}{2}\right) - \frac{\sinh\left(\frac{h\zeta}{2}\right)m}{h} \right) \\
e_2(\zeta) &= \frac{2\sinh\left(\frac{h\zeta}{2}\right)e^{\frac{m\zeta}{2}}}{2\left(\frac{\delta-\psi}{D}\right)\frac{h}{\sinh\left(\frac{h\zeta}{2}\right)}e^{\frac{m\zeta}{2}}} \\
e_3(\zeta) &= \frac{h}{2\left(\frac{\delta-\psi}{D}\right)\sinh\left(\frac{h\zeta}{2}\right)e^{\frac{m\zeta}{2}}} \\
e_4(\zeta) &= e^{\frac{m\zeta}{2}} \left(\cosh\left(\frac{h\zeta}{2}\right) + \frac{\sinh\left(\frac{h\zeta}{2}\right)m}{h} \right) \\
b_1(\zeta) &= \int_0^\zeta f_1(\zeta, \eta)(\cdot)_I d\eta \\
f_1(\zeta, \eta) &= \frac{-2e^{\frac{(\zeta-\eta)m}{2}}\sinh\left(\frac{h(\zeta-\eta)}{2}\right)}{Dh} \\
k_1(\zeta) &= \int_0^\zeta f_1(\zeta, \eta)f(\zeta)d\eta \\
b_2(\zeta) &= \int_0^\zeta f_2(\zeta, \eta)(\cdot)_I d\eta
\end{aligned} \tag{2.17}$$

$$f_2(\zeta, \eta) = -\frac{e^{\frac{(\zeta-\eta)m}{2}}}{D} \left[\cosh\left(\frac{h(\zeta-\eta)}{2}\right) + \frac{\sinh\left(\frac{h(\zeta-\eta)}{2}\right)m}{h} \right]$$

$$k_2(\zeta) = \int_0^\zeta f_2(\zeta, \eta)f(\zeta)d\eta$$

$$m = \frac{v}{D}$$

$$h = \sqrt{\left(\frac{v}{D}\right)^2 + 4\left(\frac{\delta-\psi}{D}\right)}$$

$$f_3(\zeta) = e_1(\zeta) - \frac{e_2(\zeta)e_3^{(1)}}{e_4^{(1)}}$$

where $e_1^{(1)}$, $e_2^{(1)}$, $e_3^{(1)}$, $e_4^{(1)}$, $b_1^{(1)}$, $b_2^{(1)}$, $k_1^{(1)}$, $k_2^{(1)}$, $f_1^{(1)}$, $f_2^{(1)}$ and $f_3^{(1)}$ are the corresponding terms calculated at $\zeta = L = 1$.

2.3.2 Discrete Adjoint Operators

The adjoint operators are required for developing the model predictive control. The expressions for adjoints (A_d^*, B_d^*) of the discrete operators (A_d, B_d) are written in the following form:

$$A_d^*(\cdot) = - \begin{bmatrix} (\cdot)_F \\ (\cdot)_I \end{bmatrix} + 2\delta \begin{bmatrix} R_{FF}^* & R_{IF}^* \\ R_{FI}^* & R_{II}^* \end{bmatrix} \begin{bmatrix} (\cdot)_F \\ (\cdot)_I \end{bmatrix} \quad (2.18)$$

$$B_d^* = \sqrt{2\delta} \begin{bmatrix} (R_{FF}B)^* \\ (R_{IF}B)^* \end{bmatrix}^T \quad (2.19)$$

The components of the adjoint operators are computed based on the definition ($\langle A_d\Phi, \Psi^* \rangle = \langle \Phi, A_d^*\Psi^* \rangle$) and results in following operators:

$$R_{FF}^*(\cdot)_F = R_{FF}(\cdot)_F$$

$$R_{IF}^*(\cdot)_I = \int_0^L \begin{bmatrix} e_1 - \frac{e_2 e_3^{(1)}}{e_4^{(1)}} \\ \delta - a_1 - R f_3^{(1)} \end{bmatrix} (\cdot)_I d\zeta$$

$$R_{FI}^*(\cdot)_F(\zeta) = \left(\begin{array}{c} \frac{f_1^{(1)}}{\frac{\delta - a_1}{R} - f_3^{(1)}} - \frac{\frac{e_2^{(1)} f_2^{(1)}}{e_4^{(1)}}}{\frac{\delta - a_1}{R} - f_3^{(1)}} \\ \end{array} \right) (\cdot)_F$$

$$R_{II}^*(\cdot)_I(\zeta) = \left(-f_2^{(1)} \int_0^L \left[\frac{e_2^{(1)}}{e_4^{(1)} (\delta - a_1 - R f_3^{(1)})} f_3(\eta) + \frac{e_2(\eta)}{e_4^{(1)}} \right] (\cdot)_I d\eta \right) + \quad (2.20)$$

$$\left(f_1^{(1)} \int_0^L \left[\frac{f_3(\eta)}{(\delta - a_1 - R f_3^{(1)})} \right] (\cdot)_I d\eta + \int_\zeta^L f_1(\eta, \zeta) (\cdot)_I d\eta \right)$$

$$(R_{FF}B)^*(\cdot)_F = \left(\begin{array}{c} \frac{a_2 f_3^{(1)}}{\frac{(\delta - a_1)^2}{R} - f_3^{(1)}(\delta - a_1)} + \frac{a_2}{\delta - a_1} \\ \end{array} \right) (\cdot)_F$$

$$(R_{IF}B)^*(\cdot)_I = \left(\frac{\frac{a_2}{R}}{\frac{\delta - a_1}{R} - f_3^{(1)}} \right) \int_0^L \left[e_1(\zeta) - \frac{e_3^{(1)} e_2(\zeta)}{e_4^{(1)}} \right] (\cdot)_I d\zeta$$

2.4 Luenberger Observer Design

In a real process system controller realization, having access to all the state variables cannot be feasible, especially when DPS are considered. In order to address this issue in the design of the model predictive control, the Luenberger observer is introduced for reconstruction of the state variables by taking the output measurement into account. First, the design of observer for the coupled parabolic PDE-ODE system in the continuous setting is considered. Then, the continuous observer gain is transferred into the discrete one using Cayley-Tustin discretization. The Luenberger observer has the form given by:

$$\begin{aligned}\dot{\hat{x}}(\zeta, t) &= A\hat{x}(\zeta, t) + Bu(t) + L_c[y(t) - \hat{y}(t)] + f(\zeta)d(t) \\ \hat{y}(t) &= C\hat{x}(\zeta, t)\end{aligned}\quad (2.21)$$

where $L_c = \begin{bmatrix} L_F \\ L_I(\zeta) \end{bmatrix}$ is the continuous observer gain. By subtracting Equation (2.21) from its general form ($\dot{x}(\zeta, t) = Ax(\zeta, t) + Bu(t)$), one can get the dynamics of the observer error as follows:

$$\dot{\hat{e}}(\zeta, t) = (A - L_c C)\hat{e}(t), \hat{e}(0) \neq 0 \quad (2.22)$$

the design of the observer is relied on choosing L_c such that the state estimation error dynamics given by Equation (2.22) is stable. Hence, the stability of the observer can be ensured by analyzing the eigenvalues problem of the observer error:

$$(A - L_c C)\Phi = \lambda\Phi \quad (2.23)$$

which results in following equation and boundary conditions:

$$\frac{d^2\Phi_I}{d\zeta^2} - \frac{v}{D} \frac{d\Phi_I}{d\zeta} - \frac{(\lambda - \psi)}{D} \Phi_I = \frac{L_I(\zeta)}{D} \Phi_I(\zeta = 1) \quad (2.24a)$$

$$\Phi_I(\zeta = 0) = \Phi_F = -\frac{(L_F - R)\Phi_I(\zeta = 1)}{a_1 - \lambda}, \left. \frac{d\Phi_I}{d\zeta} \right|_{\zeta=1} = 0. \quad (2.24b)$$

Fig. 2.4 shows the eigenvalues placement for different values of $L_c = \begin{bmatrix} L_F \\ L_I(\zeta) \end{bmatrix}$. It should be emphasized that in the eigenvalue problem, although a spatially varying $L_I(\zeta)$ could be chosen, a constant value throughout the whole spatial domain ($L_I(\zeta) = L$) is considered and the same value assigned for the finite part ($L_F = L$). It can be seen that as the value of L_c increases, the unstable real eigenvalue is shifted to the left side (the stable region). Therefore, as depicted in Fig. 2.4 for $L_c > 0.1$ the stability of the error dynamics will be ensured by having only negative eigenvalues. Here, the resolvent is used to compute the corresponding discrete observer gain from the continuous one (Cassol and Dubljevic, 2020):

$$L_d = \sqrt{2\delta} \begin{bmatrix} R_{FF} & R_{FI} \\ R_{IF} & R_{II} \end{bmatrix} \begin{bmatrix} L_F \\ L_I(\zeta) \end{bmatrix}. \quad (2.25)$$

Therefore, the reconstructed state in the discrete setting can be expressed as:

$$\begin{aligned}\hat{x}_{k+1} &= A_d \hat{x}_k + B_d u_k + L_d (y_k - \hat{y}_k) + M_d d_k \\ \hat{y}_k &= C_d \hat{x}_k + D_d u_k + N_d d_k, y_k = C_d x_k + D_d u_k + N_d d_k\end{aligned}\tag{2.26}$$

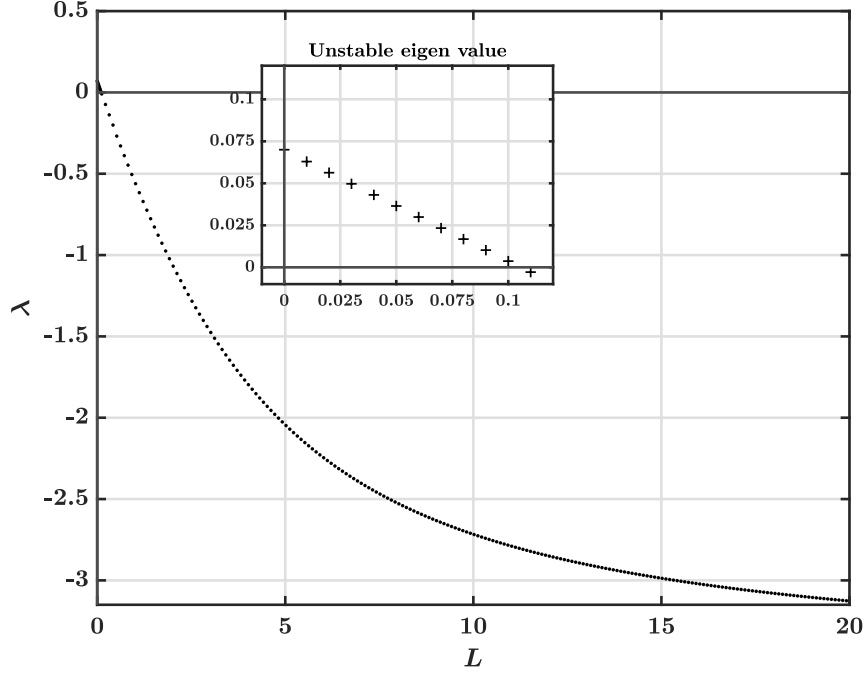


Figure 2.4: Shifting the unstable eigenvalue of the observer for different values of the observer gain.

2.5 Model Predictive Control for Linear Coupled ODE-PDE System

2.5.1 Optimization Problem

The linear discrete-time model dynamics represented in Equations (2.12)–(2.20) is used in the formulation of the model predictive control for the coupled CSTR and tubular reactor system. The MPC developed in (Rawlings et al., 2017) regarding linear time invariant systems for the finite-dimensional setting is extended to infinite-dimensional one. In order to achieve this purpose, the following objective function should be minimized at each sampling time (k) to design the regulator of the coupled

ODE-PDE system:

$$\begin{aligned}
\min_u J &= \sum_{j=0}^{\infty} \langle \hat{x}(k+j|k), Q\hat{x}(k+j|k) \rangle \\
&+ \langle u(k+j+1|k), Fu(k+j+1|k) \rangle \\
\text{s.t. } \hat{x}(k+j+1|k) &= A_d\hat{x}(k+j|k) + B_d u(k+j|k), \\
u^{\min} &\leq u(k+j|k) \leq u^{\max}, \\
\hat{x}_F^{\min} &\leq \hat{x}_F(k+j|k) \leq \hat{x}_F^{\max}, \\
\langle \hat{x}(k+N), \Phi_u \rangle &= 0
\end{aligned} \tag{2.27}$$

where $\hat{x} = \begin{bmatrix} \hat{x}_F \\ \hat{x}_I \end{bmatrix}$ refers to the reconstructed state, F is a positive definite operator,

$Q = \begin{bmatrix} Q_F \\ Q_I \end{bmatrix}$ represents positive semidefinite spatial operator associated with the state of coupled ODE-PDE system and the indices, $(k+j)$ and $(k+j+1|k)$, for both input and state variable, indicate current and future time, respectively. In order to get the finite horizon objective function, one can assume zero input beyond the control horizon (i.e., $u(k+N+1|k) = 0$) by taking the terminal penalty term into an account. The result takes the following form:

$$\begin{aligned}
\min_{u^N} J &= \sum_{j=0}^{N-1} \langle \hat{x}(k+j|k), Q\hat{x}(k+j|k) \rangle \\
&+ \langle u(k+j+1|k), Fu(k+j+1|k) \rangle \\
&+ \langle \hat{x}(k+N|k), \bar{Q}\hat{x}(k+N|k) \rangle \\
\text{s.t. } \hat{x}(k+j+1|k) &= A_d\hat{x}(k+j|k) + B_d u(k+j|k), \\
u^{\min} &\leq u(k+j|k) \leq u^{\max}, \\
\hat{x}_F^{\min} &\leq \hat{x}_F(k+j|k) \leq \hat{x}_F^{\max}, \\
\langle \hat{x}(k+N), \Phi_u \rangle &= 0.
\end{aligned} \tag{2.28}$$

After simple algebraic manipulation, the following finite-dimensional quadratic optimization problem is obtained:

$$\begin{aligned}
\min_U J &= U^T H U + 2U^T P \hat{x}(k|k) \\
&+ \langle \hat{x}(k|k), \bar{Q}\hat{x}(k|k) \rangle
\end{aligned} \tag{2.29a}$$

where \bar{Q} is terminal state penalty operator. The above equation is subjected to the following constraints:

$$\left\{ \begin{array}{l} 1. U^{\min} \leq U \leq U^{\max} \\ 2. \hat{x}_F^{\min} \leq \hat{x}_F \leq \hat{x}_F^{\max} \\ 3. \langle \hat{x}(N), \Phi_u \rangle = 0 \end{array} \right. \tag{2.29b}$$

where $U = \begin{bmatrix} u(k+1|k) & u(k+2|k) & u(k+3|k) & \dots & u(k+N|k) \end{bmatrix}^T$ and (H, P) are computed as below:

$$H = \begin{bmatrix} B_d^* \bar{Q} B_d + F & B_d^* A_d^* \bar{Q} B_d & \dots & B_d^* A_d^{*N-1} \bar{Q} B_d \\ B_d^* \bar{Q} A_d B_d & B_d^* \bar{Q} B_d + F & \dots & B_d^* A_d^{*N-2} \bar{Q} B_d \\ \vdots & \vdots & \ddots & \vdots \\ B_d^* \bar{Q} A_d^{N-1} B_d & B_d^* \bar{Q} A_d^{N-2} B_d & \dots & B_d^* \bar{Q} B_d + F \end{bmatrix}, \quad (2.30)$$

$$P = \begin{bmatrix} B_d^* \bar{Q} A_d \\ B_d^* \bar{Q} A_d^2 \\ \vdots \\ B_d^* \bar{Q} A_d^N \end{bmatrix}.$$

The model predictive control scheme used on the coupled ODE-PDE system is illustrated in Fig. 2.5. As can be seen, the full state feedback is needed for the MPC scheme, which is going to be given by the reconstructed states from the observer.

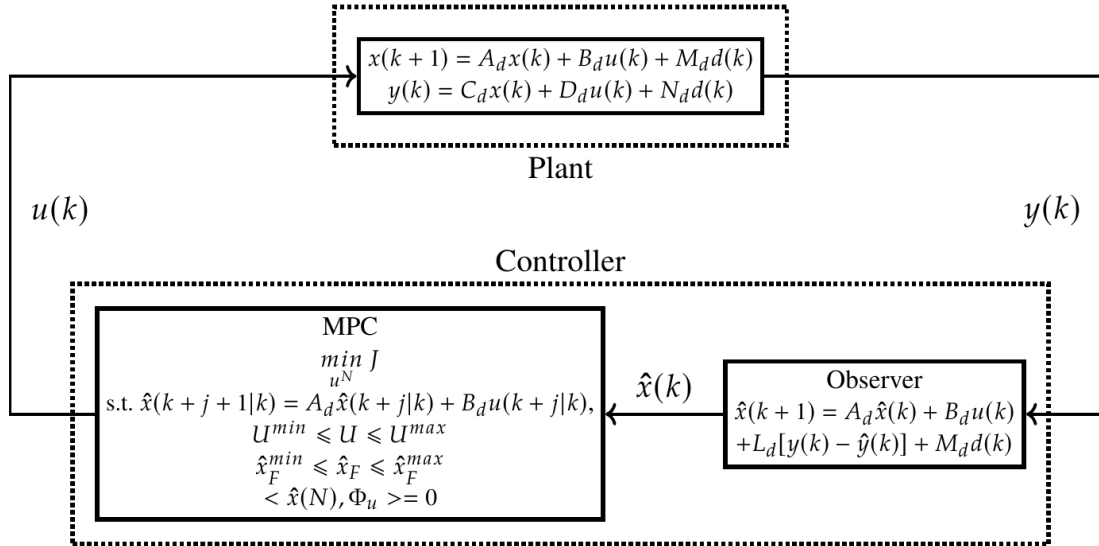


Figure 2.5: Representation of the closed loop.

2.5.2 Terminal State Penalty Operator

The terminal state penalty term, the operator $\bar{Q} = \begin{bmatrix} \bar{Q}_F \\ \bar{Q}_I \end{bmatrix}$, can be found from the solution of the following discrete Lyapunov equation:

$$A_d^* \bar{Q} A_d - \bar{Q} = -Q. \quad (2.31)$$

The above solution of the discrete Lyapunov equation based on Cayley-Tustin method

is the same unique solution of \bar{Q} in Equation (2.31) in continuous setting ($A^*\bar{Q} + \bar{Q}A = -Q$) (Xu and Dubljevic, 2017). Since the solution of \bar{Q} cannot be obtained directly; in other words, because of the necessity of using integral operators coming from discrete operators for calculating \bar{Q} , the procedure followed here is to connect the discrete and continuous Lyapunov equations. Here, one can rewrite the continuous Lyapunov equation in the following format (Curtain and Zwart, 1995):

$$\langle Ax_1, \bar{Q}x_2 \rangle + \langle \bar{Q}x_1, Ax_2 \rangle = - \langle x_1, Qx_2 \rangle. \quad (2.32)$$

By considering $x_1 = \hat{\Phi}^m$ and $x_2 = \hat{\Psi}^m$ and using the fact that λ^m and $\hat{\Psi}^m$ are the eigenvalue and eigen function of the system (i.e., $A\hat{\Phi}^m = \lambda^m\hat{\Phi}^m$), the equation leads to:

$$\begin{aligned} \langle \lambda^m \hat{\Phi}^m, \bar{Q} \hat{\Psi}^m \rangle + \langle \bar{Q} \hat{\Phi}^m, \lambda^m \hat{\Psi}^m \rangle &= \lambda^m \langle \hat{\Phi}^m, \bar{Q} \hat{\Psi}^m \rangle \\ + \lambda^m \langle \bar{Q} \hat{\Phi}^m, \hat{\Psi}^m \rangle &= - \langle \hat{\Phi}^m, Q \hat{\Psi}^m \rangle \end{aligned} \quad (2.33)$$

\bar{Q} is a bounded symmetric operator ($D(A^*) = D(A)$) and it is self-adjoint (see, (Curtain and Zwart, 1995)) which implies $\langle \hat{\Phi}^m, \bar{Q} \hat{\Psi}^m \rangle = \langle \bar{Q} \hat{\Phi}^m, \hat{\Psi}^m \rangle = \bar{Q}^m$, accordingly the following simplified equation is achieved:

$$\bar{Q}^m = \frac{- \langle \hat{\Phi}^m, Q \hat{\Psi}^m \rangle}{2\lambda^m}. \quad (2.34)$$

Finally, the solution of the continuous Lyapunov equation gives the expression for the infinite part (PDE) of the terminal state penalty operator (\bar{Q}_I) which can be expressed as below:

$$\bar{Q}_I(\cdot)_I = \sum_{m=0}^{\infty} \frac{- \langle \hat{\Phi}_I^m, Q_I \hat{\Psi}_I^m \rangle}{2\lambda^m} \langle (\cdot)_I, \hat{\Psi}_I^m \rangle \hat{\Phi}_I^m \quad (2.35)$$

where $\hat{\Phi}_I^m$ and $\hat{\Psi}_I^m$ refer to the normalized eigenfunction and adjoint eigenfunction of infinite part of the system, respectively. In Equation (2.35), the summation is computed for increasing number of different eigenvalues, until the applied operator converges to a constant value. In this work the first 20 eigen modes are considered in the simulation. For the finite part (ODE), $A_F = A_F^* = a_1$. According to Lyapunov equation, \bar{Q}_F is easily obtained and given by the following expression:

$$\bar{Q}_F(\cdot)_F = \frac{Q_F}{2a_1}(\cdot)_F \quad (2.36)$$

2.5.3 Stability Constraint

Based on the definition of a positive definite operator, it is possible to show that \bar{Q} is a positive operator if only the stable nodes are taken into account (Curtain and Zwart, 1995). In order to guarantee stabilization of the system, a stability constraint is

applied in the optimization problem and is represented by an equality constraint (Xu and Dubljevic, 2017). It is assumed that the controller will gain stabilization by rejecting the unstable modes. Hence, this condition can be written as below:

$$\langle \hat{x}(N), \Phi_u \rangle = 0 \quad (2.37)$$

where Φ_u refer to unstable eigenfunctions associated with positive eigenvalues. The corresponding equality constraint, which cancels the unstable modes at end of the horizon, is constructed as follows:

$$\begin{aligned} & \left[\langle A_d^{N-1} B_d, \Phi_u \rangle \quad \dots \quad \langle B_d, \Phi_u \rangle \right] U \\ & = - \langle A_d^N \hat{x}(k|k), \Phi_u \rangle . \end{aligned} \quad (2.38)$$

If there is a feasible input sequence given by optimization problem, the above equality constraint is satisfied for the constrained convex optimization problem given by Equation (2.29a). Therefore, stabilization can be obtained, and the unstable modes will be canceled by end of the horizon. Here, due to the feasibility of the optimization represented by constrained quadratic problem in the zero-disturbance case, feasibility implies stability and optimal stabilizability. This extension is based on the well-known results from the finite-dimensional theory (Mayne, 2014; Rawlings et al., 2017).

2.6 Simulation Results

In this section, the simulation study is performed for the proposed controller of the coupled ODE-PDE system. First, the design of the observer is discussed in the discrete setting with reconstruction of states in an open-loop condition by using Cayley-Tustin method, then the performance of the ensuing Model Predictive Control is demonstrated and compared with the open-loop response.

Table 2.1: Parameter values used in numerical simulation

Parameters	Values
v	1.8
F	1
D	0.35
a_1	-0.25
ψ	-1
a_2	1
R	0.5
u^{min}	-0.09
u^{max}	0
x_F^{min}	0
x_F^{max}	0.65

2.6.1 Observer Design and Open-Loop Response

Based on Equations (2.8)–(2.13), one can reconstruct the dynamics of the discrete representation for both finite and infinite parts of the system with the set of parameters given in Table 2.1. As discussed in Section 2.4, to guarantee the stability of the observer, $L_c = 5$ is chosen as the observer gain. By using Equation (2.25) the discrete version of the corresponding observer gain is computed. The initial conditions for the mentioned observer and original system are considered to be constants in the entire space, $\hat{x}_0 = 0$ and $x_0 = 1$, respectively. In simulation $\Delta t = 0.04$ is considered which implies $\delta = 50$ and for numerical integration $\Delta z = 0.005$ is chosen. Then, according to Equation (2.26), the reconstructed state is obtained, and the corresponding error dynamics is evaluated. As shown in Fig. 2.6, the dynamics of the observer error converges to zero, which means the developed observer has a good performance. Hence, in the case of a realistic system, the Model Predictive Control can be applied using just the output measurement.

As discussed in Section 2.2.2 regarding the instability of the coupled ODE-PDE system, Fig. 2.7a demonstrates the space-time evolution of the tubular reactor ($x_I(\zeta, t)$) for $0 \leq t \leq 20$ which grows unbounded as expected. Following this, the corresponding dynamics of the CSTR ($x_F(t)$) with pertaining initial condition is depicted in Fig. 2.7b.

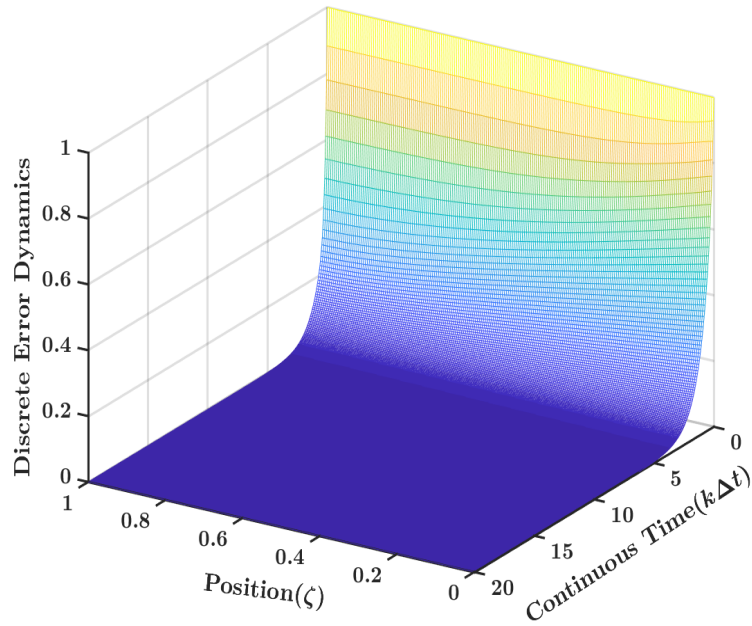
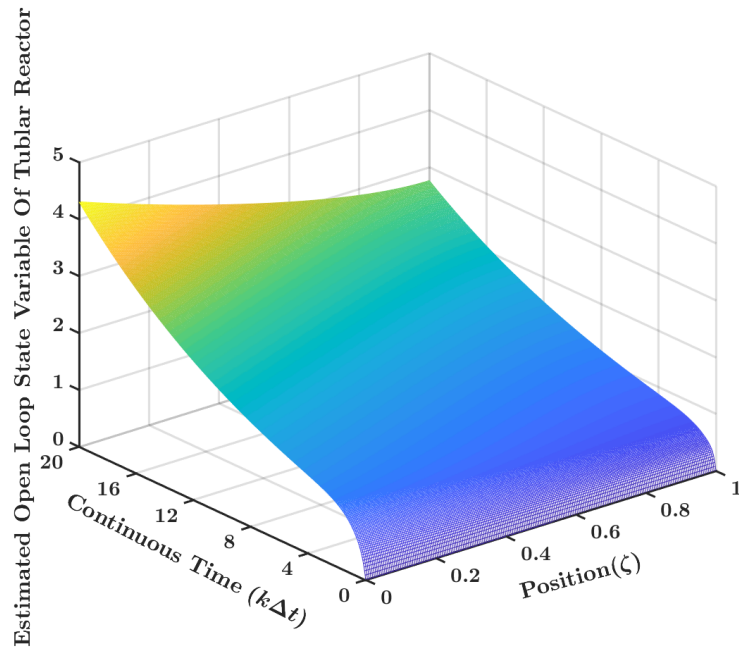
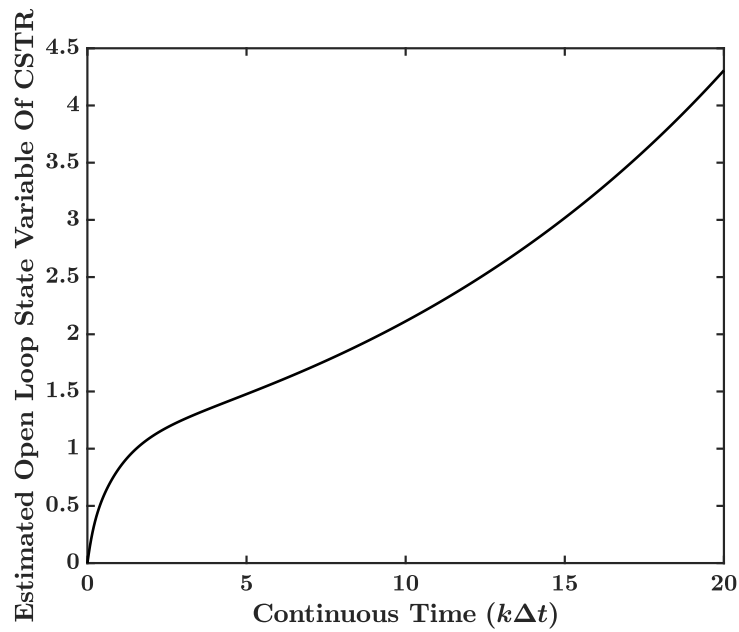


Figure 2.6: Evolution of the discrete error dynamics with the value $L_c = 5$ for observer gain.



(a)



(b)

Figure 2.7: (a) The estimated state profile evolution ($x_I(\zeta, k)$) through dispersive tubular reactor constructed on the basis of discrete-time coupled ODE-PDE system in an open-loop condition; (b) Dynamics reconstruction of the scalar variable within the CSTR in an open-loop condition.

2.6.2 MPC Implementation

In this part, based on the scheme represented by Fig. 2.5, the successful application of the proposed constrained model predictive controller is demonstrated on the basis of Cayley-Tustin time discretization with optimization problem described by Equations (2.27)–(2.38).

The implementation of the system under model predictive control with and without constraints (see Equation (2.29b)) in time domain $0 \leq t \leq 20$ is shown in Fig. 2.8 b) and Fig. 2.8 d). By choosing $Q_F = 2.5$, $Q_I(\zeta) = 1.5$ and $N = 65$ for the MPC control horizon, it is possible to see that the controller is able to comply with the input and states constraints (dash-dotted lines) imposed into the coupled ODE-PDE system. Moreover, regarding the instability of the system, as described in Section 2.5.3, one can notice that the stability constraint is also fulfilled by canceling the unstable mode at end of the horizon (see Fig. 2.9).

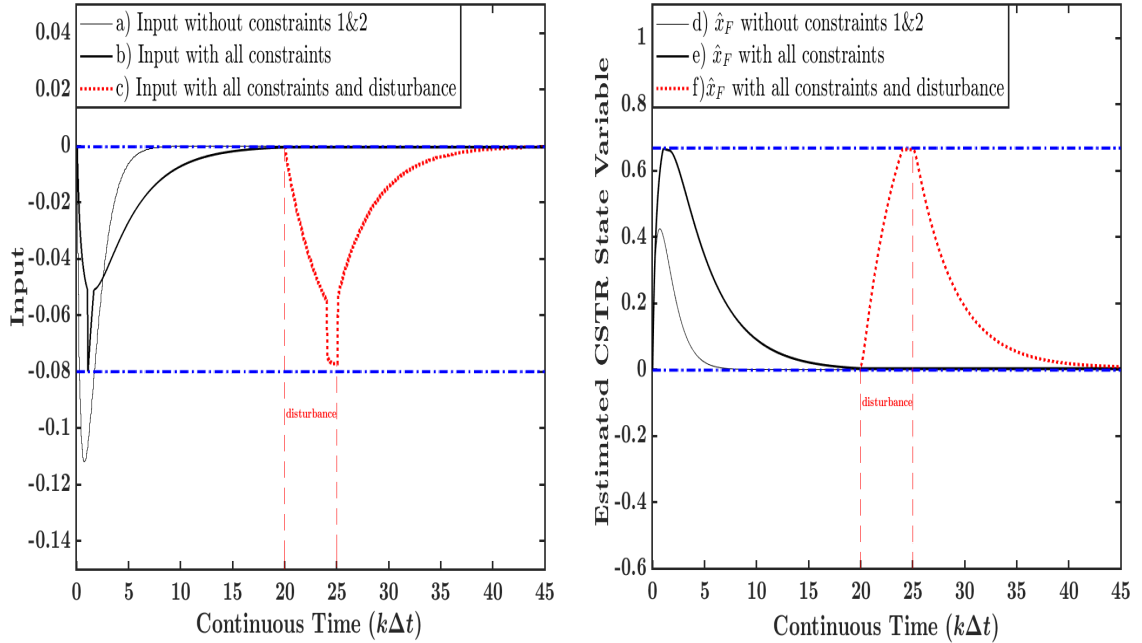


Figure 2.8: a), b) and c) demonstrate the comparison between input profiles under model predictive control law: with and without input/state constraints, with constraints and with disturbance for $20 \leq t \leq 25$; d), e) and f) denote reconstructed dynamics of the scalar variable within the CSTR under model predictive law: with and without input/state constraints, with constraints and with disturbance for $20 \leq t \leq 25$.

On the other hand, in order to provide a comparison of the dynamics of scalar variable x_F in CSTR with input and state constraints, the simulation is performed again to justify two scenarios, for the first one only stability constraint is considered in the MPC algorithm while in the second one all constraints (stability, input and

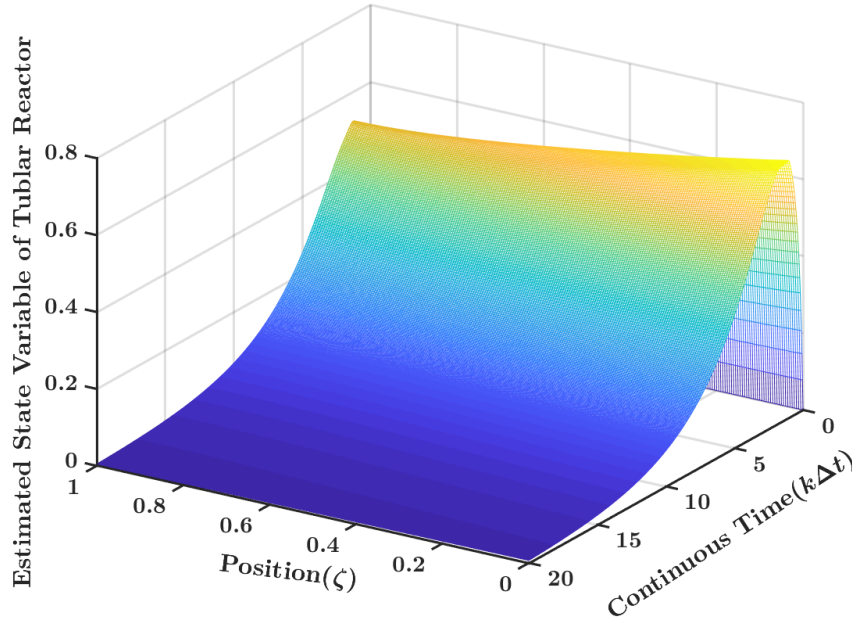


Figure 2.9: Evolution of the stabilized spatial profile for the tubular reactor with all constraints.

state) are present. Fig. 2.8 d) and Fig. 2.8 e) show this analogy with corresponding control actions given by Fig. 2.8 a) and Fig. 2.8 b). As expected in the first setting, the CSTR dynamics is faster compared to the latter case as no state/input constraints need to be satisfied.

Another simulation has been performed to explore the behaviour of the MPC algorithm for handling the mentioned constraints, the step disturbance is applied through the infinite part of the system (tubular reactor) for $20 \leq t \leq 25$. The idea here is to examine the performance of the MPC algorithm for stabilization and the state/input constraints satisfaction. $y_I = 0.5$ and $k_I = 0.6$ are chosen as the parameters in Equation (2.2) describing spatial varying function $f(\zeta)$. Fig. 2.8 c) and Fig. 2.8 f) verify the good performance of MPC for handling the constraints when the disturbance is present.

By analyzing Fig. 2.8 c), one can notice that after the step disturbance is applied, the state variable of the CSTR stays at the upper limit (x_F^{max}) until $t = 25$, then decreases and once again goes back to zero (at $t = 45$) based on the control action given by Fig. 2.8 c).

2.7 Summary

In this chapter, the design of a model predictive controller and discrete observer for a coupled ODE-PDE system was investigated. In particular, the lumped and distributed system were coupled by the boundaries, with the manipulated variable acting

on the ODE. The system stability characteristics were first analyzed by studying the system's eigenvalues. A discrete representation of the system was necessary in the controller design; thus, the Cayley-Tustin time discretization was applied, preserving the original system characteristics. An unstable operation condition was considered, and the MPC and observer design had to take this into account. To develop the discrete observer, the design in the continuous-time setting was first derived, then the discrete observer was obtained based on the continuous gain. The MPC was designed to obtain the optimal control sequence while handling input constraints and stabilizing the system using a terminal constraint. Finally, numerical simulations were shown to present the performance of the controller in the closed loop. As expected, the controller was able to achieve stabilization, while handling the constraints. If a disturbance is made, the controller can deal with the effects made in the system while satisfying the constraints.

References

- Ai, L. and San, Y. (2013). Model predictive control for nonlinear distributed parameter systems based on ls-svm. *Asian Journal of Control*, 15(5):1407–1416.
- Armaou, A. and Christofides, P. (2002). Dynamic optimization of dissipative pde systems using nonlinear order reduction. *Chemical Engineering Science*, 57(24):5083–5114.
- Bonis, I., Xie, W., and Theodoropoulos, C. (2012). A linear model predictive control algorithm for nonlinear large-scale distributed parameter systems. *AIChE Journal*, 58(3):801–811.
- Cassol, G. O. and Dubljevic, S. (2020). Discrete output regulator design for the linearized saint–venant–exner model. *Processes*, 8(8).
- Chen, C. C. (1994). A continuous bulk polymerization process for crystal polystyrene. *Polymer-Plastics Technology and Engineering*, 33(1):55–81.
- Chen, H. and Allgöwer, F. (1998). *Nonlinear Model Predictive Control Schemes with Guaranteed Stability*. Springer Netherlands.
- Curtain, R. and Zwart, H. (1995). *An Introduction to Infinite Dimensional Linear Systems Theory*. Springer.
- Dubljevic, S. and Christofides, P. D. (2006). Predictive control of parabolic pdes with boundary control actuation. *Chemical Engineering Science*, 61(18):6239 – 6248.
- Dubljevic, S., El-Farra, N. H., Mhaskar, P., and Christofides, P. D. (2006). Predictive control of parabolic pdes with state and control constraints. *International Journal of Robust and Nonlinear Control*, 16(16):749–772.
- Eaton, J. W. and Rawlings, J. B. (1992). Model-predictive control of chemical processes. *Chemical Engineering Science*, 47(4):705 – 720.
- Fogler (2005). *H.S., elements of chemical reaction engineering*. prentice-hall.
- García, C. E., Prett, D. M., and Morari, M. (1989). Model predictive control: Theory and practice—a survey. *Automatica*, 25(3):335 – 348.
- Hairer, E., Lubich, C., and Wanner, G. (2006). *Geometric Numerical Integration: Structure-Preserving Algorithms for Ordinary Differential Equations; 2nd ed.* Springer.
- Hasan, A., Aamo, O. M., and Krstic, M. (2016). Boundary observer design for hyperbolic pde–ode cascade systems. *Automatica*, 68:75 – 86.
- Ito, K. and Kunisch, K. (2002). Receding horizon optimal control for infinite dimensional systems. *ESAIM: Control, Optimisation and Calculus of Variations*, 8:741–760.

- Kazantzis, N. and Kravaris, C. (1999). Energy-predictive control: a new synthesis approach for nonlinear process control. *Chemical Engineering Science*, 54(11):1697 – 1709.
- Krstic, M. and A.Smyshlyaev (2008). *Boundary Control of Pdes: A Course on Backstepping Designs*. Society for Industrial and Applied Mathematics.
- Krstic, M. and Smyshlyaev, A. (2008). Backstepping boundary control for first-order hyperbolic PDEs and application to systems with actuator and sensor delays. *System and Control letters*, 57:750–758.
- Liu, L., Huang, B., and Dubljevic, S. (2014). Model predictive control of axial dispersion chemical reactor. *Journal of Process Control*, 24(11):1671 – 1690.
- Mayne, D., Rawlings, J., Rao, C., and Sokaert, P. (2000). Constrained model predictive control: Stability and optimality. *Automatica*, 36(6):789–814.
- Mayne, D. Q. (2014). Model predictive control: Recent developments and future promise. *Automatica*, 50(12):2967 – 2986.
- Meglio, F. D., Argomedeo, F. B., Hu, L., and Krstic, M. (2018). Stabilization of coupled linear heterodirectional hyperbolic pde–ode systems. *Automatica*, 87:281 – 289.
- Moghadam, A. A., Aksikas, I., Dubljevic, S., and Forbes, J. F. (2013). Boundary optimal (lq) control of coupled hyperbolic pdes and odes. *Automatica*, 49(2):526 – 533.
- Mohammadi, L., Aksikas, I., Dubljevic, S., and Forbes, J. F. (2015). Optimal boundary control of coupled parabolic PDE – ODE systems using infinite-dimensional representation. *Journal of Process Control*, 33:102–111.
- Muske, K. R. and Rawlings, J. B. (1993). Model predictive control with linear models. *AIChE Journal*, 39(2):262–287.
- Oh, M. and Pantelides, C. (1996). A Modelling and Simulation Language for Combined Lumped and Distributed Parameter Systems. *Computers and Chemical Engineering*.
- Åström, K. J. and Wittenmark, B. (1990). *Computer-Controlled Systems: Theory and Design (2nd Ed.)*. Prentice-Hall, Inc.
- Rawlings, J., Mayne, D., and Diehl, M. (2017). *Model Predictive Control: Theory, Computation, and Design*. Nob Hill Publishing.
- Rawlings, J. B. (2000). Tutorial overview of model predictive control. *IEEE Control Systems Magazine*, 20(3):38–52.
- Ray, W. (1981). *Advanced process control*. New York McGraw-Hill.

- Richalet, J., Rault, A., Testud, J., and Papon, J. (1978). Model predictive heuristic control: Applications to industrial processes. *Automatica*, 14(5):413 – 428.
- Scokaert, P. O. M., Mayne, D. Q., and Rawlings, J. B. (1999). Suboptimal model predictive control (feasibility implies stability). *IEEE Transactions on Automatic Control*.
- Shang, H., Forbes, J. F., and Guay, M. (2004). Model predictive control for quasilinear hyperbolic distributed parameter systems. *Industrial & Engineering Chemistry Research*, 43(9):2140–2149.
- Susto, G. A. and Krstic, M. (2010). Control of pde–ode cascades with neumann interconnections. *Journal of the Franklin Institute*, 347(1):284 – 314.
- Tang, S. and Xie, C. (2011). State and output feedback boundary control for a coupled pde–ode system. *Systems & Control Letters*, 60(8):540 – 545.
- V.Havu and Malinen, J. (2007). The cayley transform as a time discretization scheme. *Numerical Functional Analysis and Optimization*, 28(7-8):825–851.
- Xu, Q. and Dubljevic, S. (2017). Linear Model Predictive Control for Transport-Reaction Processes. *AIChE Journal*, 63(7).

3

Model Predictive Control of Non-Isothermal Axial Dispersion Tubular Reactors with Recycle

3.1 Introduction

Many transport-reaction processes present in petrochemical, biochemical and pharmaceutical unit operations belong to distributed parameter system (DPS) models. Within a finite spatial domain, the mathematical formulation of the mentioned processes, arising from the first-principle modeling, usually takes the form of a set of parabolic partial differential equations (PDEs) in which the intrinsic feature of reaction, convection and diffusion phenomena can be captured. The non-isothermal axial dispersion reactors have attracted great attention since their models account for a large number of reactor realizations in industry (see Varma and Aris 1977 for a survey). In particular, the dynamical properties and control for axial dispersion tubular reactors, where mass and thermal phenomena are taking place, has been the objective of numerous studies over the years (see Hlavacek and Hofmann 1970a,b; Cohen and Poore 1974; Georgakis et al. 1977; Bošković and Krstić 2002), as several complexities are observed in the dynamical description and in the practical realization of the reactor operation (Marwaha and Luss, 2003). In addition, when a dispersive chemical tubular reactor is considered with recycle of energy and mass flow, the model analysis and subsequent controller design become more challenging and require careful consideration since competitive effects of mass and heat transfer are present in recycle and it is known that may induce instability in apparently stable reactor operations (Luss and Amundson, 1967).

The salient feature of the axial dispersion reactor model is the mathematical de-

scription given by parabolic partial differential equations (PDEs) which can admit a variety of boundary modeling realizations to account for the physically meaningful setting present in industry. Among several modeling realizations, the Danckwerts boundary conditions (Danckwerts, 1953) reflect the physically relevant inlet flux transport and zero flux conditions at the reactor outlet. In general, the reactor models are numerically solved by application of standard (high-order) and reduced-order PDE-to-ordinary differential equation (ODE) including finite difference discretization schemes (Badillo-Hernandez et al., 2019), methods relied on dynamically moving the discretization mesh to minimize the discretization error (Liu and Jacobsen, 2004), or by applying the various spectral methods such as proper orthogonal decomposition (POD) to study oscillatory reactors regimes (Bizon et al., 2008). Along with the modeling efforts, the controller designs and associated spatial discretization techniques are proposed for PDEs to obtain sets of ordinary differential equations (ODEs), and then the reduced models (if possible) are utilized for the synthesis of finite dimensional controllers (see Curtain 1982; Balas 1979; Ray 1981; Antoniadis and Christofides 2000). The significant drawback of this approach, notably when it comes to parabolic PDEs, is that the order of the discretization used (in the case of finite difference methods applied to approximate spatial derivatives) and/or number of modes that must be considered to reach the desired order of model approximation, which may lead to high dimensional controllers, mainly difficult to be implemented. Consequently, the regulator design for dissipative PDEs has been the objective of many studies over the years, and different design methodologies were considered, such as approximate inertial manifolds, dynamic optimization, robust control and linear quadratic control in the frequency domain (e.g. Christofides and Daoutidis 1997; Armaou and Christofides 2002; Aksikas et al. 2017 to cite a few). In the same vein, there are several contributions focused on the stability and dynamical properties of the axial dispersion tubular reactors with multiple steady states (Jensen and Ray, 1982; Dochain, 2018; Bildea et al., 2004).

Although in designing a controller, the stabilization of the system is investigated by the aforementioned studies, the issue of input and state constraints, which are naturally present in the process, is generally not considered for the transport-reaction systems with recycle. Hence, within the optimal framework, the model predictive control (MPC), or the so-called online receding horizon control, is introduced by control practitioners to compute the required manipulated variable for optimizing open-loop performance objective subjected to constraints (Muske and Rawlings, 1993). A significant number of contributions has been focused on properties of MPC controllers for parabolic PDEs, including spatial discretization methods, constraints validation with system performance for a class of the Riesz spectral systems with separable spectrums, pice-wise predictive feedback control and data-based modeling using repeatedly online linearization (Dufour et al., 2003; Dubljevic et al., 2006; Bonis et al., 2012).

As the implementation of MPC applications in digital computer controllers, the discrete version of the overall system is mainly required for control realizations. Over the years, for the conversion of the models or controllers into a discrete time setting, the classical methods such as explicit or implicit Euler, Runge-Kutta and etc. are

usually taken into account. It is proven from linear system theory that by increasing the sampling period, the accuracy of discretization can be degraded and leads to the mapping a stable continuous system into an unstable discrete one (Aström and Wittenmark, 1990; Kazantzis and Kravaris, 1999). This issue gets more prominent when it comes to distributed parameter systems, given by the infinite dimensional state-space control realization needs to be accounted for in the controller design. Motivated by aforementioned issues, this work explores a robust and accurate transformation of continuous linear infinite dimensional system to a discrete one by the application of Cayley-Tustin time discretization technique (Crank-Nicolson midpoint integration rule), in which the system properties and intrinsic energy of the DPS model are preserved (i.e., Hamiltonian preserving) (V.Havu and Malinen, 2007; Xu and Dubljevic, 2017). In addition, the practical realizations usually account for the output controller designs (Xie et al., 2019) due to the fact that infinite dimensional system states cannot be directly measured. Hence, the discrete observer developed in this work is based on the Cayley-Tustin method, which does not account for any model reduction or/and spatial approximation, as the discretization of the underlying operators is the usual procedure used in the literature to reconstruct the state variables given by transport-reaction processes (e.g. Dochain 2001, 2000; Mohd Ali et al. 2015; Alonso et al. 2004; Bitzer and Zeitz 2002).

In this manuscript, the claimed novelty is the extension of linear MPC designs for finite-dimensional system (Mayne, 2014; Rawlings et al., 2017) to the case of infinite-dimensional one which accounts for transport-reaction system properties considering a system of coupled parabolic PDEs which represent a non-isothermal axial dispersion tubular reactor with mass and thermal recycle flow. In addition, the proposed findings provide an insight into the dynamical properties of the system since the model of interest considers different mass and heat Peclet numbers in the spatial operators accounting for the distinction between heat and mass transport phenomena. Moreover, a different values for mass and thermal Peclet numbers lead to more complexity in model representation and prevent the analytic solution for eigenvalues and corresponding eigenfunctions. Due to the fact that one cannot realize the measurement of mass and temperature along the reactor, the discrete observer for the system of parabolic PDEs is proposed. The discrete-time observer design accounts for the available output measurement taken at the exit of the reactor (considered to be the reactor temperature) and reconstructs the system states. Finally, the controller design provides optimal stabilization of the system with the inclusion of state and input constraints, as well as input disturbance rejection in the control law.

The manuscript is organized as follows: Section 3.2 addresses the model description of the axial dispersion tubular reactor with recycle. In Section 3.3, the linearized system is derived and the system is defined in an appropriate abstract Hilbert space. This is followed by the linear system stability analysis and obtaining the relevant eigenfunctions and adjoint eigenfunctions of the system, in Section 3.4. In Section 3.5, the time discretization of the overall system is accomplished by the Cayley-Tustin technique. Then, the discrete observer design is provided in Section 3.6, while the optimization problem for a coupled unstable parabolic PDEs is presented in Section 3.7. Finally, the performance of the proposed controller is demonstrated with a simulation

study in Section 3.8.

3.2 Case study: Biochemical reactors

3.2.1 Model formulation

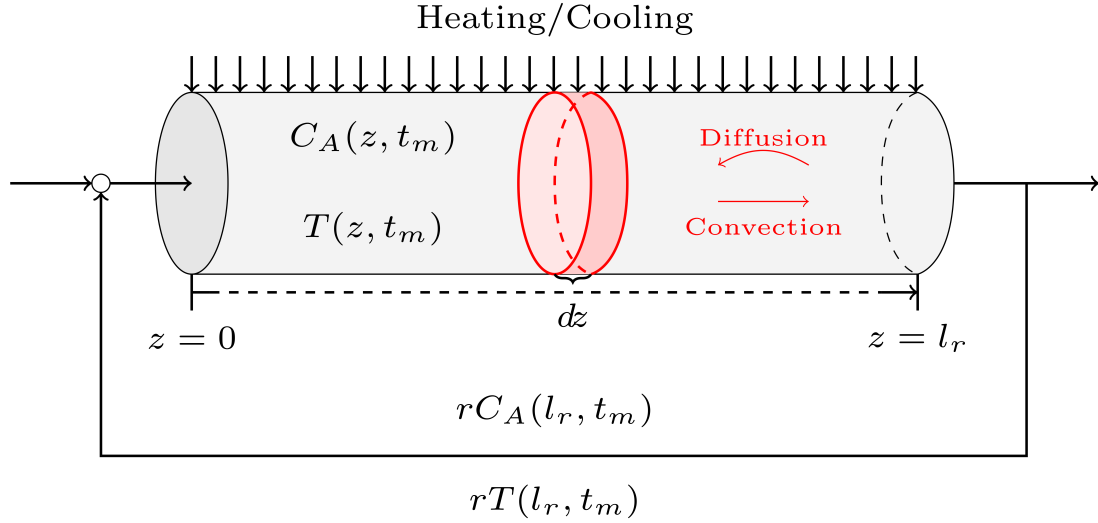


Figure 3.1: Schematic view of a non-isothermal axial dispersion tubular reactor with recycle

The chemical process shown in Fig.3.1 represents a non-isothermal tubular reactor involving convection, molecular diffusion with macroscopic back mixing (dispersion) (Levenspiel, 1999), and a first-order irreversible reaction $A \rightarrow B$, where the reaction is considered to be exothermic. After passing through a separator, the unreacted component A is recycled and fed back to the tubular reactor. The dynamics of the system can be directly deduced from energy and mass balances on a slice with infinitesimal thickness dz shown in Fig.3.1. The mentioned process is described by the class of convection-diffusion-reaction parabolic PDEs on domain $\{t_m \in \mathbb{R}^+, z \in [0, l_r]\}$ as follows (Jensen and Ray, 1982):

$$\begin{aligned} \frac{\partial C_A}{\partial t_m} &= D \frac{\partial^2 C_A}{\partial z^2} - v \frac{\partial C_A}{\partial z} - k e^{-\frac{E}{RT}} C_A \\ \frac{\partial T}{\partial t_m} &= \frac{\lambda}{\rho_f c_p} \frac{\partial^2 T}{\partial z^2} - v \frac{\partial T}{\partial z} - \frac{\Delta H_r}{\rho_f c_p} k e^{-\frac{E}{RT}} C_A + \frac{4h}{\rho C_p d_t} (T_c - T) \end{aligned} \quad (3.1)$$

assuming transport lags in the connecting lines are not significant, the associated

Danckwerts' boundary conditions (Danckwerts, 1953) are given by:

$$\begin{aligned}\frac{\partial C_A}{\partial z}\Big|_{z=0} &= \frac{v}{D} \left(C_A\Big|_{z=0} - (1-r)C_{A_{Feed}} - rC_A\Big|_{z=L} \right) \\ \frac{\partial T}{\partial z}\Big|_{z=0} &= \frac{\rho_f v c_p}{\lambda} \left(T\Big|_{z=0} - (1-r)T_{Feed} - rT\Big|_{z=L} \right) \\ \frac{\partial C_A}{\partial z}\Big|_{z=L} &= \frac{\partial T}{\partial z}\Big|_{z=L} = 0\end{aligned}\quad (3.2)$$

where the state components are $C_A(z, t_m)$ and $T(z, t_m)$ representing the concentration ($\frac{mol}{l}$) of reactant and the temperature (K) profile through the tubular reactor, respectively. $z \in [0, l_r]$ is the position (m) and $t_m \geq 0$ is the time variable (s). The parameters of the axial dispersion reactor with recycle is given in Table 3.1.

Table 3.1: Parameters of the chemical tubular reactor system used to model Eq.(3.1)

Variable	Unit	Description
l_r	m	Length of the tubular reactor
d_t	m	Diameter of the tubular reactor
R	kJ/kgK	Gas constant
λ	kJ/msK	Axial energy dispersion coefficient
v	m/s	Fluid superficial velocity
D	m^2/s	Axial mass diffusivity
T_c	K	Jacket temperature
h	kJ/m^2Ks	Heat transfer coefficient for wall
ρ_f	kg/m^3	Fluid density
C_p	kJ/kgK	Heat capacity of reacting fluid
E	kJ/kg	Activation energy
ΔH_r	kJ/kg	Heat of reaction*
r	—	Recycle ratio

* For endothermic reactions $\Delta H_r > 0$, and for exothermic reactions $\Delta H_r < 0$.

For the sake of simplicity, one can transform the aforementioned system of equations into the dimensionless form by introducing the following change of coordinates:

$$\zeta = \frac{z}{L}, \quad t = \frac{t_m v}{L} \quad (3.3)$$

As T_{Feed} and $C_{A_{Feed}}$ are considered to be constant values, the change of variables can be written as:

$$m_1 = \frac{C_{Feed} - C_A}{C_{Feed}}, \quad m_2 = \frac{T - T_{Feed}}{T_{Feed}}, \quad T_w(t) = \frac{T_c(t) - T_{Feed}}{T_{feed}} \quad (3.4)$$

by substitution, we get the following:

$$\begin{aligned}
\frac{\partial m_1}{\partial t} &= \frac{1}{Pe_m} \frac{\partial^2 m_1}{\partial \zeta^2} - \frac{\partial m_1}{\partial \zeta} + k_a (1 - m_1) e^{\left(\frac{\eta m_2}{1+m_2}\right)} \\
\frac{\partial m_2}{\partial t} &= \frac{1}{Pe_T} \frac{\partial^2 m_2}{\partial \zeta^2} - \frac{\partial m_2}{\partial \zeta} + \delta k_a (1 - m_1) e^{\left(\frac{\eta m_2}{1+m_2}\right)} + \sigma (T_w - m_2) \\
\frac{\partial m_1}{\partial \zeta} \Big|_{\zeta=0} &= Pe_m \left(m_1 \Big|_{\zeta=0} - Rm_1 \Big|_{\zeta=1} \right) \\
\frac{\partial m_2}{\partial \zeta} \Big|_{\zeta=0} &= Pe_T \left(m_2 \Big|_{\zeta=0} - Rm_2 \Big|_{\zeta=1} \right) \\
\frac{\partial m_1}{\partial \zeta} \Big|_{\zeta=1} &= \frac{\partial m_2}{\partial \zeta} \Big|_{\zeta=1} = 0
\end{aligned} \tag{3.5}$$

with

$$\begin{aligned}
Pe_m &= \frac{vL}{D}, Pe_T = \frac{\rho v C_p L}{\lambda}, k_a = \frac{kL}{v} e^{-\eta}, \\
\delta &= \frac{-\Delta H_r C_{A_{Feed}}}{\rho C_p T_{Feed}}, \eta = \frac{E}{RT_{Feed}}, \sigma = \frac{4hL}{\rho C_p v d_t}
\end{aligned}$$

Pe_m and Pe_T are defined as mass and heat Peclet numbers describing the relative significance of diffusion and convection in the chemical tubular reactor given in Fig.3.1.

3.2.2 Steady state solutions

The steady state solutions of the reaction-convection-diffusion PDEs in Eq.(3.5) can be obtained by solving the following ordinary differential equations with their associated boundary conditions:

$$\begin{aligned}
\frac{1}{Pe_m} \frac{d^2 m_{1_{ss}}}{d\zeta^2} - \frac{dm_{1_{ss}}}{d\zeta} + k_a (1 - m_{1_{ss}}) e^{\left(\frac{\eta m_{2_{ss}}}{1+m_{2_{ss}}}\right)} &= 0 \\
\frac{1}{Pe_T} \frac{d^2 m_{2_{ss}}}{d\zeta^2} - \frac{dm_{2_{ss}}}{d\zeta} + \delta k_a (1 - m_{1_{ss}}) e^{\left(\frac{\eta m_{2_{ss}}}{1+m_{2_{ss}}}\right)} + \sigma (T_{w_{ss}} - m_{2_{ss}}) &= 0 \\
\frac{dm_{1_{ss}}}{d\zeta} \Big|_{\zeta=0} &= Pe_m \left(m_{1_{ss}} \Big|_{\zeta=0} - Rm_{1_{ss}} \Big|_{\zeta=1} \right) \\
\frac{dm_{2_{ss}}}{d\zeta} \Big|_{\zeta=0} &= Pe_T \left(m_{2_{ss}} \Big|_{\zeta=0} - Rm_{2_{ss}} \Big|_{\zeta=1} \right) \\
\frac{dm_{1_{ss}}}{d\zeta} \Big|_{\zeta=1} &= \frac{dm_{2_{ss}}}{d\zeta} \Big|_{\zeta=1} = 0
\end{aligned} \tag{3.6}$$

It is well known from literature that due to the nonlinearity in kinetic term representing the interconnection of temperature and concentration, particularly for exothermic reactions, multiple steady state profiles, either stable or unstable, can be generated (Heinemann and Poore, 1982; Hastir et al., 2020). It should be emphasized that in practical applications, the operating points of interest may correspond to an unstable equilibrium profile observed by the above equations.

By considering the following parameters and using shooting method, one can identify the existence of multiple equilibrium steady state profiles as it is illustrated in

Fig.3.2:

$$Pe_m = 4, Pe_T = 6, T_{feed} = 600, T_{w_{ss}} = 380, C_{A_{feed}} = 1,$$

$$\sigma = 0.9, r = 0.3, k_a = 0.6, \delta = 0.8, \eta = 20$$

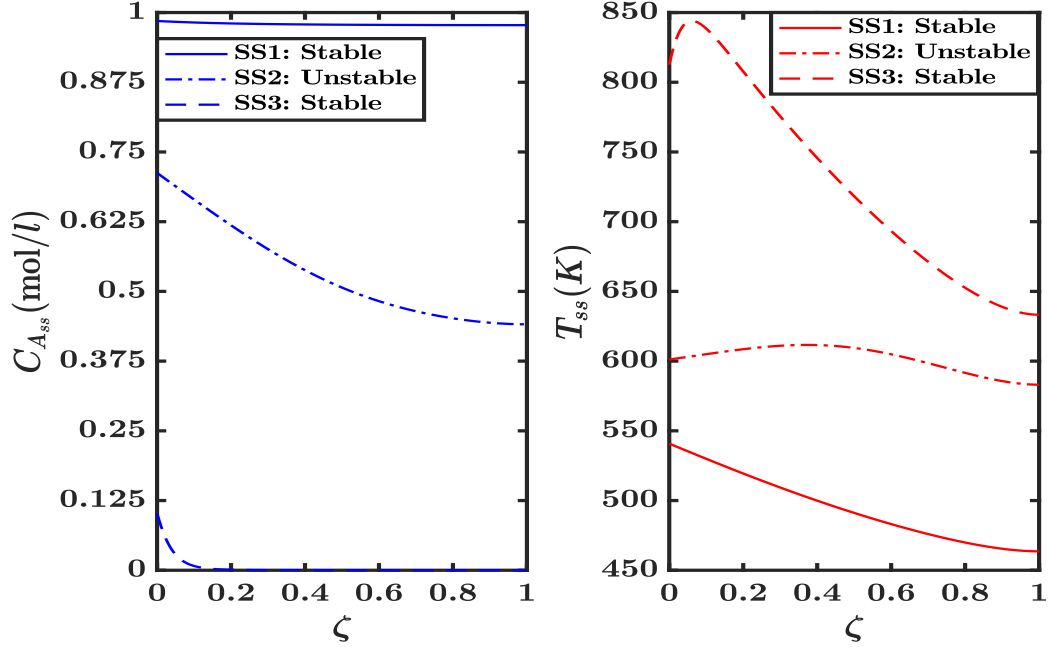


Figure 3.2: Multiple equilibrium profiles of obtained for a non-isothermal tubular reactor with recycle.

The results show that three steady state solutions are possible solutions to the system given by Eq.(3.6). The equilibrium profile of interest is the middle one between the low and high conversion profiles (represented by dash-dotted lines). As expected, this is the unstable equilibrium profile obtained by Eq.(3.6). Therefore, it is important to implement a robust and reliable controller to keep the tubular reactor working at this unstable operating points of interest. In the following sections, the stability analysis is performed and subsequently, design of the model predictive controller is addressed based on the linearized model around the unstable equilibrium profile.

3.3 Linearized model

3.3.1 System linearization

Consider the following deviation variables:

$$\begin{bmatrix} x_1(\zeta, t) = m_1(\zeta, t) - m_{1_{ss}}(\zeta) \\ x_2(\zeta, t) = m_2(\zeta, t) - m_{2_{ss}}(\zeta) \end{bmatrix} \quad (3.7)$$

we assume the cooling jacket temperature ($T_c(t)$) as the manipulated input variable and the reactor outlet temperature as the measured output of the system which is required to reconstruct the states in the subsequent observer design. Then, the new input and output can be defined as follows:

$$\begin{bmatrix} u(t) = T_w(t) - T_{w_{ss}} \\ y(t) = m_2(\zeta = 1, t) - m_{2_{ss}}(\zeta = 1) \end{bmatrix} \quad (3.8)$$

The reaction rate is linearized around its steady-state as it depends on the dimensionless concentration and temperature of the reactor:

$$\begin{aligned} f_{nl}(m_1, m_2) &= k_a(1 - m_1)e^{\frac{\eta m_2}{1 + m_2}} \approx f_{nl}(m_{1_{ss}}, m_{2_{ss}}) + \\ &R_1(m_1 - m_{1_{ss}}) + R_2(m_2 - m_{2_{ss}}), \\ g_{nl}(m_1, m_2) &= \delta k_a(1 - m_1)e^{\frac{\eta m_2}{1 + m_2}} \approx \delta g_{nl}(m_{1_{ss}}, m_{2_{ss}}) \\ &+ \delta R_1(m_1 - m_{1_{ss}}) + \delta R_2(m_2 - m_{2_{ss}}) \end{aligned} \quad (3.9)$$

with the following coefficients:

$$R_1(\zeta) = -k_a e^{\frac{\eta m_{2_{ss}}(\zeta)}{1 + m_{2_{ss}}(\zeta)}}, \quad R_2(\zeta) = \frac{\eta k_a (1 - m_{1_{ss}}(\zeta)) e^{\frac{\eta m_{2_{ss}}(\zeta)}{1 + m_{2_{ss}}(\zeta)}}}{(1 + m_{2_{ss}}(\zeta))^2}$$

where $R_1(\zeta)$, $R_2(\zeta)$, $\delta R_1(\zeta)$ and $\delta R_2(\zeta)$ are the Jacobian of the nonlinear terms. In the linearized system, we consider the spatial averaged coefficients over the space (\bar{R}_1 and \bar{R}_2), defined as below:

$$\begin{cases} \bar{R}_1 = \int_0^1 R_1(\zeta) d\zeta \\ \bar{R}_2 = \int_0^1 R_2(\zeta) d\zeta \end{cases} \quad (3.10)$$

Finally, the linearized representation of the original system in Eq.(3.5) takes the following form:

$$\begin{aligned}
\frac{\partial x_1}{\partial t} &= \frac{1}{Pe_m} \frac{\partial^2 x_1}{\partial \zeta^2} - \frac{\partial x_1}{\partial \zeta} + \bar{R}_1 x_1 + \bar{R}_2 x_2 \\
\frac{\partial x_2}{\partial t} &= \frac{1}{Pe_T} \frac{\partial^2 x_2}{\partial \zeta^2} - \frac{\partial x_2}{\partial \zeta} + \delta \bar{R}_1 x_1 + \delta \bar{R}_2 x_2 + \sigma (u(t) - x_2) \\
\frac{\partial x_1}{\partial \zeta} \Big|_{\zeta=0} &= Pe_m \left(x_1 \Big|_{\zeta=0} - r x_1 \Big|_{\zeta=1} \right) \\
\frac{\partial x_2}{\partial \zeta} \Big|_{\zeta=0} &= Pe_T \left(x_2 \Big|_{\zeta=0} - r x_2 \Big|_{\zeta=1} \right) \\
\frac{\partial x_1}{\partial \zeta} \Big|_{\zeta=1} &= \frac{\partial x_2}{\partial \zeta} \Big|_{\zeta=1} = 0, \\
y(t) &= x_2 \Big|_{\zeta=1}
\end{aligned} \tag{3.11}$$

3.3.2 Infinite-dimensional system representation

The system of coupled parabolic PDEs given by Eq.(3.11) can be rewritten as the following state space equations:

$$\begin{aligned}
\dot{x}(\zeta, t) &= Ax(\zeta, t) + Bu(t) \\
y(t) &= Cx(\zeta, t)
\end{aligned} \tag{3.12}$$

where x is the state, $x(\zeta, t) = \begin{bmatrix} x_1(\zeta, t) \\ x_2(\zeta, t) \end{bmatrix}$, and the operator A is defined as a linear operator $\mathfrak{L}(X)$ (X is defined as Hilbert space $L^2[0, 1] \times L^2[0, 1]$):

$$\begin{aligned}
A(\cdot) &= \begin{bmatrix} \frac{1}{Pe_m} \frac{\partial^2}{\partial \zeta^2} - \frac{\partial}{\partial \zeta} + \bar{R}_1 & \bar{R}_2 \\ \delta \bar{R}_1 & \frac{1}{Pe_T} \frac{\partial^2}{\partial \zeta^2} - \frac{\partial}{\partial \zeta} + \delta \bar{R}_2 - \sigma \end{bmatrix} (\cdot) \\
&= \begin{bmatrix} A_{11} & A_{12} \\ A_{21} & A_{22} \end{bmatrix} (\cdot)
\end{aligned} \tag{3.13}$$

such that $D(A) = \left\{ x = (x_1, x_2)^T \in X : x(\zeta) \in L^2[0, 1] \mid x(\zeta), \frac{dx}{d\zeta}, \frac{d^2x}{d\zeta^2} \text{ a.c.}, \frac{dx_1}{d\zeta} \Big|_{\zeta=1} = \frac{dx_2}{d\zeta} \Big|_{\zeta=1} = 0, \frac{dx_1}{d\zeta} \Big|_{\zeta=0} = Pe_m \left(x_1 \Big|_{\zeta=0} - r x_1 \Big|_{\zeta=1} \right) \text{ and } \frac{dx_2}{d\zeta} \Big|_{\zeta=0} = Pe_T \left(x_2 \Big|_{\zeta=0} - r x_2 \Big|_{\zeta=1} \right) \right\}$. Moreover, the actuation is presented as $B = \begin{bmatrix} 0 \\ \sigma \end{bmatrix}$ representing the linear input

operator $\mathfrak{L}(\mathbb{R}, X)$, and $C = \begin{bmatrix} 0 & \int_0^1 \delta(\zeta - 1)(\cdot) d\zeta \end{bmatrix}$ indicates the linear output operator providing boundary point observation in the control setting. The above system dynamics operator A has a well defined eigenvalue problem, which depends on the Peclet numbers and recycle ratio r . The solution of the eigenvalue problem provides spectral system characteristics, such as eigenvalues and associated eigenfunctions.

3.4 Linear system stability analysis ($Pe_T \neq Pe_m$)

Based on the linear system representation, it is possible to analyze the internal stability by solving the eigenvalue problem associated with the system, see Eq.(3.11). In particular, the stability assessment is performed with different settings of the Peclet numbers which is less studied in the literature (see Hastir et al. 2020), as the constant value for Peclet numbers ($Pe_T = Pe_m$) implies the assumption of same transport properties of the mass and heat flow in the axial dispersion reactor, see Antoniadou and Christofides (2000, 2001) as examples of this case.

Consequently, the eigenvalues (λ) and eigenfunctions of the operators A and A^* will be specified to access the system stability and to determine the terminal cost in the model predictive controller, which will be demonstrated in the ensuing sections.

3.4.1 Eigenvalues and eigenfunctions of the operator A

The linear system representation is utilized to analyze the internal stability of the operator A by solving the following eigenvalue problem for the unforced ($u(t) = 0$) coupled parabolic PDEs:

$$A\Phi = \lambda\Phi \quad (3.14)$$

where the operator A is defined by Eq.(3.13). Let us write the system eigenfunctions $\Phi(\zeta)$ as below:

$$\Phi(\zeta) = \begin{bmatrix} \Phi_1(\zeta) \\ \Phi_2(\zeta) \end{bmatrix} \quad (3.15)$$

by substitution in Eq.(3.14), one can get the system of second order ordinary differential equations. The system can be rewritten as $\dot{Y}(\zeta) = \bar{A}Y$, where \bar{A} is defined as a matrix with constant components of Eq.(3.11) and Y is the following vector of eigenfunctions (Φ_1, Φ_2) and the corresponding derivatives:

$$Y = \begin{bmatrix} \Phi_1 \\ \frac{d\Phi_1}{d\zeta} \\ \Phi_2 \\ \frac{d\Phi_2}{d\zeta} \end{bmatrix} \quad (3.16)$$

Hence, the solution can be expressed as below:

$$Y(\zeta) = e^{\bar{A}(\zeta-1)}Y(1) = N_{i,j}Y(1) \quad (3.17)$$

$N_{4 \times 4}(\zeta)$ is defined as the exponential matrix, with index i and j referring to the component of the matrix. Applying the boundary conditions presented in Eq.(3.14) leads to the following nonlinear equation, which is numerically solvable and gives the system's eigenvalues:

$$f(\lambda) = k_1k_4 - k_2k_3 = 0 \quad (3.18)$$

with

$$\begin{aligned}
k_1 &= Pe_m N_{1,1}^{(\zeta=0)} - N_{2,1}^{(\zeta=0)} - Pe_m r, \\
k_2 &= Pe_m N_{1,3}^{(\zeta=0)} - N_{2,3}^{(\zeta=0)}, \\
k_3 &= Pe_m N_{3,1}^{(\zeta=0)} - N_{4,1}^{(\zeta=0)}, \\
k_4 &= Pe_T N_{3,3}^{(\zeta=0)} - N_{4,3}^{(\zeta=0)} - Pe_T r
\end{aligned} \tag{3.19}$$

Remark 1. *In this work, as a system with different Peclet numbers and the Danckwerts' conditions is considered, finding the analytic solution for spectral system characteristics is not applicable in this case. Thus, the numerical solution for this equation is presented.*

The solution of Eq.(3.19) generates the eigenvalue spectrum containing the stable and unstable modes (λ_u, λ_s) associated with corresponding eigenfunctions (Φ_u, Φ_s) constructed as the function basis of the operator A in Eq.(3.13). Thus, based on Eq.(3.18), the eigenvalue problem is solved for the unstable equilibrium profile, see Fig.3.2. In addition, from Fig.3.3, it can be seen that there is only one real unstable eigenvalue generated by the coupled parabolic PDEs system with the operating conditions considered. It is interesting to explore the relative importance of the mass and heat Peclet numbers on the calculated eigenvalues of the system. Hence, by changing the value for the mass diffusivity (which is related to Pe_m) and considering the same value for Pe_T , new steady state solutions are found and, once again, the eigenvalue problem is solved for the unstable equilibrium profile. The eigenvalues distributions are presented in Fig.3.3. In this case, it is possible to see that increasing Pe_m leads to more complex eigenvalues. In Section 3.7.1, the stabilization of the system will be addressed by rejecting the unstable modes under the developed model predictive controller.

3.4.2 Eigenfunctions of the operator A^*

For any $x \in D(A)$ and $y \in D(A^*)$, one can write the following definition:

$$\langle Ax, y \rangle = \langle x, A^*y \rangle \tag{3.20}$$

employing integration by parts and substituting the boundary conditions given in Eq.(3.11), results in the following adjoint operator A^* (see Appendix C):

$$\begin{aligned}
A^*(\cdot) &= \begin{bmatrix} \frac{1}{Pe_m} \frac{\partial^2}{\partial \zeta^2} + \frac{\partial}{\partial \zeta} + \bar{R}_1 & \delta \bar{R}_1 \\ \bar{R}_2 & \frac{1}{Pe_T} \frac{\partial^2}{\partial \zeta^2} + \frac{\partial}{\partial \zeta} + \delta \bar{R}_2 - \sigma \end{bmatrix} (\cdot) \\
&= \begin{bmatrix} A_{11}^* & A_{12}^* \\ A_{21}^* & A_{22}^* \end{bmatrix} (\cdot)
\end{aligned} \tag{3.21}$$

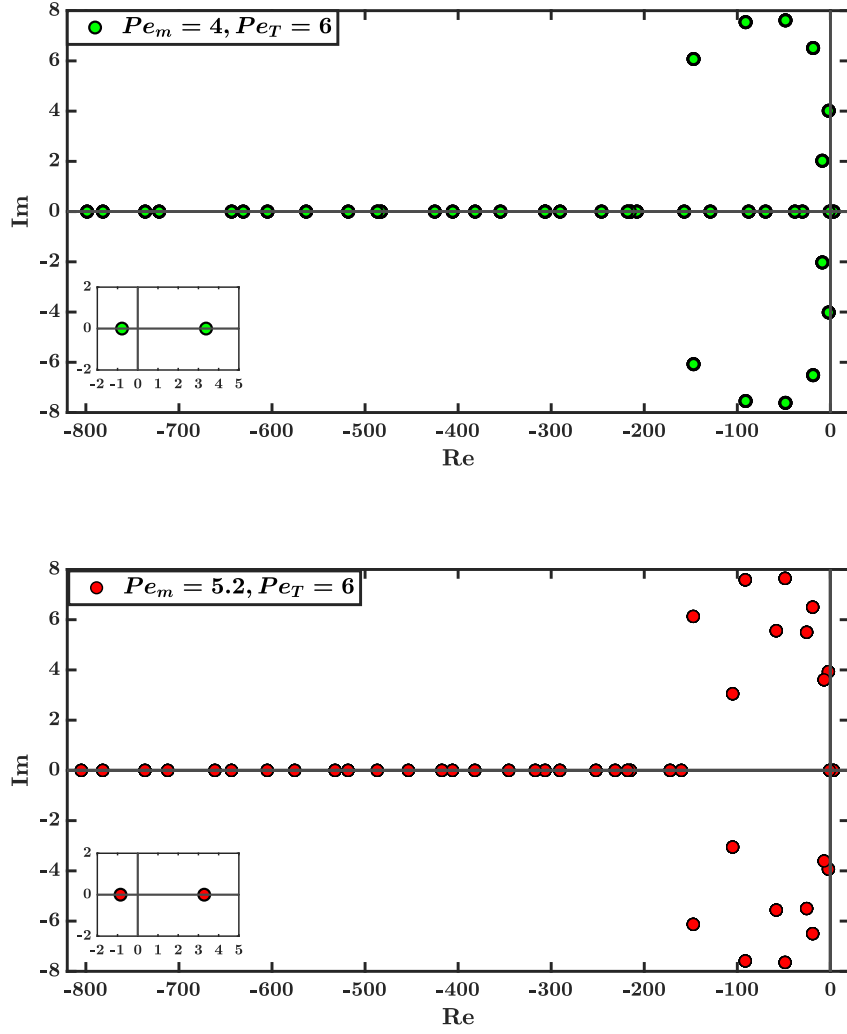


Figure 3.3: Comparison of the eigenvalue distribution with different setting for Peclet numbers.

with the new boundary condition represented as below:

$$\begin{aligned}
 \frac{\partial y_1}{\partial \zeta} \Big|_{\zeta=1} &= -Pe_m \left(y_1 \Big|_{\zeta=1} - r y_1 \Big|_{\zeta=0} \right) \\
 \frac{\partial y_2}{\partial \zeta} \Big|_{\zeta=1} &= -Pe_T \left(y_2 \Big|_{\zeta=1} - r y_2 \Big|_{\zeta=0} \right) \\
 \frac{\partial y_1}{\partial \zeta} \Big|_{\zeta=0} &= \frac{\partial y_2}{\partial \zeta} \Big|_{\zeta=0} = 0
 \end{aligned} \tag{3.22}$$

A similar procedure, as described in Section 3.4.1 is followed to compute the adjoint eigenfunction of the coupled class of parabolic PDEs. The associated eigenfunction for the adjoint operator is given by:

$$\Phi^*(\zeta) = \begin{bmatrix} \Phi_1^*(\zeta) \\ \Phi_2^*(\zeta) \end{bmatrix} \quad (3.23)$$

Finally, we define $\hat{\Phi}_m(\zeta)$ and $\hat{\Phi}_n^*(\zeta)$ as the normalized eigenfunction and corresponding bi-orthogonal ones respectively. Indeed, based on Eqs.(3.15)-(3.23) they can be constructed by:

$$\hat{\Phi}_m(\zeta) = \frac{\Phi_m(\zeta)}{\sqrt{\int_0^1 (\Phi_{1_m}(\zeta)\Phi_{1_m}^*(\zeta) + \Phi_{2_m}(\zeta)\Phi_{2_m}^*(\zeta))d\zeta}} \quad (3.24)$$

$$\hat{\Phi}_n^*(\zeta) = \frac{\Phi_n^*(\zeta)}{\sqrt{\int_0^1 (\Phi_{1_n}(\zeta)\Phi_{1_n}^*(\zeta) + \Phi_{2_n}(\zeta)\Phi_{2_n}^*(\zeta))d\zeta}}$$

where indices m, n indicate the corresponding eigenvalue of the coupled parabolic PDEs.

3.5 Cayley-Tustin time discretization

3.5.1 Discrete time representation

In this subsection, for the mentioned coupled convection-diffusion parabolic PDEs, mapping the continuous time setting to discrete one is considered by the application of the Cayley-Tustin time discretization method. Let us consider Δt as the sampling time, then by applying Crank-Nicolson time discretization to Eq.(3.12), one can get the following:

$$\frac{x(j\Delta t) - x((j-1)\Delta t)}{\Delta t} \approx A \frac{x(j\Delta t) + x((j-1)\Delta t)}{2} + Bu(j\Delta t), \quad j \geq 1 \quad (3.25)$$

$$y(j\Delta t) \approx C \frac{x(k\Delta t) + x((k-1)\Delta t)}{2} + Du(k\Delta t), \quad j \geq 1 \quad (3.26)$$

Next, we consider $u(j\Delta t)/\sqrt{\Delta t}$ as the approximation of $u(j\Delta t)$, and the convergence of $u(j\Delta t)/\sqrt{\Delta t}$ to $u(j\Delta t)$ as $\Delta t \rightarrow 0$ can be verified in several ways, similarly for $y(j\Delta t)$, see V.Havu and Malinen (2007). Accordingly, the following finite dimensional discrete time dynamics can be achieved which is known as Tustin transform (Franklin et al., 1998) in digital control framework:

$$\frac{x(j\Delta t) - x((j-1)\Delta t)}{\Delta t} \approx A \frac{x(j\Delta t) + x((j-1)\Delta t)}{2} + B \frac{u(j\Delta t)}{\sqrt{\Delta t}}, \quad j \geq 1 \quad (3.27)$$

$$\frac{y(j\Delta t)}{\sqrt{\Delta t}} \approx C \frac{x(j\Delta t) + x((j-1)\Delta t)}{2} + D \frac{u(j\Delta t)}{\sqrt{\Delta t}}, \quad j \geq 1 \quad (3.28)$$

By simple manipulation, and assuming piecewise constant input within time intervals, the discrete time counter part of Eqs.(3.12) takes the following form:

$$\begin{aligned} x(\zeta, k) &= A_d x(\zeta, k-1) + B_d u(k) \\ y(k) &= C_d x(\zeta, k-1) + D_d u(k) \end{aligned} \quad (3.29)$$

with $\alpha = 2/\Delta t$ and the discrete spatial operators (A_d, B_d, C_d, D_d) given as:

$$\begin{bmatrix} A_d & B_d \\ C_d & D_d \end{bmatrix} = \begin{bmatrix} -I + 2\alpha [\alpha I - A]^{-1} & \sqrt{2\alpha} [\alpha I - A]^{-1} B \\ \sqrt{2\alpha} C [\alpha I - A]^{-1} & C [\alpha I - A]^{-1} B \end{bmatrix} \quad (3.30)$$

$\mathfrak{R}(s, A) = (sI - A)^{-1}$ and $(sI - A)^{-1} B = \mathfrak{R}(s, A) B$ are defined as the resolvent operators for A and B , respectively. In the above expression, it is important to emphasize that the original model expressed by Eq.(3.12) does not have feedthrough operator while the discrete system Eq.(3.29) poses a well-defined feedthrough operator which is realized as transfer function, $D_d = G(\alpha) = C [\alpha - A]^{-1} B$, and includes one to one relation between continuous and discrete setting (V.Havu and Malinen, 2007; Xu and Dubljevic, 2017). The physically realizable distributed parameter systems generally do not contain feedforward operator ($D = 0$). This implies $G(\alpha)$ is strictly proper and do not involve instantaneous transfer from the input signal to the output one, such that $G(\alpha)$ is defined as a function evaluated at $s = \alpha$.

Remark 2. *The Crank-Nicolson is a type of discretization scheme derived from the implicit midpoint rule and preserves the system dynamical properties (stability, observability and controllability). This method of discretization is also referred to as the lowest order symplectic integration algorithm in Gauss quadrature based Runge-Kutta methods (Hairer et al., 2006).*

3.5.2 Resolvents and discrete operators

The resolvent operator $\mathfrak{R}(s, A) = (sI - A)^{-1}$ of the operator A can be obtained by considering the system with a zero input condition which yields:

$$\mathfrak{R}(s, A)(\cdot) = \begin{bmatrix} \mathfrak{R}_{11} & \mathfrak{R}_{12} \\ \mathfrak{R}_{21} & \mathfrak{R}_{22} \end{bmatrix} \begin{bmatrix} (\cdot)_1 \\ (\cdot)_2 \end{bmatrix} \quad (3.31)$$

Proof. All the resolvent operators can be directly found by applying Laplace transform to the class of parabolic PDEs described by Eq.(3.11):

$$\frac{\partial}{\partial \zeta} \underbrace{\begin{bmatrix} x_1(\zeta, s) \\ \frac{\partial x_1(\zeta, s)}{\partial \zeta} \\ x_2(\zeta, s) \\ \frac{\partial x_2(\zeta, s)}{\partial \zeta} \end{bmatrix}}_{X(\zeta, s)} = \underbrace{\begin{bmatrix} 0 \\ -Pe_m x_1(\zeta, 0) \\ 0 \\ -Pe_T x_2(\zeta, 0) \end{bmatrix}}_{Z_1(\zeta, 0)} + \underbrace{\begin{bmatrix} 0 \\ 0 \\ 0 \\ -Pe_T \sigma u(s) \end{bmatrix}}_{Z_2(s)} \quad (3.32)$$

$$+ \underbrace{\begin{bmatrix} 0 & 1 & 0 & 0 \\ Pe_m(s - \bar{R}_1) & Pe_m & -Pe_m\bar{R}_2 & 0 \\ 0 & 0 & 0 & 1 \\ -Pe_T\delta\bar{R}_1 & 0 & Pe_T(s - \delta\bar{R}_2 + \sigma) & Pe_T \end{bmatrix}}_P \begin{bmatrix} x_1(\zeta, s) \\ \frac{\partial x_1(\zeta, s)}{\partial \zeta} \\ x_2(\zeta, s) \\ \frac{\partial x_2(\zeta, s)}{\partial \zeta} \end{bmatrix}$$

since the matrix P includes constant variables, one can obtain the general solution as:

$$X(\zeta, s) = TX(0, s) + \int_0^\zeta FZ_1(\eta, 0)d\eta + \int_0^\zeta FZ_2(s)d\eta \quad (3.33)$$

which is the solution of the ODE given by Eq.(3.32). T and F are defined as 4×4 matrices, representing the exponential matrices $e^{P\zeta}$ and $e^{P(\zeta-\eta)}$, respectively. After some manipulation, the desired resolvent operator can be expressed as $\mathfrak{R}(s, A)(\cdot) = (sI - A)^{-1}(\cdot)$ involving four components, \mathfrak{R}_{11} , \mathfrak{R}_{12} , \mathfrak{R}_{21} and \mathfrak{R}_{22} based on the operators A_{11} , A_{12} , A_{21} and A_{22} (see Appendix D.1 for the details). \square

Based on the discrete operators defined in the previous section and the resolvent in Eq.(3.31), the operator A_d can be written as the following convenient form:

$$A_d(\cdot) = - \begin{bmatrix} (\cdot)_1 \\ (\cdot)_2 \end{bmatrix} + 2\alpha \begin{bmatrix} \mathfrak{R}_{11} & \mathfrak{R}_{12} \\ \mathfrak{R}_{21} & \mathfrak{R}_{22} \end{bmatrix} \begin{bmatrix} (\cdot)_1 \\ (\cdot)_2 \end{bmatrix} \quad (3.34)$$

Similarly, one can obtain the operator B_d by using the resolvent operator $\mathfrak{R}(s, A)B = (sI - A)^{-1}B$ which can be computed by imposing zero initial condition ($X(\zeta = 0, s) = 0$) in Eq.(3.32). This leads to the following expression (see Appendix D.1):

$$B_d = \sqrt{2\alpha}\mathfrak{R}(\alpha, A)B = \begin{bmatrix} \mathfrak{R}_1 B \\ \mathfrak{R}_2 B \end{bmatrix} \quad (3.35)$$

According to Eq.(3.30) and the definition of the operators B and C presented in Section 3.3.2, the discrete operators C_d and D_d can be expressed as:

$$C_d(\cdot) = \sqrt{2\alpha}C\mathfrak{R}(\alpha, A)(\cdot) = \begin{bmatrix} \mathfrak{R}_{21}|_{\zeta=1} & \mathfrak{R}_{22}|_{\zeta=1} \end{bmatrix} \begin{bmatrix} (\cdot)_1 \\ (\cdot)_2 \end{bmatrix}, \quad (3.36)$$

$$D_d = C\mathfrak{R}(\alpha, A)B = (\mathfrak{R}_2 B)|_{\zeta=1}$$

3.5.3 Resolvents of the adjoints and corresponding discrete operators

In order to design the model predictive control, the adjoint operators (A_d^* , B_d^*) are required as well in the controller design. Hence, in a similar manner described in the previous subsection, the expressions for the corresponding adjoint resolvent operators

can be found by applying Laplace transform on the adjoint system given by Eq.(3.21) and Eq.(3.22):

$$\mathfrak{R}(\alpha, A^*)(\cdot) = \begin{bmatrix} \mathfrak{R}_{11}^* & \mathfrak{R}_{12}^* \\ \mathfrak{R}_{21}^* & \mathfrak{R}_{22}^* \end{bmatrix} \begin{bmatrix} (\cdot)_1 \\ (\cdot)_2 \end{bmatrix} \quad (3.37)$$

This yields the final form of the operator A_d^* given by:

$$A_d^*(\cdot) = - \begin{bmatrix} (\cdot)_1 \\ (\cdot)_2 \end{bmatrix} + 2\alpha \begin{bmatrix} \mathfrak{R}_{11}^* & \mathfrak{R}_{12}^* \\ \mathfrak{R}_{21}^* & \mathfrak{R}_{22}^* \end{bmatrix} \begin{bmatrix} (\cdot)_1 \\ (\cdot)_2 \end{bmatrix} \quad (3.38)$$

and one can construct the discrete operator B_d^* as below:

$$B_d^*(\cdot) = \sqrt{2\alpha}(\mathfrak{R}(\alpha, A)B)^*(\cdot) = \begin{bmatrix} (\mathfrak{R}_1 B)^* \\ (\mathfrak{R}_2 B)^* \end{bmatrix}^T \begin{bmatrix} (\cdot)_1 \\ (\cdot)_2 \end{bmatrix} \quad (3.39)$$

All the expressions of the resolvent components are provided in Appendix D.2.

3.6 Observer design for a coupled parabolic PDEs

To address the issue of having access to all the state variables, the discrete output observer is considered in this work. The Luenberger observer is one of the practical and easy to realize observers which is considered in a discrete modern controller realizations. However, the discrete operators cannot be directly used in the design of observer gains in discrete-time setting. Therefore, design is performed first in the continuous time setting. Then, the discrete observer gain is obtained from the continuous one by utilizing Cayley-Tustin discretization scheme and link between the gains obtained in continuous and discrete setting.

3.6.1 Design for continuous-time observer

For the state reconstruction of the transport distributed parameter systems, particularly for the class of diffusion-convection-reaction parabolic PDEs, one can consider the following general representation without the feedforward term (i.e., D):

$$\begin{aligned} \dot{x}(\zeta, t) &= Ax(\zeta, t) + Bu(t) \\ y(t) &= Cx(\zeta, t) \end{aligned} \quad (3.40)$$

and the Luenberger observer can be presented by the following standard form:

$$\begin{aligned} \dot{\hat{x}}(\zeta, t) &= A\hat{x}(\zeta, t) + Bu(t) + L_T[y(t) - \hat{y}(t)] \\ \hat{y}(t) &= C\hat{x}(\zeta, t) \end{aligned} \quad (3.41)$$

where the reconstructed state $\hat{x}(\zeta, t)$ is defined as a copy of the system dynamics and considers the output of the plant provided in affine manner. By subtracting Eq.(3.41)

from its general form Eq.(3.40) and defining observer error by $\hat{e}(\zeta, t) = x(\zeta, t) - \hat{x}(\zeta, t)$, yields the below expression:

$$\dot{\hat{e}}(\zeta, t) = (A - L_T C)\hat{e}(t) = A_o \hat{e}(\zeta, t) \quad (3.42)$$

the above design relies on choosing the appropriate spatially varying gain $L_T(\zeta) = \begin{bmatrix} L_1(\zeta) \\ L_2(\zeta) \end{bmatrix}$ such that the operator A_o in the state estimation error dynamics given by Eq.(3.42) is stable. Therefore, to ensure the stability of the observer, one can analyze the corresponding eigenvalues of Eq.(3.42):

$$A_o \phi_o = \lambda_o \phi_o \quad (3.43)$$

By the same method explained in Section 3.4, after imposing the boundary conditions, the eigenvalue problem for the operator A_o leads to a set of numerically solvable nonlinear equations. The design objective is to determine the observer region of stability by considering the proper value for the observer gain which is achieved by ensuring that all eigenvalues have negative real parts. Hence, one can consider various spatial functions $L_T(\zeta)$ in order to guarantee that eigenvalue problem in Eq.3.43 provides stable error dynamics. Subsequently, once the observer gain is determined one needs to link this spatial gain to the corresponding discrete gain $L_d(\zeta)$. The link between the continuous and discrete observer gain is provided in ensuing section.

3.6.2 Design for discrete-time observer

A discrete version of the observer, similar to the discrete version of the plant model, is constructed as follows:

$$\begin{aligned} \hat{x}(\zeta, k) &= A_d \hat{x}(\zeta, k-1) + B_d u(k) + L_d [y(k) - \hat{y}(k)] \\ \hat{y}(k) &= C_{d_o} \hat{x}(\zeta, k-1) + D_{d_o} u(k) + M_{d_o} y(k) \end{aligned} \quad (3.44)$$

where A_d and B_d have been defined in Eq.(3.30). The other discrete operators, (C_{d_o} , D_{d_o} , L_d , M_{d_o}), are given as:

$$\begin{aligned} C_{d_o}(\cdot) &= \sqrt{2\alpha} [I + C(\alpha I - A)L_T]^{-1} C [\alpha I - A]^{-1}(\cdot) \\ D_{d_o} &= [I + C(\alpha I - A)L_T]^{-1} C [\alpha I - A]^{-1} B \\ M_{d_o} &= (I + C(\alpha I - A)^{-1} L_T)^{-1} C(\alpha I - A)^{-1} L_T \\ L_d &= \sqrt{2\alpha} [\alpha I - A]^{-1} L_T \end{aligned} \quad (3.45)$$

notice that L_d has similar structure to B_d , as y_k can be determined as an input to the observer.

Lemma 1. *If the continuous observer gain (L_T) is chosen such that (A_o) is stable, then the discrete version of the observer in Eq.(3.44) is stable as well. In other words, the Cayley-Tustin time discretization will preserve the system properties.*

Proof. In order to show the states constructed by observer will converge to the system state, one can realize the discrete observer error dynamics as:

$$\hat{e}_d(\zeta, k) = x(\zeta, k) - \hat{x}(\zeta, k) \quad (3.46)$$

and by some algebraic manipulation (see Appendix F), the relation between discrete and continuous setting is obtained and leads to the following form of the discrete error:

$$\hat{e}_d(\zeta, k) = (A_d - L_d C_d) \hat{e}_d(\zeta, k - 1) = (-I + 2[\alpha I - A + L_T C]^{-1}) \hat{e}_d(\zeta, k - 1) \quad (3.47)$$

□

where $(-I + 2[\alpha I - A + L_T C]^{-1})$ is the discrete representation of $A_o = (A - L_T C)$. Thus, if the continuous observer gain (L_T) is chosen such that (A_o) is stable, then the proposed discrete observer is able to reconstruct the states, as A_o generates a stable discrete representation if the Cayley-Tustin time discretization is applied.

It should be mentioned that the presented methodology does not involve any model reduction associated with the discrete Luenberger observer design, and no spatial approximation has been considered compared to the spatial discretization schemes mainly used in the literature, see Dochain (2001, 2000); Mohd Ali et al. (2015); Alonso et al. (2004); Bitzer and Zeitz (2002).

3.7 Model predictive control for unstable coupled parabolic PDEs

This section addresses the design of the proposed model predictive controller for the coupled parabolic PDEs. The discrete-time model dynamics with eigenfunctions of the system are used to find the solution of the optimization problem.

3.7.1 Optimization problem

In this subsection, based on the scheme given in Fig.3.4, the MPC design is developed for the infinite dimensional setting. As can be seen, the full state feedback is used by the MPC scheme, which is going to be estimated by the observer. The design of the regulator is emerged from the finite dimensional linear time invariant systems, see Rawlings et al. (2017).

Here, the following open-loop objective function is utilized as a foundation of a controller design providing minimization at each sampling time (k):

$$\min_{u^N} \sum_{l=0}^{\infty} \langle \hat{x}(\zeta, k + l|k), Q \hat{x}(\zeta, k + l|k) \rangle + \langle u(k + l + 1|k), F u(k + l + 1|k) \rangle$$

$$\begin{aligned} \text{s.t. } & \hat{x}(\zeta, k + l|k) = A_d \hat{x}(\zeta, k + l - 1|k) + B_d u(k + l|k), \\ & u^{\min} \leq u(k + l|k) \leq u^{\max}, \\ & \hat{x}^{\min} \leq \hat{x}(\zeta = \zeta_c, k + l|k) \leq \hat{x}^{\max}, \\ & \langle \hat{x}(\zeta, k + N), \hat{\Phi}_u \rangle = 0 \end{aligned}$$

(3.48)

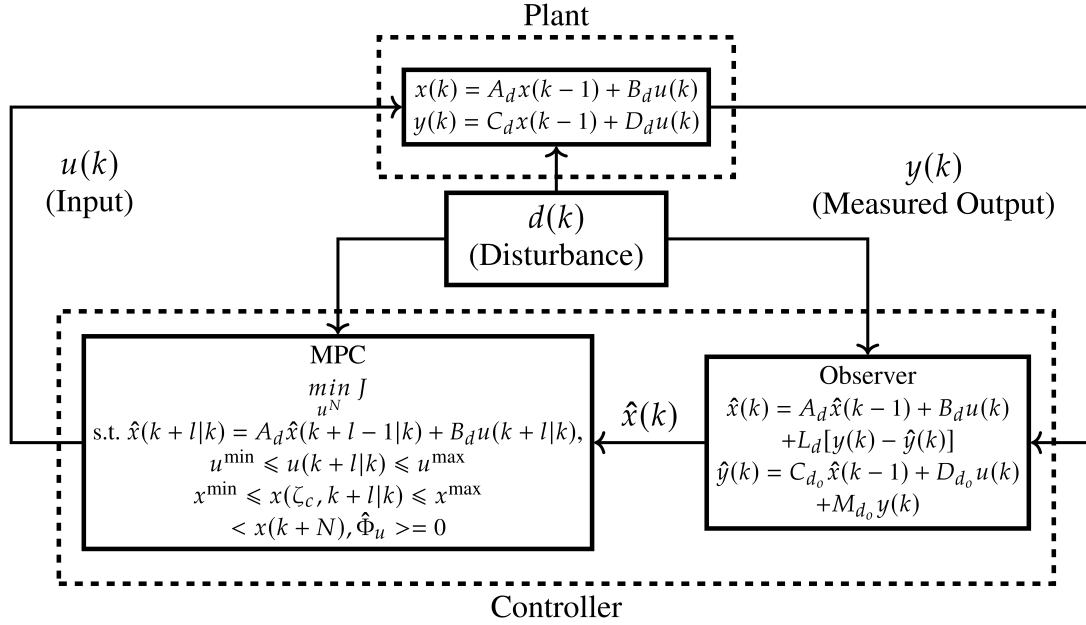


Figure 3.4: Scheme of the model predictive controller used for the non-isothermal axial dispersion tubular reactor with recycle

where $\hat{x}(\zeta, k) = [\hat{x}_1(\zeta, k) \quad \hat{x}_2(\zeta, k)]^T$ indicates the state variables of the system, F is a positive definite operator, $Q = \begin{bmatrix} Q_1(\zeta) & 0 \\ 0 & Q_2(\zeta) \end{bmatrix}$ responsible for positive semidefinite spatial operator associated with the state of coupled parabolic PDEs, $(k+l)$ and $(k+l+1|k)$ are considered for current and future time, respectively. By assigning zero-input beyond the control horizon ($u(k \geq N+1|k) = 0$), the aforementioned infinite horizon objective function can be cast as the the following finite horizon version (i.e, N-horizon length):

$$\begin{aligned} \min_{u^N} J &= \sum_{l=0}^{N-1} \langle \hat{x}(\zeta, k+l|k), Q \hat{x}(\zeta, k+l|k) \rangle \\ &+ \langle u(k+l+1|k), F u(k+l+1|k) \rangle + \langle \hat{x}(\zeta, k+N|k), \bar{Q} \hat{x}(\zeta, k+N|k) \rangle \\ \text{s.t. } &\hat{x}(\zeta, k+l|k) = A_d \hat{x}(\zeta, k+l-1|k) + B_d u(k+l|k), \\ &u^{\min} \leq u(k+l|k) \leq u^{\max}, \\ &\hat{x}^{\min} \leq \hat{x}(\zeta = \zeta_c, k+l|k) \leq \hat{x}^{\max}, \\ &\langle \hat{x}(\zeta, k+N), \hat{\Phi}_u \rangle = 0 \end{aligned} \quad (3.49)$$

where \bar{Q} is obtained as the following terminal cost operator for the system of coupled parabolic PDEs (see Appendix E):

$$\bar{Q}(\cdot) = \sum_{m=0}^{\infty} \sum_{n=0}^{\infty} \frac{-\langle C \hat{\Phi}_m, Q C \hat{\Psi}_n \rangle}{\lambda_m + \lambda_n} \langle (\cdot), \hat{\Psi}_n \rangle \hat{\Phi}_m \quad (3.50)$$

Regarding the equality constraint ($\langle \hat{x}(\zeta, k + N), \hat{\Phi}_u \rangle = 0$), the following equation needs to be integrated in the convex optimization problem presented by Eq.(3.49):

$$\begin{aligned} & \left[\langle A_d^{N-1} B_d, \hat{\Phi}_u \rangle \quad \langle A_d^{N-2} B_d, \hat{\Phi}_u \rangle \quad \dots \quad \langle B_d, \hat{\Phi}_u \rangle \right] U \\ & = - \langle A_d^N \hat{x}(\zeta, k|k), \hat{\Phi}_u \rangle \end{aligned} \quad (3.51)$$

where $\hat{\Phi}_u$ is described as the relevant normalized unstable eigenfunctions associated with positive eigenvalues. Therefore, with feasible input sequence given by optimization problem, the equality constraint is satisfied and the unstable modes will be canceled at the end of the horizon.

By straightforward algebraic manipulation, one can express the objective function in Eq.(3.49) as the following quadratic optimization form:

$$\min_U J = 2U^T \langle I, P\hat{x}(\zeta, k|k) \rangle + U^T \langle I, H \rangle U + \langle \hat{x}(\zeta, k|k), \bar{Q}\hat{x}(\zeta, k|k) \rangle \quad (3.52a)$$

which is subjected to the following constraints:

$$\begin{aligned} U^{\min} & \leq U \leq U^{\max} \\ \hat{x}^{\min} & \leq [SU + T\hat{x}(\zeta, k|k)] \Big|_{\zeta=\zeta_c} \leq \hat{x}^{\max} \\ S_u U + T_u \hat{x}(\zeta, k|k) & = 0 \end{aligned} \quad (3.52b)$$

with:

$$H = \begin{bmatrix} B_d^* \bar{Q} B_d + F & B_d^* A_d^* \bar{Q} B_d & \dots & B_d^* A_d^{*N-1} \bar{Q} B_d \\ B_d^* \bar{Q} A_d B_d & B_d^* \bar{Q} B_d + F & \dots & B_d^* A_d^{*N-2} \bar{Q} B_d \\ \vdots & \vdots & \ddots & \vdots \\ B_d^* \bar{Q} A_d^{N-1} B_d & B_d^* \bar{Q} A_d^{N-2} B_d & \dots & B_d^* \bar{Q} B_d + F \end{bmatrix}, \quad (3.53)$$

$$P = \begin{bmatrix} B_d^* \bar{Q} A_d \\ B_d^* \bar{Q} A_d^2 \\ \vdots \\ B_d^* \bar{Q} A_d^N \end{bmatrix}, \quad T = \begin{bmatrix} A_d \\ A_d^2 \\ \vdots \\ A_d^N \end{bmatrix}, \quad S = \begin{bmatrix} B_d & 0 & \dots & 0 \\ A_d B_d & B_d & \dots & 0 \\ \vdots & \vdots & \ddots & \vdots \\ A_d^{N-1} B_d & A_d^{N-2} B_d & \dots & B_d \end{bmatrix},$$

$$T_u = [A_d], \quad S_u = [A_d^{N-1} B_d \quad A_d^{N-2} B_d \quad \dots \quad B_d],$$

$$U = [u(k+1|k) \quad u(k+2|k) \quad u(k+3|k) \quad \dots \quad u(k+N|k)]^T$$

The above standard formulation of the quadratic optimization problem leads to finite-dimensional quadratic programming with linear constraints. If feasible, then the constraints and optimality are fulfilled while the controller ensures the system stabilization.

3.7.2 Input disturbance rejection

In the chemical plant demonstrated in Fig.3.1, heating/cooling jacket may involve possible temperature disturbance. To deal with this issue, in this subsection we implement the disturbance rejection based on the optimization problem discussed earlier. The axial dispersion tubular reactor system with recycle is a coupled parabolic PDEs system, which can be rewritten as:

$$\begin{aligned} \dot{x}(\zeta, t) &= Ax(\zeta, t) + B\tilde{u}(t) \\ y(t) &= Cx(\zeta, t) \end{aligned} \quad (3.54)$$

where $\tilde{u}(k)$ defined as the input variable with possible disturbance and given by

$$\tilde{u}(t) = u(t) + d(t) \quad (3.55)$$

Then, the reformulated discrete version of the plant can be written as below:

$$\begin{aligned} x(\zeta, k) &= A_d x(\zeta, k-1) + B_d \tilde{u}(k) \\ y(k) &= C_d x(\zeta, k-1) + D_d \tilde{u}(k) \end{aligned} \quad (3.56)$$

Based on the optimization problem given by Eq.(3.48), in a similar manner and by substitution input $u(k)$ with aforementioned manipulated variable $\tilde{u}(k)$, one can obtain the following new quadratic form of the objective function:

$$\begin{aligned} \min_U \quad & J = 2U^T [\langle I, P\hat{x}(\zeta, k|k) \rangle + \langle I, FG \rangle] + U^T \langle I, H \rangle U \\ & + \langle \hat{x}(\zeta, k|k), Q\hat{x}(\zeta, k|k) \rangle + \langle G, FG \rangle \\ \text{s.t.} \quad & U^{\min} \leq U + G \leq U^{\max} \\ & \hat{x}^{\min} \leq [S(U + G) + T\hat{x}(\zeta, k|k)] \Big|_{\zeta=\zeta_c} \leq \hat{x}^{\max} \\ & S_u(U + G) + T_u\hat{x}(\zeta, k|k) = 0 \end{aligned} \quad (3.57)$$

where U and the operators H , P , T , T_u , S and S_u have been defined previously. G is defined as below:

$$G = \begin{bmatrix} d(k+1|k) & d(k+2|k) & d(k+3|k) & \dots & d(k+N|k) \end{bmatrix}^T \quad (3.58)$$

Therefore, with feasible input, the proposed constrained optimization problem can also be accounted for input disturbance rejection.

3.8 Simulation results

This section is dedicated to the implementation of the model predictive controller for the axial dispersion tubular reactor with recycle, see the scheme in Fig.3.4. The particular choice of parameters given by Table 3.2 leads to three equilibria for the system as shown in Fig.3.2. The outer two profiles are stable, while the middle one is unstable

and will be considered in the simulation study. Based on the model predictive control designed in Section 3.7, our objective is to stabilize the system while complying with input/state constraints. The developed controller can also address the issue of having possible known input disturbance in the system. Due to the construction of the optimization problem, as discussed in Section 3.4, one can perform the eigenvalue problem to calculate the eigenvalues, eigenfunctions and adjoint eigenfunctions for the unstable coupled parabolic PDEs system.

Table 3.2: Values of the parameters used in numerical simulations

Variable	Value	Unit
Pe_m	4	—
Pe_T	6	—
k_a	0.6	—
δ	0.8	—
σ	0.9	—
r	0.3	—
η	20	—
T_{Feed}	600	K
$C_{A_{Feed}}$	1	$\frac{mol}{l}$
$T_{w_{ss}}$	380	K

Based on Fig.3.4, the discrete observer is considered in the close-loop setting. As discussed in Section 3.6, the stability of the observer is evaluated by the analysis of observer error dynamics. Thus, the corresponding eigenvalue problem in Eq.(3.43) is studied for increasing values of the observer gains. Two cases are investigated: one provides a constant value for the observer gain in the entire spatial domain (L); the other considers a linear spatially varying function ($L(\zeta) = L\zeta$) for the mentioned observer gain. In general, one can propose different types of the spatial functions $L(\zeta)$ and calculate the region of stability by considering Eq.(3.43).

Subsequently, in order to have a better realization of the proposed design, the most positive eigenvalue for each gain is extracted and shown in Fig.3.5. From Fig.3.5, it can be seen that, for the case with $L_1(\zeta) = L_2(\zeta) = L$, as the value of the gain is increased, the unstable eigenvalue is shifted to the left side of the complex plain, while at the same time increasing gain leads to the shift of the stable pair of the eigenvalues to the right half plane, making the observer error dynamics unstable again. Hence, the stability region for this observer design refers to $1.20 \leq L \leq 1.70$ and $12.60 \leq L \leq 35$, while for the second case, the desired stability region is $7.85 \leq L \leq 35$.

We show simulation studies of observer for a model of an axial dispersion tubular reactor with recycle. The gain $L = 24$ is chosen as the constant observer gain in the whole spatial domain and the related discrete version is computed based on Eq.(3.45). Considering zero initial condition for the observer dynamics, the equivalent discrete error dynamic written in Eq.(3.47) is evaluated and shown in Fig.3.6. It can be confirmed that the error dynamics is decaying exponentially such that the stability of

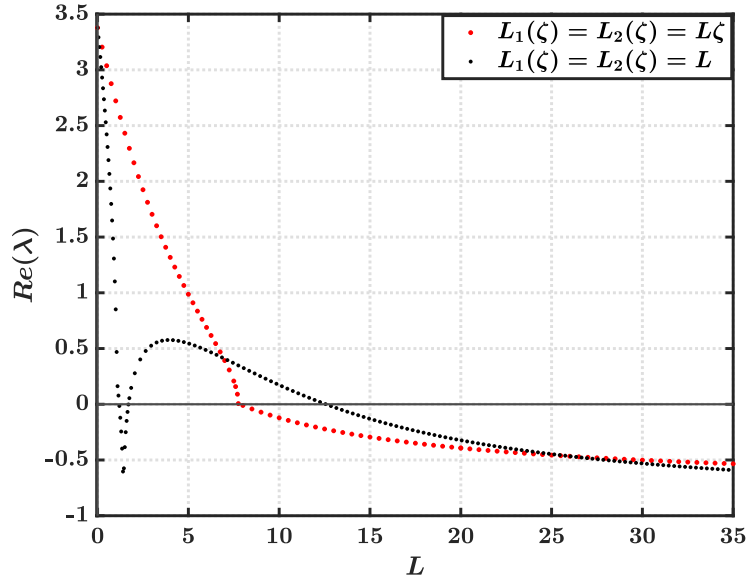


Figure 3.5: Transition of the unstable eigenvalue to stable one by increasing the values for L .

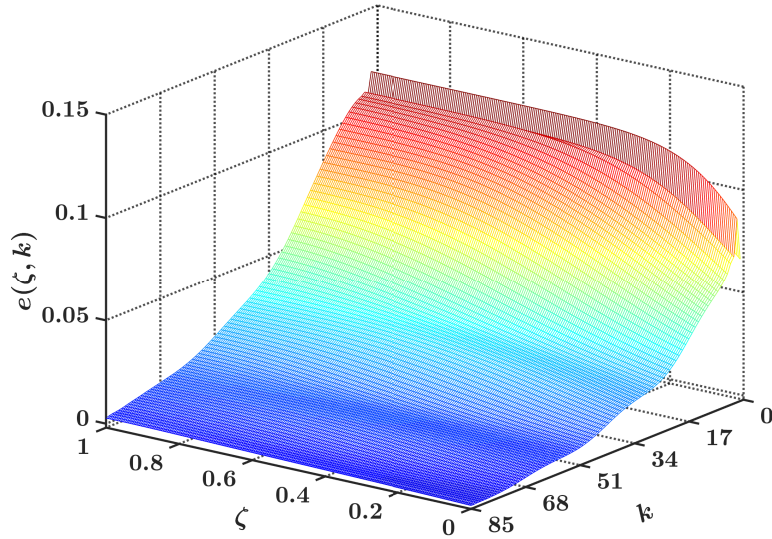
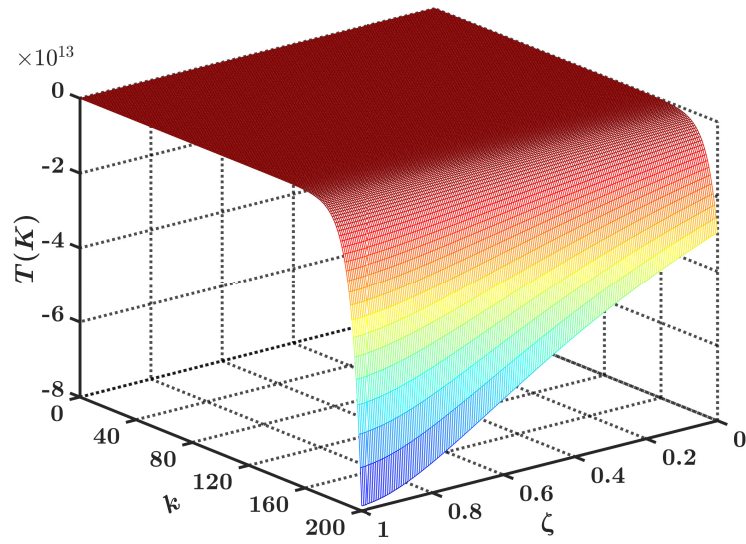


Figure 3.6: Discrete error dynamics given by Eq.(3.47) for $L = 24$.

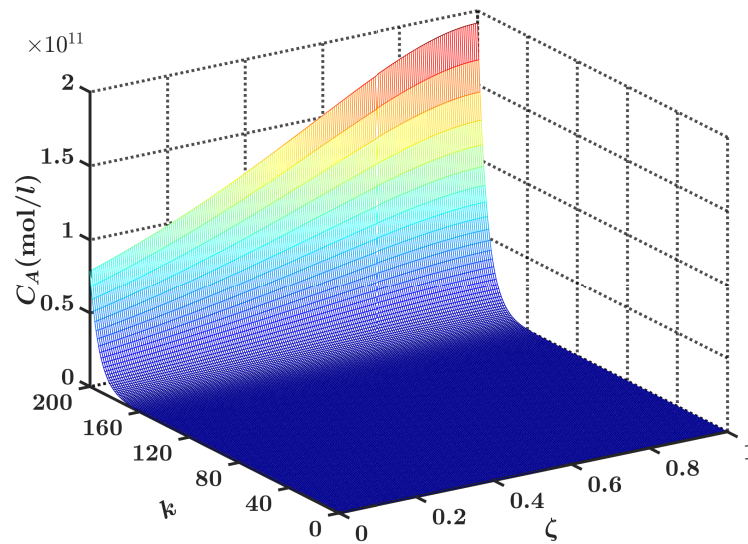
the observer is guaranteed.

Based on the developed observer, one can use Eq.(3.44) to obtain the reconstructed states in the discrete-time setting for both temperature and concentration through the dispersive tubular reactor. In numerical simulation, $x_0(\zeta)$ belongs to the domain of A , $\Delta t = 0.04$ which implies $\alpha = 50$ and $\Delta z = 0.005$ for numerical integration.

Next, the normalized eigenfunctions of the system with corresponding biorthonormal ones are used to determine the terminal cost operator presented in Eq.(3.50). The



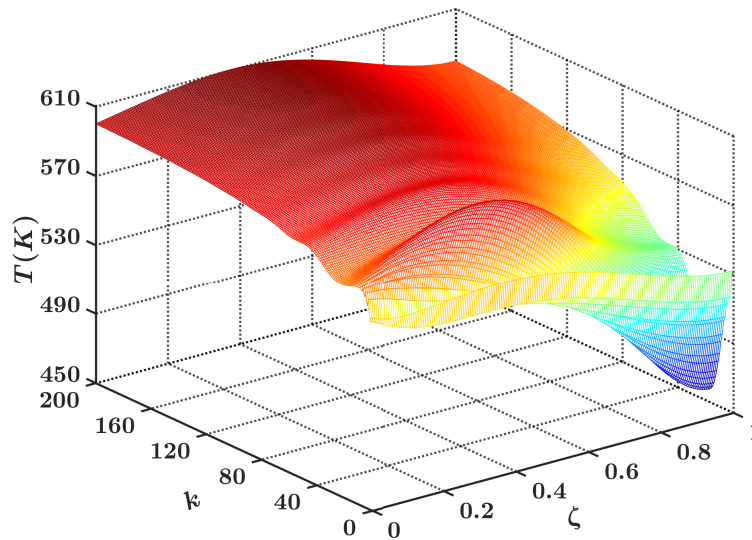
(a) Temperature



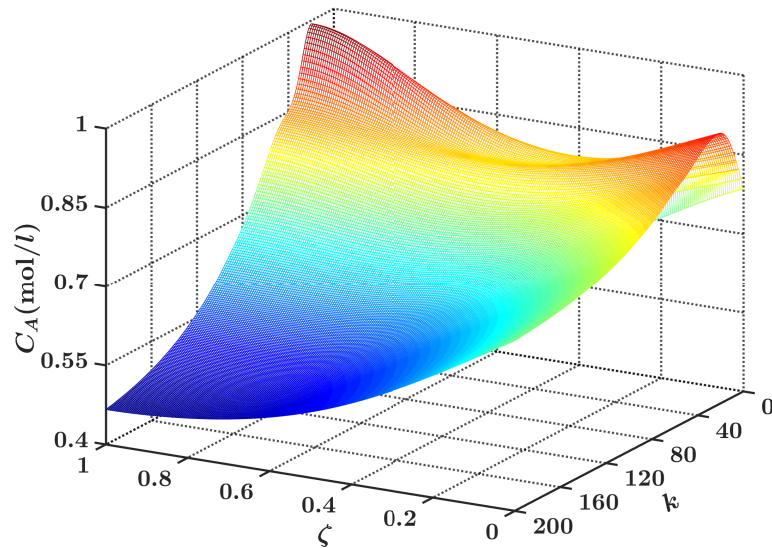
(b) Concentration

Figure 3.7: The evolution of the estimated state profiles through the axial dispersion tubular in an open-loop condition.

manipulation of the MPC is obtained by the application of the constrained optimization problem (see Eqs. (3.48)-(3.53)) on the basis of Cayley-Tustin time discretization with $Qx = 2x$, $F = 0.2$ and $N = 10$ as the control horizon. From Fig.3.8, it is possible to verify that the close-loop system under model predictive control is successful in stabilizing the unstable mode at end of the horizon and satisfy the stability constraint for the system of coupled parabolic PDEs.



(a) Temperature



(b) Concentration

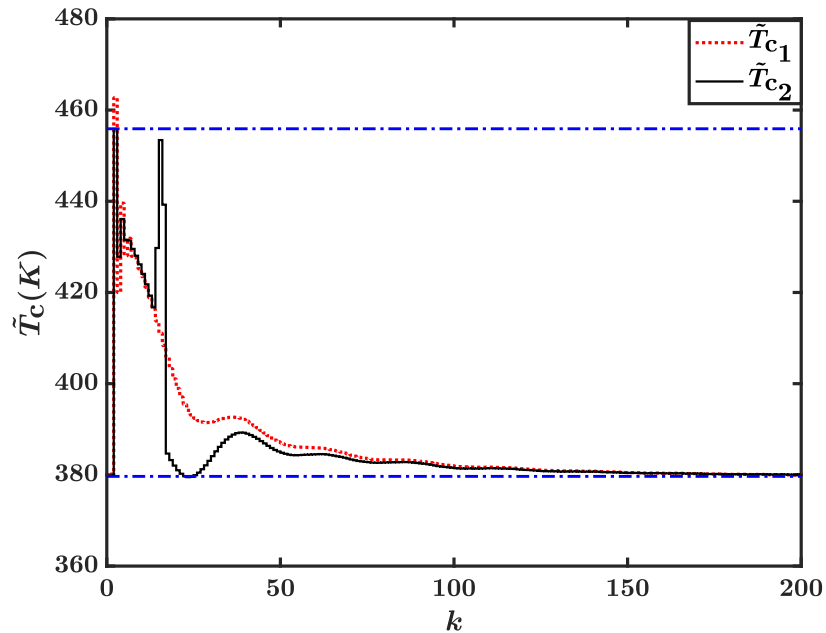
Figure 3.8: Dynamics reconstruction of the stabilized spatial profiles for the axial dispersion tubular reactor constructed on the basis of a discrete time coupled parabolic PDEs system.

As emphasized in Section 3.7.2, in this chemical plant, tuning the temperature of the wall may involve possible temperature disturbance. In this work, we consider a square wave function as the known disturbance injected into the system. Based on the quadratic optimization problem stated in Eq.(3.57) and the scheme given by

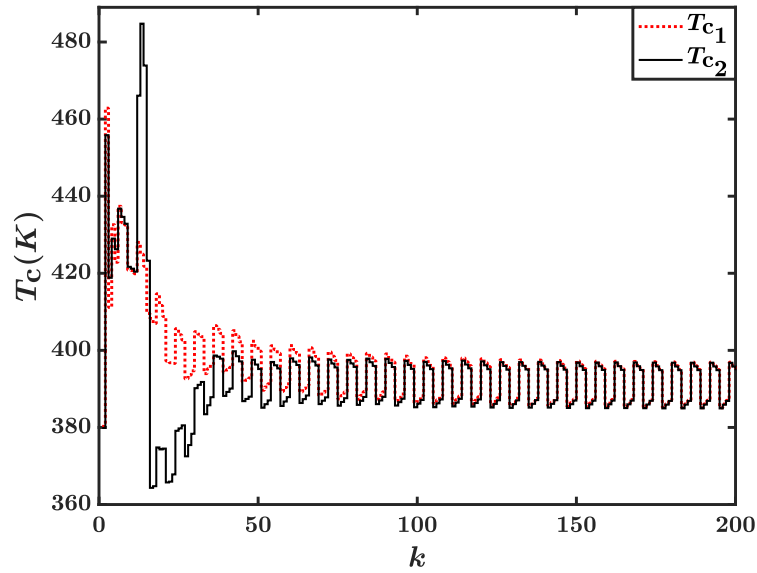
Fig.3.4, two scenarios are justified in the simulation study. For the first one, all the constraints (stability, state and input) with the input disturbance are assigned to the objective function. However, in the latter case, MPC is only subjected to stabilizing the coupled parabolic PDEs with consideration of input disturbance. From Fig.3.9 (a), it can be seen that the input with disturbance while all constraints are activated, can satisfy the upper and lower limitations of manipulated input variable compared to the second scenario which only stability constraint is applied on the system. The related controlled actions with respect to disturbance rejection are presented in Fig.3.9 (b).

Moreover, in a realistic physical systems various cases can be considered as the points where state constraints can be imposed. For example, the reactor outlet concentration, or the temperature constraint along the reactor to account with any hot-spot generated throughout the axial dispersion reactor. Here, the concentration of the component at end of the chemical tubular reactor ($\zeta = 1$) is introduced as the state constraint in the MPC controller. The result for corresponding state limitation is demonstrated in Fig.3.9 (c) according to the input manipulations.

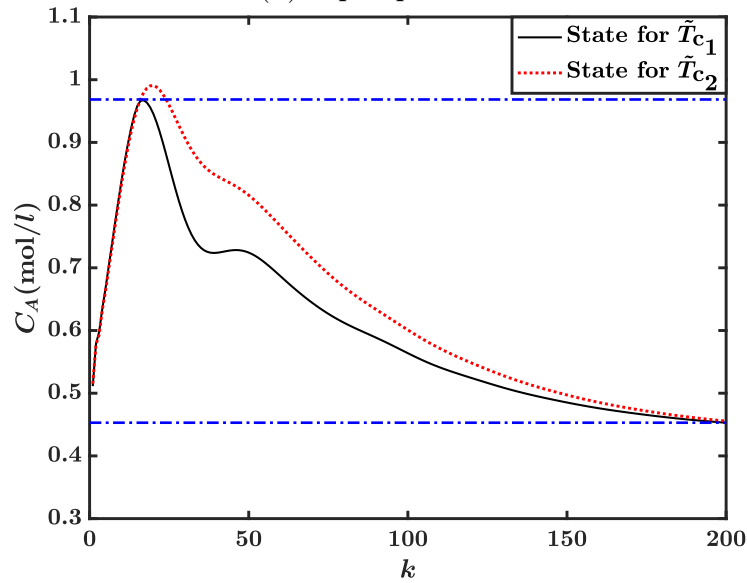
In a chemical process, the noise originating from operational environment may also affect the close-loop system. Thus, another case study is considered, as measurement noise is included in the system output (temperature at reactor outlet). In Fig.3.10, the simulation is performed in order to show the system output with measurement noise, generated as a white noise with standard variance $\kappa = 0.05$ and zero mean. As it is possible to notice, the model predictive controller is able to maintain the operation of the non-isothermal axial dispersion reactor at the desired steady state.



(a) Input profiles with disturbance.



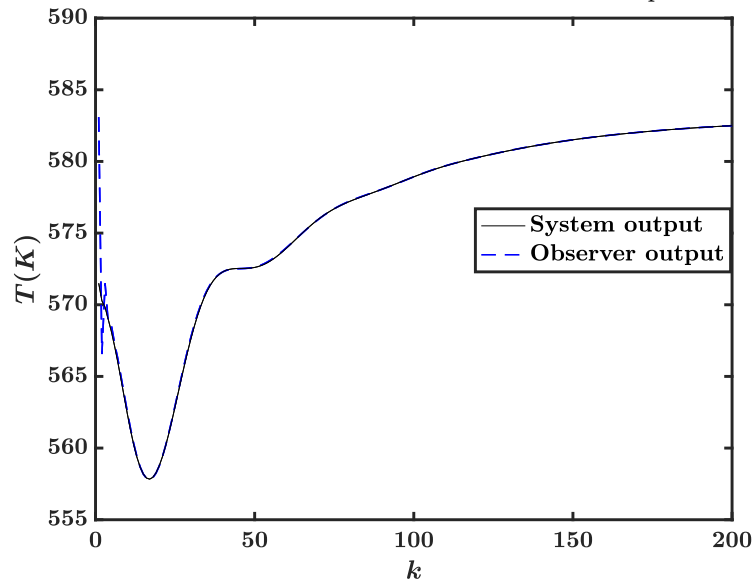
(b) Input profiles.



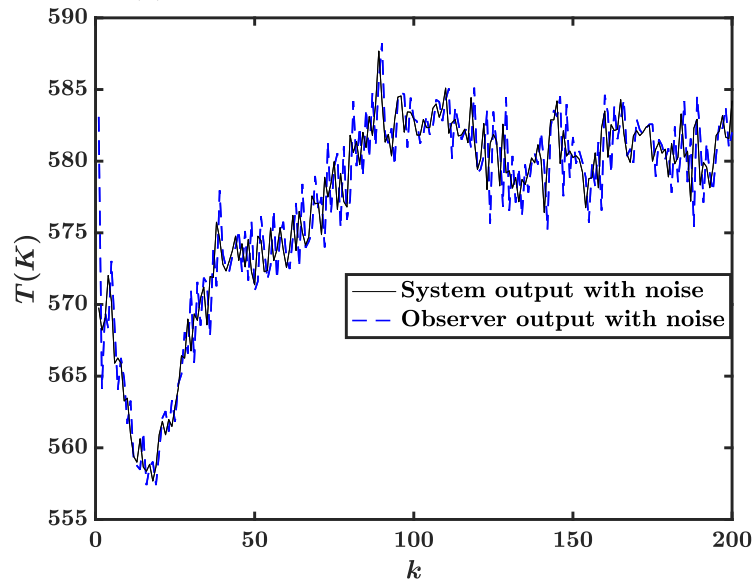
(c) Concentration profiles for inputs with disturbance.

Figure 3.9: Comparison between the inputs with square wave disturbance, controlled inputs and concentration profiles under model predictive controller subjected to all constraints (solid-lines) or only stability constraint (dotted lines).

Based on the above simulation studies, it possible to see that the developed constrained optimal controller can provide system stabilization, complying with constraints and reject the possible input disturbance. In addition, the observer reconstructs the states of the dispersive tubular reactor properly through the system output such that MPC is applicable in the chemical plant.



(a) System output and observer output.



(b) System output and observer output with measurement noise.

Figure 3.10: Comparison of the system output (solid lines) and observer output (dashed lines) with and without measurement noise in the non-isothermal tubular reactor under the model predictive control and using the Luenberger observer in Eq.(3.44).

3.9 Summary

In this chapter, the design of a model predictive controller and discrete observer were investigated for an axial dispersion tubular reactor with recycle. The discrete version of the overall system is provided by the application of the Cayley-Tustin time discretization on the linearization of a coupled nonlinear convection-diffusion-reaction

PDEs system. The discrete observer is considered without any model reduction or spatial approximation while the system properties (such as controllability, observability and stability) are preserved. An unstable operating condition with different energy and mass Peclet numbers is considered for the tubular reactor. Besides the stabilizing condition given by a terminal constraint, the physical limitation of the process (state and input constraints) with possible disturbance in control manipulation were placed in the formulation of the constrained optimization problem. The simulation results demonstrated the good performance of the controller by regulating the cooling jacket temperature of the reactor. As expected, the system under the proposed model predictive controller was able to achieve stabilization and provide constraints satisfaction while rejecting the input disturbance. The proposed optimal control scheme with consideration of constraints is designed to help the chemical process to operate efficiently in accordance with the process limitations.

References

- Aksikas, I., Moghadam, A. A., and Forbes, J. F. (2017). Optimal linear–quadratic control of coupled parabolic–hyperbolic pdes. *International Journal of Control*, 90(10):2152–2164.
- Alonso, A. A., Kevrekidis, I. G., Banga, J. R., and Frouzakis, C. E. (2004). Optimal sensor location and reduced order observer design for distributed process systems. *Computers & Chemical Engineering*, 28(1):27 – 35. Escape 12.
- Antoniades, C. and Christofides, P. (2000). Non-linear feedback control of parabolic partial differential difference equation systems. *International Journal of Control*, 73(17):1572–1591.
- Antoniades, C. and Christofides, P. D. (2001). Studies on nonlinear dynamics and control of a tubular reactor with recycle. *Nonlinear Analysis: Theory, Methods & Applications*, 47(9):5933 – 5944.
- Armaou, A. and Christofides, P. D. (2002). Dynamic optimization of dissipative pde systems using nonlinear order reduction. *Chemical Engineering Science*, 57(24):5083 – 5114.
- Aström, K. J. and Wittenmark, B. (1990). *Computer-Controlled Systems: Theory and Design (2nd Ed.)*. Prentice-Hall, Inc.
- Badillo-Hernandez, U., Alvarez, J., and Alvarez-Icaza, L. (2019). Efficient modeling of the nonlinear dynamics of tubular heterogeneous reactors. *Computers & Chemical Engineering*, 123:389 – 406.
- Balas, M. J. (1979). Feedback control of linear diffusion processes. *International Journal of Control*, 29(3):523–534.
- Bildea, C. S., Dimian, A. C., Cruz, S. C., and Iedema, P. D. (2004). Design of tubular reactors in recycle systems. *Computers & Chemical Engineering*, 28(1):63 – 72. Escape 12.
- Bitzer, M. and Zeitz, M. (2002). Design of a nonlinear distributed parameter observer for a pressure swing adsorption plant. *Journal of Process Control*, 12(4):533 – 543.
- Bizon, K., Continillo, G., Russo, L., and Smuła, J. (2008). On pod reduced models of tubular reactor with periodic regimes. *Computers & Chemical Engineering*, 32(6):1305 – 1315.
- Bonis, I., Xie, W., and Theodoropoulos, C. (2012). A linear model predictive control algorithm for nonlinear large-scale distributed parameter systems. *AIChE Journal*, 58(3):801–811.
- Bošković, D. M. and Krstić, M. (2002). Backstepping control of chemical tubular reactors. *Computers & Chemical Engineering*, 26(7):1077 – 1085.

- Christofides, P. D. and Daoutidis, P. (1997). Finite-dimensional control of parabolic pde systems using approximate inertial manifolds. *Journal of Mathematical Analysis and Applications*, 216(2):398 – 420.
- Cohen, D. S. and Poore, A. B. (1974). Tubular chemical reactors: the “lumping approximation” and bifurcation of oscillatory states. *SIAM Journal on Applied Mathematics*, 27(3):416–429.
- Curtain, R. (1982). Finite-dimensional compensator design for parabolic distributed systems with point sensors and boundary input. *IEEE Transactions on Automatic Control*, 27(1):98–104.
- Danckwerts, P. (1953). Continuous flow systems: Distribution of residence times. *Chemical Engineering Science*, 2(1):1 – 13.
- Dochain, D. (2000). State observers for tubular reactors with unknown kinetics. *Journal of Process Control*, 10(2):259 – 268.
- Dochain, D. (2001). State observation and adaptive linearizing control for distributed parameter (bio)chemical reactors. *International Journal of Adaptive Control and Signal Processing*, 15(6).
- Dochain, D. (2018). Analysis of the multiplicity of steady-state profiles of two tubular reactor models. *Computers & Chemical Engineering*, 114:318 – 324.
- Dubljevic, S., El-Farra, N. H., Mhaskar, P., and Christofides, P. D. (2006). Predictive control of parabolic pdes with state and control constraints. *International Journal of Robust and Nonlinear Control*, 16(16):749–772.
- Dufour, P., Touré, Y., Blanc, D., and Laurent, P. (2003). On nonlinear distributed parameter model predictive control strategy: on-line calculation time reduction and application to an experimental drying process. *Computers & Chemical Engineering*, 27.
- Franklin, G. F., Powell, J. D., Workman, M. L., et al. (1998). *Digital control of dynamic systems*, volume 3. Addison-wesley Reading, MA.
- Georgakis, C., Aris, R., and Amundson, N. R. (1977). Studies in the control of tubular reactors-i general considerations. *Chemical Engineering Science*, 32(11):1359 – 1369.
- Hairer, E., Lubich, C., and Wanner, G. (2006). *Geometric numerical integration: structure-preserving algorithms for ordinary differential equations*, volume 31. Springer Science & Business Media.
- Hastir, A., Lamoline, F., Winkin, J. J., and Dochain, D. (2020). Analysis of the existence of equilibrium profiles in nonisothermal axial dispersion tubular reactors. *IEEE Transactions on Automatic Control*, 65(4):1525–1536.

- Heinemann, R. F. and Poore, A. B. (1982). The effect of activation energy on tubular reactor multiplicity. *Chemical Engineering Science*, 37(1):128 – 131.
- Hlavacek, V. and Hofmann, H. (1970a). Modeling of chemical reactors - xvi: Steady state axial heat and mass transfer in tubular reactors - an analysis of the uniqueness of solutions. *Chemical Engineering Science*, 25(1):187 – 199.
- Hlavacek, V. and Hofmann, H. (1970b). Modeling of chemical reactors - xvii: Steady state axial heat and mass transfer in tubular reactors - numerical investigation of multiplicity. *Chemical Engineering Science*, 25(1):173 – 185.
- Jensen, K. F. and Ray, W. (1982). The bifurcation behavior of tubular reactors. *Chemical Engineering Science*, 37(2):199 – 222.
- Kazantzis, N. and Kravaris, C. (1999). Energy-predictive control: a new synthesis approach for nonlinear process control. *Chemical Engineering Science*, 54(11):1697 – 1709.
- Levenspiel, O. (1999). Chemical reaction engineering. *Industrial & Engineering Chemistry Research*, 38(11):4140–4143.
- Liu, Y. and Jacobsen, E. W. (2004). On the use of reduced order models in bifurcation analysis of distributed parameter systems. *Computers & Chemical Engineering*, 28(1):161 – 169. Escape 12.
- Luss, D. and Amundson, N. R. (1967). Stability of loop reactors. *AIChE Journal*, 13(2):279–290.
- Marwaha, B. and Luss, D. (2003). Hot zones formation in packed bed reactors. *Chemical Engineering Science*, 58(3):733 – 738.
- Mayne, D. Q. (2014). Model predictive control: Recent developments and future promise. *Automatica*, 50(12):2967 – 2986.
- Mohd Ali, J., Ha Hoang, N., Hussain, M., and Dochain, D. (2015). Review and classification of recent observers applied in chemical process systems. *Computers & Chemical Engineering*, 76:27 – 41.
- Muske, K. R. and Rawlings, J. B. (1993). Model predictive control with linear models. *AIChE Journal*, 39(2):262–287.
- Rawlings, J., Mayne, D., and Diehl, M. (2017). *Model Predictive Control: Theory, Computation, and Design*. Nob Hill Pub.
- Ray, W. (1981). *Advanced process control*. New York McGraw-Hill.
- Varma, A. a. and Aris, R. (1977). Stirred pots and empty tubes. In *Chemical Reactor Theory*, pages 79–154. Prentice-Hall.

- V.Havu and Malinen, J. (2007). The cayley transform as a time discretization scheme. *Numerical Functional Analysis and Optimization*, 28(7-8):825–851.
- Xie, J., Xu, Q., Ni, D., and Dubljevic, S. (2019). Observer and filter design for linear transport-reaction systems. *European Journal of Control*, 49:26 – 43.
- Xu, Q. and Dubljevic, S. (2017). Linear model predictive control for transport-reaction processes. *AIChE Journal*, 63(7):2644–2659.

4

Conclusion and Recommendations

4.1 Conclusion

In this work, the design of the model predictive control was investigated for distributed parameter systems and coupled LPS-DPS models. Two different chemical process models were considered: one described a coupled CSTR and tubular reactor with recycle for some complex chemical reactions such as polymerization process and the other one illustrated non-isothermal dispersive chemical tubular reactor with recycle commonly used in chemical and bio-processing. Furthermore, in this work, the foundation of systematic modeling for a linear DPS and coupled LPS-DPS for the predictive controller was shown without any spatial approximation or order reduction. The stability analysis is performed for both systems with consideration of diffusivity effects on eigenvalues distribution. Moreover, we also considered different Peclet numbers in the non-isothermal biochemical reactor in which the relative importance of heat and mass phenomena is preserved in the system dynamics. The discrete-time versions of original systems were obtained by the Cayley-Tustin time discretization method by applying Laplace transform to the original systems. Since it is expected that only output measurement at the outflow of the reactors is available as a measurable variable: therefore, the discrete output observers were developed to reconstruct the states for a system of ODE-PDE and a system of coupled convection-diffusion-reaction PDEs. The effects of spatial observer gains in shifting the unstable eigenvalue of error dynamics have also been demonstrated and discussed. It was shown that the proposed controller was able to optimize the system performance, while handling input and state constraints, ensuring the system stabilization and rejecting the possible disturbance in reactor operation.

4.2 Future work

An important area for future study is to reformulate model predictive controller for an unstable chemical system modelled by a set of hyperbolic-parabolic PDEs coupled to ODEs. In many chemical processes, mass/energy transfer can be described by parabolic PDEs, but distributed delays emerging from measurement (sensors) are modelled by hyperbolic PDEs. Furthermore, ODEs can be added to describe the dynamics of several lumped parameters systems. Since the techniques for solution of these two types of PDEs in addition to ODEs will be different particularly when it comes to Lyapunov equation; hence, it would be worthwhile to explore how to exploit three different approaches (parabolic PDE, hyperbolic PDE and ODE) represented by one complex industrial system.

Another promising area is development of advanced process control strategies which also account for the economic aspects of the process in distributed parameter systems besides the stability and physical limitations. This will effect on some variations in realization of constrained optimization problem and the subsequent controllers.

Bibliography

- A. Bensoussan, G. Prato, M. D. and Mitter, S. (2007). *Representation and Control of Infinite Dimensional Systems*. Birkhauser, Boston.
- Ai, L. and San, Y. (2013). Model predictive control for nonlinear distributed parameter systems based on ls-svm. *Asian Journal of Control*, 15(5):1407–1416.
- Aksikas, I., Fuxman, A., Forbes, J. F., and Winkin, J. J. (2009). Lq control design of a class of hyperbolic pde systems: Application to fixed-bed reactor. *Automatica*, 45(6):1542 – 1548.
- Aksikas, I., Moghadam, A. A., and Forbes, J. F. (2017). Optimal linear–quadratic control of coupled parabolic–hyperbolic pdes. *International Journal of Control*, 90(10):2152–2164.
- Aksikas, I., Winkin, J., and Dochain, D. (2007). Optimal lq-feedback regulation of a nonisothermal plug flow reactor model by spectral factorization. *Automatic Control, IEEE Transactions on*, 52:1179 – 1193.
- Alessio, A. and Bemporad, A. (2009). *A Survey on Explicit Model Predictive Control*, volume 384. Springer Berlin Heidelberg.
- Alizadeh Moghadam, A., Aksikas, I., Dubljevic, S., and Forbes, J. F. (2013). Boundary optimal (LQ) control of coupled hyperbolic PDEs and ODEs. *Automatica*, 49(2):526–533.
- Antoniades, C. and Christofides, P. (2000). Non-linear feedback control of parabolic partial differential difference equation systems. *International Journal of Control*, 73(17):1572–1591.
- Armaou, A. and Ataei, A. (2014). Piece-wise constant predictive feedback control of nonlinear systems. *Journal of Process Control*, 24(4):326 – 335.
- Armaou, A. and Christofides, P. (2002). Dynamic optimization of dissipative pde systems using nonlinear order reduction. *Chemical Engineering Science*, 57(24):5083–5114.
- Badillo-Hernandez, U., Alvarez, J., and Alvarez-Icaza, L. (2019). Efficient modeling of the nonlinear dynamics of tubular heterogeneous reactors. *Computers & Chemical Engineering*, 123:389 – 406.

- Balas, M. J. (1979). Feedback control of linear diffusion processes. *International Journal of Control*, 29(3):523–534.
- Bildea, C. S., Dimian, A. C., Cruz, S. C., and Iedema, P. D. (2004). Design of tubular reactors in recycle systems. *Computers & Chemical Engineering*, 28(1):63 – 72. Escape 12.
- Bizon, K., Continillo, G., Russo, L., and Smuła, J. (2008). On pod reduced models of tubular reactor with periodic regimes. *Computers & Chemical Engineering*, 32(6):1305 – 1315.
- Bonis, I., Xie, W., and Theodoropoulos, C. (2012). A linear model predictive control algorithm for nonlinear large-scale distributed parameter systems. *AIChE Journal*, 58(3):801–811.
- Borsche, R., Colombo, R. M., and Garavello, M. (2012). Mixed systems : ODEs – Balance laws. *Journal of Differential Equations*, 252(3):2311–2338.
- Bošković, D. M. and Krstić, M. (2002). Backstepping control of chemical tubular reactors. *Computers & Chemical Engineering*, 26(7):1077 – 1085.
- Carlos, E. G. A. R. A., Preti, M., and Morari, M. (1989). Model Predictive Control : Theory and Practice a Survey. 25(3).
- Chen, C. C. (1994). A continuous bulk polymerization process for crystal polystyrene. *Polymer-Plastics Technology and Engineering*, 33(1):55–81.
- Chen, H. and Allgöwer, F. (1998). *Nonlinear Model Predictive Control Schemes with Guaranteed Stability*. Springer Netherlands.
- Christofides, P. (2001). *Nonlinear and robust control of PDE systems. Methods and applications to transport-reaction processes*.
- Christofides, P. D. and Daoutidis, P. (1996). Feedback Control of Hyperbolic PDE Systems. *AIChE Journal*, 42(11):3063–3086.
- Christofides, P. D. and Daoutidis, P. (1997). Finite-dimensional control of parabolic pde systems using approximate inertial manifolds. *Journal of Mathematical Analysis and Applications*, 216(2):398 – 420.
- Cohen, D. S. and Poore, A. B. (1974). Tubular chemical reactors: the “lumping approximation” and bifurcation of oscillatory states. *SIAM Journal on Applied Mathematics*, 27(3):416–429.
- Curtain, R. (1982). Finite-dimensional compensator design for parabolic distributed systems with point sensors and boundary input. *IEEE Transactions on Automatic Control*, 27(1):98–104.
- Curtain, R. and Zwart, H. (1995a). *An Introduction to Infinite Dimensional Linear Systems Theory*. Springer.

- Curtain, R. F. and Zwart, H. (1995b). *An introduction to Infinite-Dimensional Linear Systems Theory*. New York: Springer-Verlag.
- Danckwerts, P. (1953). Continuous flow systems: Distribution of residence times. *Chemical Engineering Science*, 2(1):1 – 13.
- Dochain, D. (2018). Analysis of the multiplicity of steady-state profiles of two tubular reactor models. *Computers & Chemical Engineering*, 114:318 – 324.
- Dubljevic, S. and Christofides, P. D. (2006a). Predictive control of parabolic pdes with boundary control actuation. *Chemical Engineering Science*, 61(18):6239 – 6248.
- Dubljevic, S. and Christofides, P. D. (2006b). Predictive output feedback control of parabolic partial differential equations (pdes). *Industrial & Engineering Chemistry Research*, 45(25):8421–8429.
- Dubljevic, S., El-Farra, N. H., Mhaskar, P., and Christofides, P. D. (2006). Predictive control of parabolic pdes with state and control constraints. *International Journal of Robust and Nonlinear Control*, 16(16):749–772.
- Dubljevic, S., Mhaskar, P., El-farra, N. H., and Christofides, P. D. (2005). Predictive control of transport-reaction processes. *Computers and chemical engineering*, 29:2335–2345.
- Dufour, P., Touré, Y., Blanc, D., and Laurent, P. (2003). On nonlinear distributed parameter model predictive control strategy: on-line calculation time reduction and application to an experimental drying process. *Computers & Chemical Engineering*, 27.
- Eaton, J. W. and Rawlings, J. B. (1992). Model-predictive control of chemical processes. *Chemical Engineering Science*, 47(4):705 – 720.
- Fogler (2005). *H.S., elements of chemical reaction engineering*. prentice-hall.
- Franklin, G. F., Powell, J. D., Workman, M. L., et al. (1998). *Digital control of dynamic systems*, volume 3. Addison-wesley Reading, MA.
- García, C. E., Prett, D. M., and Morari, M. (1989). Model predictive control: Theory and practice—a survey. *Automatica*, 25(3):335 – 348.
- Georgakis, C., Aris, R., and Amundson, N. R. (1977). Studies in the control of tubular reactors-i general considerations. *Chemical Engineering Science*, 32(11):1359 – 1369.
- Hairer, E., Lubich, C., and Wanner, G. (2006). *Geometric Numerical Integration: Structure-Preserving Algorithms for Ordinary Differential Equations; 2nd ed.* Springer.

- Hasan, A., Aamo, O. M., and Krstic, M. (2016). Boundary observer design for hyperbolic pde-ode cascade systems. *Automatica*, 68:75 – 86.
- Hastir, A., Lamoline, F., Winkin, J. J., and Dochain, D. (2020). Analysis of the existence of equilibrium profiles in nonisothermal axial dispersion tubular reactors. *IEEE Transactions on Automatic Control*, 65(4):1525–1536.
- Heinemann, R. F. and Poore, A. B. (1982). The effect of activation energy on tubular reactor multiplicity. *Chemical Engineering Science*, 37(1):128 – 131.
- Hlavacek, V. and Hofmann, H. (1970a). Modeling of chemical reactors - xvi: Steady state axial heat and mass transfer in tubular reactors - an analysis of the uniqueness of solutions. *Chemical Engineering Science*, 25(1):187 – 199.
- Hlavacek, V. and Hofmann, H. (1970b). Modeling of chemical reactors - xvii: Steady state axial heat and mass transfer in tubular reactors - numerical investigation of multiplicity. *Chemical Engineering Science*, 25(1):173 – 185.
- Ito, K. and Kunisch, K. (2002). Receding horizon optimal control for infinite dimensional systems. *ESAIM: Control, Optimisation and Calculus of Variations*, 8:741–760.
- Izadi, M., Abdollahi, J., and Dubljevic, S. S. (2015). Pde backstepping control of one-dimensional heat equation with time-varying domain. *Automatica*, 54:41 – 48.
- Jensen, K. F. and Ray, W. (1982). The bifurcation behavior of tubular reactors. *Chemical Engineering Science*, 37(2):199 – 222.
- Kazantzis, N. and Kravaris, C. (1999). Energy-predictive control: a new synthesis approach for nonlinear process control. *Chemical Engineering Science*, 54(11):1697 – 1709.
- Khatibi, S., Cassol, G. O., and Dubljevic, S. (2020). Linear model predictive control for a cascade ode-pde system. *American Control Conference (ACC)*.
- Khatibi, S., Ozorio Cassol, G., and Dubljevic, S. (2020a). Linear model predictive control for a coupled cstr and axial dispersion tubular reactor with recycle. *Mathematics*, 8.
- Khatibi, S., Ozorio Cassol, G., and Dubljevic, S. (2020b). Model predictive control of non-isothermal axial dispersion tubular reactors with recycle. Unpublished.
- Krstic, M. and A.Smyshlyaev (2008). *Boundary Control of Pdes: A Course on Backstepping Designs*. Society for Industrial and Applied Mathematics.
- Krstic, M. and Smyshlyaev, A. (2008). Backstepping boundary control for first-order hyperbolic PDEs and application to systems with actuator and sensor delays. *System and Control letters*, 57:750–758.

- Levenspiel, O. (1999). Chemical reaction engineering. *Industrial & Engineering Chemistry Research*, 38(11):4140–4143.
- Liu, L., Huang, B., and Dubljevic, S. (2014). Model predictive control of axial dispersion chemical reactor. *Journal of Process Control*, 24(11):1671 – 1690.
- Liu, Y. and Jacobsen, E. W. (2004). On the use of reduced order models in bifurcation analysis of distributed parameter systems. *Computers & Chemical Engineering*, 28(1):161 – 169. Escape 12.
- Luss, D. and Amundson, N. R. (1967). Stability of loop reactors. *AIChE Journal*, 13(2):279–290.
- Marwaha, B. and Luss, D. (2003). Hot zones formation in packed bed reactors. *Chemical Engineering Science*, 58(3):733 – 738.
- Mayne, D., Rawlings, J., Rao, C., and Sokaert, P. (2000). Constrained model predictive control: Stability and optimality. *Automatica*, 36(6):789–814.
- Mayne, D. Q. (2014). Model predictive control: Recent developments and future promise. *Automatica*, 50(12):2967 – 2986.
- Meglio, F. D., Argomedeo, F. B., Hu, L., and Krstic, M. (2018). Stabilization of coupled linear heterodirectional hyperbolic pde–ode systems. *Automatica*, 87:281 – 289.
- Mohammadi, L., Aksikas, I., Dubljevic, S., and Forbes, J. F. (2015). Optimal boundary control of coupled parabolic PDE – ODE systems using infinite-dimensional representation. *Journal of Process Control*, 33:102–111.
- Muske, K. R. and Rawlings, J. B. (1993). Model predictive control with linear models. *AIChE Journal*, 39(2):262–287.
- Oh, M. and Pantelides, C. (1996). A Modelling and Simulation Language for Combined Lumped and Distributed Parameter Systems. *Computers and Chemical Engineering*.
- Pazy, A. (1996). *Semigroups of Linear Operators and Applications to Partial Differential Equations*.
- Åström, K. J. and Wittenmark, B. (1990). *Computer-Controlled Systems: Theory and Design (2nd Ed.)*. Prentice-Hall, Inc.
- Rawlings, J., Mayne, D., and Diehl, M. (2017). *Model Predictive Control: Theory, Computation, and Design*. Nob Hill Publishing.
- Rawlings, J. B. (2000). Tutorial overview of model predictive control. *IEEE Control Systems Magazine*, 20(3):38–52.

- Rawlings, J. B. and Muske, K. R. (1993). The stability of constrained receding horizon control. *IEEE Transactions on Automatic Control*, 38(10):1512–1516.
- Ray, W. (1981). *Advanced process control*. New York McGraw-Hill.
- Richalet, J., Rault, A., Testud, J., and Papon, J. (1978). Model predictive heuristic control: Applications to industrial processes. *Automatica*, 14(5):413 – 428.
- Scokaert, P. O. M., Mayne, D. Q., and Rawlings, J. B. (1999). Suboptimal model predictive control (feasibility implies stability). *IEEE Transactions on Automatic Control*.
- Shang, H., Forbes, J. F., and Guay, M. (2004). Model predictive control for quasilinear hyperbolic distributed parameter systems. *Industrial & Engineering Chemistry Research*, 43(9):2140–2149.
- Susto, G. A. and Krstic, M. (2010). Control of pde–ode cascades with neumann interconnections. *Journal of the Franklin Institute*, 347(1):284 – 314.
- Tang, S. and Xie, C. (2011). State and output feedback boundary control for a coupled pde–ode system. *Systems & Control Letters*, 60(8):540 – 545.
- Varma, A. a. and Aris, R. (1977). Stirred pots and empty tubes. In *Chemical Reactor Theory*, pages 79–154. Prentice-Hall.
- V.Havu and Malinen, J. (2007). The cayley transform as a time discretization scheme. *Numerical Functional Analysis and Optimization*, 28(7-8):825–851.
- Xu, Q. and Dubljevic, S. (2017). Linear Model Predictive Control for Transport-Reaction Processes. *AIChE Journal*, 63(7).
- Yang, Y. and Dubljevic, S. (2013). Boundary model predictive control of thin film thickness modelled by the kuramoto–sivashinsky equation with input and state constraints. *Journal of Process Control*, 23(9):1362 – 1379.

Appendix A

Discrete adjoint operators

A.1 A_d^*

The operator A_d^* for a coupled ODE-PDE system can be found based on definition ($\langle A_d \Phi, \Psi^* \rangle = \langle \Phi, A_d^* \Psi^* \rangle$). For the sake of simplicity the following terms are defined based on Equation (2.17) :

$$f_3(\zeta) = e_1(\zeta) - \frac{e_2(\zeta)e_3^{(1)}}{e_4^{(1)}}, M_1(\zeta) = \frac{\frac{1}{R}f_3(\zeta)}{\frac{\delta - a1}{R} - f_3^{(1)}}, M_2(\zeta) = \frac{\frac{e_2^{(1)}}{e_4^{(1)}}f_3(\zeta)}{\frac{\delta - a1}{R} - f_3^{(1)}} \quad (\text{A.1.1})$$

$$M_3(\zeta) = \frac{f_3(\zeta)}{\frac{\delta - a1}{R} - f_3^{(1)}}, M_4(\zeta) = \frac{e_2(\zeta)}{e_4^{(1)}}. \quad (\text{A.1.2})$$

The mentioned definition can be applied on each row of the operator A_d in Eq.(2.12) describing finite (CSTR) and infinite dimensional (Tubular reactor) of the chemical process. One can write the following:

$$A_d(\cdot)_{II,IF} = -(\cdot)_I + 2\delta (R_{IF}(\cdot)_F + R_{II}(\cdot)_I) \quad (\text{A.1.3})$$

$$\begin{aligned} \langle A_d \Phi, \Psi^* \rangle &= \int_0^L -\Phi(\zeta)\Psi^*(\zeta)d\zeta - 2\delta \int_0^L \int_0^L (M_2(\zeta)\Psi^*(\zeta)f_2(1,\eta)\Phi(\eta))d\eta d\zeta \\ &+ 2\delta \int_0^L \int_0^L (M_3(\zeta)\Psi^*(\zeta)f_1(1,\eta)\Phi(\eta)d\eta)d\zeta - 2\delta \int_0^L \int_0^L (M_4(\zeta)\Psi^*(\zeta)f_2(1,\eta)\Phi(\eta))d\eta d\zeta \\ &+ 2\delta \int_0^L \int_0^\zeta f_1(\zeta,\eta)\Phi(\eta)\Psi^*(\zeta)d\eta d\zeta + \int_0^L 2\delta M_1(\zeta)\Phi_{IF}(\zeta)d\zeta \\ &= \int_0^L -\Phi(\zeta)\Psi^*(\zeta)d\zeta - 2\delta \int_0^L \int_0^L (M_2(\zeta)\Psi^*(\zeta)d\zeta)(f_2(1,\eta)\Phi(\eta)d\eta) \\ &+ 2\delta \int_0^L \int_0^L (M_3(\zeta)\Psi^*(\zeta)d\zeta)(f_1(1,\eta)\Phi(\eta)d\eta) - 2\delta \int_0^L \int_0^L (M_4(\zeta)\Psi^*(\zeta)d\zeta)(f_2(1,\eta)\Phi(\eta)d\eta) \\ &+ 2\delta \int_0^L \int_\eta^L (f_1(\zeta,\eta)\Psi^*(\zeta)d\zeta)(\Phi(\eta)d\eta) + \int_0^L 2\delta M_1(\zeta)\Phi_{IF}(\zeta)d\zeta \quad (\text{A.1.4}) \end{aligned}$$

interchanging ζ and η results in:

$$\begin{aligned}
 &= \int_0^L -\Phi(\zeta)\Psi^*(\zeta)d\zeta - 2\delta \int_0^L \int_0^L (M_2(\eta)\Psi^*(\eta)d\eta)(f_2(1, \zeta)\Phi(\zeta)d\zeta) \\
 &+ 2\delta \int_0^L \int_0^L (M_3(\eta)\Psi^*(\eta)d\eta)(f_1(1, \zeta)\Phi(\zeta)d\zeta) - 2\delta \int_0^L \int_0^L (M_4(\eta)\Psi^*(\eta)d\eta)(f_2(1, \zeta)\Phi(\zeta)d\zeta) \\
 &\quad + 2\delta \int_0^L \int_\zeta^L (f_1(\eta, \zeta)\Psi^*(\eta)d\eta)(\Phi(\zeta)d\zeta) + \int_0^L 2\delta M_1(\zeta)\Phi_{IF}(\zeta)d\zeta \\
 &= \int_0^L \left[-\Psi^*(\zeta) - 2\delta \int_0^L (M_2(\eta)\Psi^*(\eta)d\eta)f_2(1, \zeta) + 2\delta \int_0^L (M_3(\eta)\Psi^*(\eta)d\eta)f_1(1, \zeta) \int_0^L 2\delta M_1(\zeta)\Phi_F d\zeta \right. \\
 &\quad \left. - 2\delta \int_0^L (M_4(\eta)\Psi^*(\eta)d\eta)f_2(1, \zeta) + 2\delta \int_\zeta^L (f_1(\eta, \zeta)\Psi^*(\eta)d\eta) \right] \Phi(\zeta)d\zeta + \int_0^L 2\delta M_1(\zeta)\Phi_{IF}(\zeta)d\zeta \\
 &= \langle \Phi, A_d^* \Psi^* \rangle \tag{A.1.5}
 \end{aligned}$$

Hence:

$$\begin{aligned}
 A_{d_{II,IF}}^* &= -(\cdot) - 2\delta \int_0^L (M_2(\eta)(\cdot)d\eta)f_2(1, \zeta) + 2\delta \int_0^L (M_3(\eta)(\cdot)d\eta)f_1(1, \zeta) - 2\delta \int_0^L (M_4(\eta)(\cdot)d\eta)f_2(1, \zeta) \\
 &\quad + 2\delta \int_\zeta^L (f_1(\eta, \zeta)(\cdot)d\eta) + \int_0^L 2\delta M_1(\zeta)(\cdot)_F d\zeta \tag{A.1.6}
 \end{aligned}$$

Which leads to:

$$\begin{aligned}
 R_{IF}^*(\cdot)_I &= \int_0^L \left[\frac{e_1 - \frac{e_2 e_3^{(1)}}{e_4^{(1)}}}{\delta - a_1 - R f_3^{(1)}} \right] (\cdot)_I d\zeta \\
 R_{II}^*(\cdot)_I(\zeta) &= \left(-f_2^{(1)} \int_0^L \left[\frac{e_2^{(1)}}{e_4^{(1)} (\delta - a_1 - R f_3^{(1)})} f_3(\eta) + \frac{e_2(\eta)}{e_4^{(1)}} \right] (\cdot)_I d\eta \right) + \tag{A.1.7} \\
 &\quad \left(f_1^{(1)} \int_0^L \left[\frac{f_3(\eta)}{(\delta - a_1 - R f_3^{(1)})} \right] (\cdot)_I d\eta + \int_\zeta^L f_1(\eta, \zeta)(\cdot)_I d\eta \right)
 \end{aligned}$$

For the first row (finite part) we have:

$$A_d(\cdot)_{FF,FI} = -(\cdot)_F + 2\delta (R_{FF}(\cdot)_F + R_{FI}(\cdot)_I) \tag{A.1.8}$$

One can directly obtain the following expressions from the definition ($\langle A_d \Phi, \Psi^* \rangle = \langle \Phi, A_d^* \Psi^* \rangle$):

$$R_{FF}^*(\cdot)_F = R_{FF}(\cdot)_F$$

$$R_{FI}^*(\cdot)_F(\zeta) = \left(\frac{f_1^{(1)}}{\frac{\delta - a_1}{R} - f_3^{(1)}} - \frac{\frac{e_2^{(1)} f_2^{(1)}}{e_4^{(1)}}}{\frac{\delta - a_1}{R} - f_3^{(1)}} \right) (\cdot)_F \quad (\text{A.1.9})$$

Finally,

$$A_d^*(\cdot) = - \begin{bmatrix} (\cdot)_F \\ (\cdot)_I \end{bmatrix} + 2\delta \begin{bmatrix} R_{FF}^* & R_{IF}^* \\ R_{FI}^* & R_{II}^* \end{bmatrix} \begin{bmatrix} (\cdot)_F \\ (\cdot)_I \end{bmatrix} \quad (\text{A.1.10})$$

A.2 B_d^*

For the operator B_d , it is possible to write:

$$\langle B_d u, \Psi^* \rangle = \langle u, B_d \Psi^* \rangle \quad (\text{A.2.1})$$

which u is a scalar input. The above equation directly leads to the following adjoint resolvent operators:

$$(R_{FF}B)^*(\cdot)_F = \left(\frac{a_2 f_3^{(1)}}{\frac{(\delta - a_1)^2}{R} - f_3^{(1)}(\delta - a_1)} + \frac{a_2}{\delta - a_1} \right) (\cdot)_F \quad (\text{A.2.2})$$

$$(R_{IF}B)^*(\cdot)_I = \left(\frac{\frac{a_2}{R}}{\frac{\delta - a_1}{R} - f_3^{(1)}} \right) \int_0^L \left[e_1(\zeta) - \frac{e_3^{(1)} e_2(\zeta)}{e_4^{(1)}} \right] (\cdot)_I d\zeta \quad (\text{A.2.3})$$

which can be used to compute the operator B_d^* as:

$$B_d^* = \sqrt{2\delta} \begin{bmatrix} (R_{FF}B)^* \\ (R_{IF}B)^* \end{bmatrix}^T \quad (\text{A.2.4})$$

Appendix B

Sample code

A Sample code developed for the model predictive control of a coupled LPS-DPS configuration (version Matlab):

```
%%%%%%%%%%%%%%%%%%%%%%%%%%%%%%%%%%%%%%%%%%%%%%%%%%%%%%%%%%%%%%%%%%%%%%%%%
%Codes Developed by "Seyedhamidreza Khatibi"
%%%%%%%%%%%%%%%%%%%%%%%%%%%%%%%%%%%%%%%%%%%%%%%%%%%%%%%%%%%%%%%%%%%%%%%%%
%Part1:
%Demonstration of the open loop (unforced) response for a coupled ...
    ODE-PDE
%in both discrete and continous setting
%%%%%%%%%%%%%%%%%%%%%%%%%%%%%%%%%%%%%%%%%%%%%%%%%%%%%%%%%%%%%%%%%%%%%%%%%
%Continious Setting
clc
clear
close all
global R D v a1 psi
R=0.5;
D=0.35;
a1=-0.25;
psi=-1;
v=1.8;
dt=0.04;
dz=0.005;
Node=1/dz+1;
z=0:dz:1;
N=length(z);
x0=[1;ones(N-2,1)];%I.C
[t,y]=ode45(@func,0:dt:20,x0);
%%Discrete Setting%%
Delta=2/dt;%Delta=2/h
t=0:dt:20;
Time_steps=20/dt+1;
Z=zeros(length(Time_steps),Node+1);
Y=zeros(length(Time_steps),1);
Z_IC=[1,ones(1,length(z))];%I.C
Z(1,:)=Z_IC;
for T_s=1:Time_steps-1%sampling time
    Ad=discrete_Ad(Z_IC,v,psi,Delta,z,Node);
    Z(T_s+1,:)=Ad;
```

```

    Z_IC=Ad;
end
figure(1)
zeta=0:1*dz:(Node-1)*dz;
Time_steps=20/dt+1;
k=0:1*(Time_steps-1);
[Zeta,K]=meshgrid(zeta,0:dt:(Time_steps-1)*dt);%5
mesh(Zeta,K,[y(:,2) y(:,2:(N-2)+1) y(:,(N-2)+1)])%
axesH=gca;
axesH.XAxis.TickLabelInterpreter='latex';
axesH.XAxis.TickLabelFormat='\\textbf{%g}';
axesH.YAxis.TickLabelInterpreter='latex';
axesH.YAxis.TickLabelFormat='\\textbf{%g}';
axesH.ZAxis.TickLabelInterpreter='latex';
axesH.ZAxis.TickLabelFormat='\\textbf{%g}';
xlabel({'\\textbf{Position}\\boldmath$(\\zeta)$'}, 'FontSize',12,...
'fontweight','bold','Interpreter','latex','rotation',20)
ylabel({'\\textbf{Continuous ...
    Time}'),'FontSize',12,'fontweight','bold',...
'Interpreter','latex','rotation',-20)
zlabel({'\\textbf{Open Loop Response For PDE in Continious Setting}'),...
'FontSize',12,'fontweight','bold','Interpreter','latex')
set(gca,'LineWidth',1.5);
set(gca,'FontSize',14);
set(gca,'fontweight','bold');
grid on
figure(2)
mesh(Zeta,K,Z(:,2:Node+1))
axesH2=gca;
axesH2.XAxis.TickLabelInterpreter='latex';
axesH2.XAxis.TickLabelFormat='\\textbf{%g}';
axesH2.YAxis.TickLabelInterpreter='latex';
axesH2.YAxis.TickLabelFormat='\\textbf{%g}';
axesH2.ZAxis.TickLabelInterpreter='latex';
axesH2.ZAxis.TickLabelFormat='\\textbf{%g}';
ylabel({'\\textbf{Position}\\boldmath$(\\zeta)$'}, 'FontSize',12,...
'fontweight','bold','Interpreter','latex','rotation',-20)
xlabel({'\\textbf{Continuous ...
    Time}'),'FontSize',12,'fontweight','bold',...
'Interpreter','latex','rotation',20)
zlabel({'\\textbf{Open Loop Response For PDE in Discrete Setting}'),...
'FontSize',12,'fontweight','bold','Interpreter','latex')
set(gca,'LineWidth',1.5);
set(gca,'FontSize',14);
set(gca,'fontweight','bold');
grid on
function F=func(t,x)
global R D v a1 psi
dz=0.005;
z=0:dz:1;
N=length(z);
Xi=[x(1);x(2:(N-2)+1);x(end)];
F(1,1)=a1*x(1)+R*Xi(end);
for i=2:N-1

```



```

close all
global a1 R v D psi
R=0.5;
D=0.35;
a1=-0.25;
psi=-1;
v=1.8;
fun4=@f4_original;
xss_original=[];
for k=1:20000
    if k<1000
        %real guess
        x0=(rand(1))*1;
    else
        %Complex guess
        x0=-(rand(1)-0.2)*7500+(rand(1)-0.5)*30*1j;
    end
    [xs,fval,flag]=fsolve(fun4,x0);
    if (flag==1||flag==2)&&fval≠0
        if imag(xs)<0
            xs=real(xs)-imag(xs)*1i;
        end
        xss_original=[xss_original,xs];
    end
end
%Removing repeated eigenvalues:
Ass=zeros(length(xss_original),2);
Ass(:,1)=(real(xss_original));
Ass(:,2)=(imag(xss_original));
Ass(:,1)=round(Ass(:,1),4);
[C,ia]=unique(Ass(:,1),'rows');
Bss=Ass(ia,:);
xss_original=Bss(:,1)+(Bss(:,2)).*1i;
lambda=[];
for lml=1:length(xss_original)
    if abs(imag(xss_original(end-lml+1,1)))<10^-3
        lambda=[lambda,real(xss_original(end-lml+1,1))];
    else
        lambda=[lambda,xss_original(end-lml+1,1),...
            real(xss_original(end-lml+1,1))...
            -imag(xss_original(end-lml+1,1))*1i];
    end
end
xss_original=lambda;
figure(3)
plot(real(xss_original),imag(xss_original),'ok','linewidth',2)
yline(0,'linewidth',1.5,'Color','k')
xline(0,'linewidth',1.5,'Color','k')
set(gca,'LineWidth',1.5,'Fontweigh','bold');
set(gca,'FontSize',16,'Fontweigh','bold');
ylabel('\textbf{Im}','FontSize',16,'fontweight','bold',...
'Interpreter','latex')
xlabel('\textbf{Re}','FontSize',16,'fontweight','bold','Interpreter',...
'latex')

```

```

grid
function y4_original=f4_original(x)
global a1 R v D psi
a=(x-psi)/D;
b=v/D;
T_11=(exp(b/2 - (b^2 + 4*a)^(1/2)/2)*(b^2 + 4*a)^(1/2) + ...
exp(b/2 + (b^2 + 4*a)^(1/2)/2)*(b^2 + 4*a)^(1/2) + b*exp(b/2 - ...
(b^2 + 4*a)^(1/2)/2) - b*exp(b/2 + (b^2 + 4*a)^(1/2)/2))/(2*(b^2 + ...
4*a)^(1/2));
T_21=(b^2*exp(b/2 - (b^2 + 4*a)^(1/2)/2) - b^2*exp(b/2 + ...
(b^2 + 4*a)^(1/2)/2) - exp(b/2 - (b^2 + 4*a)^(1/2)/2)*(b^2 + 4*a) + ...
exp(b/2 + (b^2 + 4*a)^(1/2)/2)*(b^2 + 4*a))/(4*a*(b^2 + 4*a)^(1/2));
T_31=-(a*exp(b/2 - (b^2 + 4*a)^(1/2)/2) - a*exp(b/2 + ...
(b^2 + 4*a)^(1/2)/2))/(b^2 + 4*a)^(1/2);
T_41=(exp(b/2 - (b^2 + 4*a)^(1/2)/2)*(b^2 + 4*a)^(1/2) + ...
exp(b/2 + (b^2 + 4*a)^(1/2)/2)*(b^2 + 4*a)^(1/2) - b*exp(b/2 - ...
(b^2 + 4*a)^(1/2)/2) + b*exp(b/2 + (b^2 + 4*a)^(1/2)/2))/(2*(b^2 + ...
4*a)^(1/2));
y4_original=(T_41.*(T_11+((a1-x)/R)))-(T_21*T_31);
end
%%%%%%%%%%%%%%%%%%%%%%%%%%%%%%%%%%%%%%%%%%%%%%%%%%%%%%%%%%%%%%%%%%%%%%%%
%Codes Developed By "Seyedhamidreza Khatibi"
%%%%%%%%%%%%%%%%%%%%%%%%%%%%%%%%%%%%%%%%%%%%%%%%%%%%%%%%%%%%%%%%%%%%%%%%
%Part3:
%Observer Design
%Note that as described in the thesis the following eigenvalue ...
    problem for
%the observer error dynamics has been solved with several observer gain
%such that with proper value for L in the continuous setting
%no positive eigenvalue observed.
%%%%%%%%%%%%%%%%%%%%%%%%%%%%%%%%%%%%%%%%%%%%%%%%%%%%%%%%%%%%%%%%%%%%%%%%
clear
clc
close all
global a1 R v D psi LI LF
R=0.5;
D=0.35;
a1=-0.25;
psi=-1;
v=1.8;
fun4=@f4_L;
ds=0.01:0.01:20;%Step Changes in Observer Gain
k_lambda=[];
all_lambda=[];
all_L=[];
for gh=1:length(ds)
    LI=ds(gh);
    LF=ds(gh);
    for k=1:10
        x0_n=-(rand(1))*1;%Also with complex guess
        [xs_jhL, fval, flag]=fsolve(fun4,x0_n);
        if (flag==1 || flag==2) && fval~=0
            k_lambda=[k_lambda,xs_jhL];
        end
    end
end

```

```

end
all_lambda=[all_lambda,max(k_lambda)];
all_L=[all_L,LI];
k_lambda=[];
end
function y4_L=f4_L(x)
global a1 R v D psi LI LF z Node
a=(x-psi)/D;
b=v/D;
T_11=(exp(b/2 - (b^2 + 4*a)^(1/2)/2)*(b^2 + 4*a)^(1/2) + exp(b/2 + ...
(b^2 + 4*a)^(1/2)/2)*(b^2 + 4*a)^(1/2) + b*exp(b/2 - ...
(b^2 + 4*a)^(1/2)/2) - b*exp(b/2 + ...
(b^2 + 4*a)^(1/2)/2))/(2*(b^2 + 4*a)^(1/2));
T_21=(b^2*exp(b/2 - (b^2 + 4*a)^(1/2)/2) - ...
b^2*exp(b/2 + (b^2 + 4*a)^(1/2)/2) - exp(b/2 - ...
(b^2 + 4*a)^(1/2)/2)*(b^2 + 4*a) + exp(b/2 + ...
(b^2 + 4*a)^(1/2)/2)*(b^2 + 4*a))/(4*a*(b^2 + 4*a)^(1/2));
T_31=-(a*exp(b/2 - (b^2 + 4*a)^(1/2)/2) - ...
a*exp(b/2 + (b^2 + 4*a)^(1/2)/2))/(b^2 + 4*a)^(1/2);
T_41=(exp(b/2 - (b^2 + 4*a)^(1/2)/2)*(b^2 + 4*a)^(1/2) + ...
exp(b/2 + (b^2 + 4*a)^(1/2)/2)*(b^2 + 4*a)^(1/2) - ...
b*exp(b/2 - (b^2 + 4*a)^(1/2)/2) + b*exp(b/2 + ...
(b^2 + 4*a)^(1/2)/2))/(2*(b^2 + 4*a)^(1/2));
A=[0 1;a v/D];
F_21=zeros(1,Node);
F_41=zeros(1,Node);
for pp=1:Node
    Floop1=expm(A.*(1-z(pp)));
    F_21(1,pp)=Floop1(1,2);
    F_41(1,pp)=Floop1(2,2);
end
s33=(F_21.*(LI/D));
H11=trapz(z(1:end),s33(1:end));
s44=(F_41.*(LI/D));
H21=trapz(z(1:end),s44(1:end));
CC=[T_11+((x-a1)/(LF-R)) T_21;T_31 T_41]\[-H11;-H21];
c1=CC(1);
c2=CC(2);
y4_L=1-(T_11*c1)-(T_21*c2)-H11;
end
%%%%%%%%%%%%%%%%%%%%%%%%%%%%%%%%%%%%%%%%%%%%%%%%%%%%%%%%%%%%%%%%%%%%%%%%
%Codes Developed By "Seyedhamidreza Khatibi"
%%%%%%%%%%%%%%%%%%%%%%%%%%%%%%%%%%%%%%%%%%%%%%%%%%%%%%%%%%%%%%%%%%%%%%%%
%Part4:
%Model Predictive Control(MPC) For a coupled CSTR and Axial dispersion
%tubular reactor including stability,input,state constarints
%%%%%%%%%%%%%%%%%%%%%%%%%%%%%%%%%%%%%%%%%%%%%%%%%%%%%%%%%%%%%%%%%%%%%%%%
clc
clear
close all
global R D v a1 a2 psi L
R=0.5;
D=0.35;
a1=-0.25;

```

```

a2=1;
psi=-1;
v=1.8;
dz=0.005;
z=0:dz:1;
Node=1/dz+1;
L=[5,5.*ones(1,Node)];
dt=0.04;
Δ=2/dt;
z_p_0=1;
z0=ones(1,length(z));
t=0:dt:45;
Time_steps=45/dt+1;
%%%%%%%%%%%%%%%%%%%%%%%%%%%%%%%%%%%%%%%%%%%%%%%%%%%%%%%%%%%%%%%%%%%%%%%% Open loop %%%%%%%%%%%%%%%%%%%%%%%%%%%%%%%%%%%%%%%%%%%%%%%%%%%%%%%%%%%%%%%%%%%%%%%%%
Z0_state=zeros(length(Time_steps),Node+1);
Z0_state_observer=zeros(length(Time_steps),Node+1);
Z_IC0_state=[z_p_0,z0];
Z_IC0_observer=[0,0.*ones(1,length(z))];
Z0_state(1,:)=Z_IC0_state;
Z0_state_observer(1,:)=Z_IC0_observer;
for T_s=1:Time_steps-1
    Ad_o_state=discrete_Ad(Z_IC0_state,v,psi,Δ,z,Node);
    Ad_o_observer=discrete_Ad(Z_IC0_observer,v,psi,Δ,z,Node);
    L_d_o=discrete_L(L,v,psi,Δ,z,Node);
    Cd_o_observer=discrete_Cd((Z_IC0_state-Z_IC0_observer),v,psi,Δ,...
    z,Node);
    Z0_state(T_s+1,:)=Ad_o_state;
    Z0_state_observer(T_s+1,:)=Ad_o_observer+(L_d_o.*Cd_o_observer);
    Z_IC0_state=Z0_state(T_s+1,:);
    Z_IC0_observer=Z0_state_observer(T_s+1,:);
end
N=65;
Q=[2.5 1.5*ones(1,Node)];
RR=1;
%Loading stable eigen values and corresponding normalized eigen ...
    functions
load Phi_original_D_35
phi_F=phi_F_original_D_35(2:20);
phi_I=phi_I_original_D_35(2:20,:);
phi_F_adj=phi_F_adj_D_35(2:20);
phi_I_adj=phi_I_adj_D_35(2:20,:);
xss=xss_original_D_35(2:18);
%%%%%%%%%%%%%%%%%%%%%%%%%%%%%%%%%%%%%%%%%%%%%%%%%%%%%%%%%%%%%%%%%%%%%%%% Calculate H & S %%%%%%%%%%%%%%%%%%%%%%%%%%%%%%%%%%%%%%%%%%%%%%%%%%%%%%%%%%%%%%%%%%%%%%%%%
Bd=discrete_Bd(v,psi,Δ,z,Node);
QB=operator_Qbar(Bd,z,length(xss),Q,xss,phi_I,phi_I_adj);
Ads_Qbar_B=discrete_Ads(QB,v,psi,Δ,z,Node);
AdB=discrete_Ad(Bd,v,psi,Δ,z,Node);
QA=operator_Qbar(AdB,z,length(xss),Q,xss,phi_I,phi_I_adj);
Ads_0=Ads_Qbar_B;
AdB_0=AdB;
for i=1:N-3
    Ads_new=discrete_Ads(Ads_0,v,psi,Δ,z,Node);
    AdB_new=discrete_Ad(AdB_0,v,psi,Δ,z,Node);
    QA_new= operator_Qbar(AdB_new,z,length(xss),Q,xss,phi_I,phi_I_adj);

```

```

    Ads_0=Ads_new;
    AdB_0=AdB_new;
    Ads_Qbar_B=[Ads_Qbar_B;Ads_new];
    AdB=[AdB;AdB_new];
    QA=[QA;QA_new];
end
for i=1:N-1
    for j=1:N-1
        if i==j
            h=discrete_Bds(QB,v,psi,delta,z,Node)+RR;
            H(i,j)=h;
            S(i,j)=Bd(1);
        elseif i<j
            h=discrete_Bds(Ads_Qbar_B(j-i,:),v,psi,delta,z,Node);
            H(i,j)=h;
            S(i,j)=0;
        else
            h=discrete_Bds(QA(i-j,:),v,psi,delta,z,Node);
            H(i,j)=h;
            S(i,j)=AdB(i-j,1);
        end
    end
end
end
H=(H+H')/2;%H is not symmetric
%%%%%%%%%%%%%%%%%%%%%%%%%%%%%%%%%%%%%%%%%%%%%%%%%%%%%%%%%%%%%%%%%%%%%%%% State with MPC %%%%%%%%%%%%%%%%%%%%%%%%%%%%%%%%%%%%%%%%%%%%%%%%%%%%%%%%%%%%%%%%%%%%%%%%%
%%Constraints%%
U_up=0;
U_low=-0.09;
X_up=0.65;
X_low=-0.09;
U=[];
Z_IC_state=[z_p_0,z0];%Initial Condition for Z
Z_IC_observer=[0,0.*ones(1,length(z))];%Initial Condition for Observer
Z=Z_IC_observer;
Z_state=Z_IC_state;
Md=discrete_Md(v,psi,delta,z,Node);
disturbance=0;
for T_s=1:Time_steps-1
    if T_s>(20/dt)
        disturbance=1;
    end
    if T_s>(25/dt)
        disturbance=0;
    end
end
%%%%%%%%%%%%%%%%%%%%%%%%%%%%%%%%%%%%%%%%%%%%%%%%%%%%%%%%%%%%%%%%%%%%%%%% Calculate P & T %%%%%%%%%%%%%%%%%%%%%%%%%%%%%%%%%%%%%%%%%%%%%%%%%%%%%%%%%%%%%%%%%%%%%%%%%
Ad_state=discrete_Ad(Z_IC_state,v,psi,delta,z,Node);
Ad_observer=discrete_Ad(Z_IC_observer,v,psi,delta,z,Node);
L_d=discrete_L(L,v,psi,delta,z,Node);
Cd_observer=discrete_Cd((Z_IC_state-Z_IC_observer),v,psi,delta,z,Node);
Ad_0=Ad_observer;
for i=1:N-2
    Ad_new=discrete_Ad(Ad_0,v,psi,delta,z,Node);
    Ad_0=Ad_new;
end

```

```

    Ad_observer=[Ad_observer;Ad_new];
end
for i=1:N-1
    p=discrete_Bds(operator_Qbar(Ad_observer(i,:),z,length(xss),Q,xss,...
    phi_I,phi_I_adj),v,psi,delta,z,Node);
    P0(i)=p;
end
P=P0';
T=Ad_observer(:,1);
%%Optimization%%
H_quad=2*H;
P_quad=2*P;
>Loading unstable eigen mode
Phi_UU=[phi_F_original_D_35(1),phi_I_original_D_35(1,:)];
Equality constraint:
Left hand side:
Phi_U=[];
for i=1:N-2
    phi_u=AdB(i,1:Node+1).*Phi_UU;
    phi_U=trapz(z(1:end),phi_u(2:end))+phi_u(1);
    Phi_U=[Phi_U;phi_U];
end
phi_u=Bd(1,1:Node+1).*Phi_UU;
phi_U=trapz(z(1:end),phi_u(2:end))+phi_u(1);
Phi_U=[Phi_U;phi_U];
Phi_U=Phi_U';
Phi_UA=fliplr(Phi_U);
Right hand side:
phi_u=Ad_observer(N-1,1:Node+1).*Phi_UU;
phi_U=trapz(z(1:end),phi_u(2:end))+phi_u(1);
Phi_UB=-phi_U;
||state, input and stability constraints||
A_quad=[eye(N-1);-eye(N-1);S;-S;Phi_UA];
b_quad=[(U_up*ones(1,N-1))';(-U_low*ones(1,N-1))';...
((X_up*ones(1,N-1))'-T);((-X_low*ones(1,N-1))'+T);Phi_UB];
||Optimization:||
u=quadprog(H_quad,P_quad',A_quad,b_quad);
u_new=u(1);
x_new=Ad_observer(1,:)+(Bd*u_new)+(L_d.*Cd_observer)+(Md*disturbance);
Z_IC_state=Ad_state+(Bd*u_new)+(Md*disturbance);
x_new(1)=x_new(2);
x_new(Node)=x_new(Node-1);
Z_IC_observer=x_new;
U=[U;u_new];
Z=[Z;x_new];
end
%Constucting discrete operators
%Ad
function Ad=discrete_Ad(x,v,psi,delta,z,Node)
global R D a1
z_p_0=x(1);
xx=x(2:end);
n=v/D;
h=sqrt(n.^2+4.*((delta-psi)./D));

```

```

s1=sinh((h./2).*z);
s2=cosh((h./2).*z);
s3=(Δ-psi)./D;
s4=exp((n./2).*z);
e1=s4.*(s2-((s1.*n)./h));
e2=2.*s4.*(s1./h);
e3=(2.*s3.*s4.*s1)./h;
e4=s4.*(s2+((s1.*n)./h));
e11=e1(Node);
e21=e2(Node);
e31=e3(Node);
e41=e4(Node);
b1(1)=0;
for j=2:Node
    b10=(-2./(D.*h)).*xx.*exp((n./2)*(z(j)-z)).*sinh((h./2)*(z(j)-z));
    b1(j)=trapz(z(1:j),b10(1:j));
end

s33=(-2./(D.*h)).*xx.*exp((n./2)*(1-z)).*sinh((h./2)*(1-z));
b11=trapz(z(1:end),s33(1:end));
b2(1)=0;
for j=2:Node
    b20=(-1./(D)).*xx.*exp((n./2)*(z(j)-z)).*(cosh((h./2)*(z(j)-z))...
        +(((sinh((h./2)*(z(j)-z)).*n)./h));
    b2(j)=trapz(z(1:j),b20(1:j));
end

s44=(-1./(D)).*xx.*exp((n./2)*(1-z)).*(cosh((h./2)*(1-z))+...
    (((sinh((h./2)*(1-z)).*n)./h));
b21=trapz(z(1:end),s44(1:end));

R_FF((((z_p_0/R))./(((Δ-a1)/R)-e11+((e21.*e31)./e41)))));
R_FI((((-((e21.*b21)./e41)+b11))./(((Δ-a1)/R)-e11+((e21.*e31)./e41)))));
R_IF(((e1-((e2.*e31)./e41)).*(((z_p_0/R))./(((Δ-a1)/R)-e11+...
    ((e21.*e31)./e41)))));
R_II(((e1-((e2.*e31)./e41)).*(((Δ-a1)/R)-e11+((e21.*b21)./e41)+b11))./(((Δ-a1)/R)-...
    e11+((e21.*e31)./e41)))+b1-((e2.*b21)./e41));

Ad=-[z_p_0,xx]+2.*Δ.*[R_FF+R_FI,R_IF+R_II];
end
%Ads
function Ads=discrete_Ads(x,v,psi,Δ,z,Node)
global R D a1
z_p_0=x(1);
xx=x(2:end);
n=v/D;
h=sqrt(n.^2+4.*((Δ-psi)./D));
s1=sinh((h./2).*z);
s2=cosh((h./2).*z);
s3=(Δ-psi)./D;
s4=exp((n./2).*z);
e1=s4.*(s2-((s1.*n)./h));
e2=2.*s4.*(s1./h);
e3=(2.*s3.*s4.*s1)./h;
e4=s4.*(s2+((s1.*n)./h));

```

```

e11=e1(Node);
e21=e2(Node);
e31=e3(Node);
e41=e4(Node);
c1=1./R;
c2=e21./e41;
c3=(( $\Delta$ -a1)/R)-e11+((e21.*e31)./e41);
c4_eta=e2./e41;
c5=e21./e41;
c6=c3;
f_z=(e1-((e2.*e31)./e41));
f1_z_1=(-2./(D.*h)).*1.*exp((n./2)*(1-z)).*sinh((h./2)*(1-z));
f2_z_1=(-1./(D)).*1.*exp((n./2)*(1-z)).*(cosh((h./2)*(1-z))+...
((sinh((h./2)*(1-z))).*n)./h);
f_eta=f_z;
R_FF_s=(c1./c6).*z_p_0;
R_FI_s=((f1_z_1./c6)-(c5.*f2_z_1)./c6).*z_p_0;
integrant_IF=(c1.*f_z)./c3.*xx;
R_IF_s=trapz(z(1:end),integrant_IF(1:end));
integrant_R_II_s_1=(c2.*f_eta)./c3.*xx;
R_II_s_1=-f2_z_1.*trapz(z(1:end),integrant_R_II_s_1(1:end));
integrant_R_II_s_2=(f_eta)./c3.*xx;
R_II_s_2=f1_z_1.*trapz(z(1:end),integrant_R_II_s_2(1:end));
integrant_R_II_s_3=(c4_eta).*xx;
R_II_s_3=-f2_z_1.*trapz(z(1:end),integrant_R_II_s_3(1:end));
af(Node)=0;
for j=1:Node-1
    f1_eta_zeta=(-2./(D.*h)).*1.*...
    exp((n./2)*(z-z(j))).*sinh((h./2)*(z-z(j)));
    af0=xx.*f1_eta_zeta;
    af(j)=trapz(z(j:end),af0(j:end));
end
R_II_s_4=af;
R_II_s=R_II_s_1+R_II_s_2+R_II_s_3+R_II_s_4;
Ads=-[z_p_0,xx]+2.* $\Delta$ .*[R_FF_s+R_IF_s,R_FI_s+R_II_s];
end
%Bd
function Bd=discrete_Bd(v,psi, $\Delta$ ,z,Node)
global R D a1 a2
n=v/D;
h=sqrt(n.^2+4.*(( $\Delta$ -psi)./D));
s1=sinh((h./2).*z);
s2=cosh((h./2).*z);
s3=( $\Delta$ -psi)./D;
s4=exp((n./2).*z);
e1=s4.*(s2-((s1.*n)./h));
e2=2*s4.*(s1./h);
e3=(2.*s3.*s4.*s1)./h;
e4=s4.*(s2+((s1.*n)./h));
e11=e1(Node);
e21=e2(Node);
e31=e3(Node);
e41=e4(Node);
R_FF_B=((R./( $\Delta$ -a1)).*((e11-((e21.*e31)./e41)).*...

```

```

((a2/R) ./ ((Δ-a1) ./R) - e11 + ((e21.*e31) ./e41))) + (a2 ./ (Δ-a1));
R_IF_B = ((e1 - ((e2.*e31) ./e41)) .* ((a2/R) ./ ((Δ-a1) ./R) - ...
e11 + ((e21.*e31) ./e41)));
Bd = sqrt(2*Δ) .* [R_FF_B, R_IF_B];
end
%Bds
function Bds = discrete_Bds(spatial_operator, v, psi, Δ, z, Node)
spatial_operator_F = spatial_operator(1);
spatial_operator_I = spatial_operator(2:end);
global R D a1 a2
n = v/D;
h = sqrt(n.^2 + 4.*((Δ-psi) ./D));
s1 = sinh((h./2) .*z);
s2 = cosh((h./2) .*z);
s3 = (Δ-psi) ./D;
s4 = exp((n./2) .*z);
e1 = s4.*(s2 - ((s1.*n) ./h));
e2 = 2*s4.*(s1 ./h);
e3 = (2.*s3.*s4.*s1) ./h;
e4 = s4.*(s2 + ((s1.*n) ./h));
e11 = e1(Node);
e21 = e2(Node);
e31 = e3(Node);
e41 = e4(Node);
R_FF_Bs = ((R ./ (Δ-a1)) .* ((e11 - ((e21.*e31) ./e41)) .* ...
((a2/R) ./ ((Δ-a1) ./R) - e11 + ((e21.*e31) ./e41))) + (a2 ./ (Δ-a1));
c12 = e31 ./e41;
c10 = ((a2/R) ./ ((Δ-a1) ./R) - e11 + ((e21.*e31) ./e41));
integrant_bds = (e1 - (c12.*e2)) .* spatial_operator_I;
R_IF_Bs = c10 .* trapz(z(1:end), integrant_bds(1:end));
Bds = sqrt(2*Δ) .* (R_FF_Bs .* spatial_operator_F + R_IF_Bs);
end
%Cd
function Cd = discrete_Cd(x, v, psi, Δ, z, Node)
global R D a1
z_p_0 = x(1);
xx = x(2:end);
n = v/D;
h = sqrt(n.^2 + 4.*((Δ-psi) ./D));
s1 = sinh((h./2) .*z);
s2 = cosh((h./2) .*z);
s3 = (Δ-psi) ./D;
s4 = exp((n./2) .*z);
e1 = s4.*(s2 - ((s1.*n) ./h));
e2 = 2*s4.*(s1 ./h);
e3 = (2.*s3.*s4.*s1) ./h;
e4 = s4.*(s2 + ((s1.*n) ./h));
e11 = e1(Node);
e21 = e2(Node);
e31 = e3(Node);
e41 = e4(Node);
b1(1) = 0;
for j = 2:Node
    b10 = (-2 ./ (D.*h)) .* xx .* exp((n./2) * (z(j) - z)) .* sinh((h./2) * (z(j) - z));

```

```

    b1(j)=trapz(z(1:j),b10(1:j));

end

s33=(-2./(D.*h)).*xx.*exp((n./2)*(1-z)).*sinh((h./2)*(1-z));
b11=trapz(z(1:end),s33(1:end));

b2(1)=0;
for j=2:Node
    b20=(-1./(D)).*xx.*exp((n./2)*(z(j)-z)).*...
        (cosh((h./2)*(z(j)-z))+((sinh((h./2)*(z(j)-z))).*n)./h));
    b2(j)=trapz(z(1:j),b20(1:j));

end
s44=(-1./(D)).*xx.*exp((n./2)*(1-z)).*(cosh((h./2)*(1-z))+...
    ((sinh((h./2)*(1-z))).*n)./h));
b21=trapz(z(1:end),s44(1:end));
R_IF_1=((e11-(e21.*e31)./e41)).*((z_p_0./R))./((Δ-a1)/R)-e11+...
    ((e21.*e31)./e41));
R_II_1=((e11-(e21.*e31)./e41)).*...
    ((-(e21.*b21)./e41)+b11)./((Δ-a1)/R)-e11+((e21.*e31)./e41))+...
    b11-(e21.*b21)./e41);
Cd=sqrt(2*Δ)*(R_IF_1+R_II_1);
end
%Md
function Md=discrete_Md(v,psi,Δ,z,Node)
global R D a1
f_zeta_disturbance=[zeros(1,length(1:(Node-1)/2)),...
    0.6.*ones(1,length((Node-1)/2)+1:Node)];
n=v/D;
h=sqrt(n.^2+4.*((Δ-psi)./D));
s1=sinh((h./2).*z);
s2=cosh((h./2).*z);
s3=(Δ-psi)./D;
s4=exp((n./2).*z);
e1=s4.*(s2-((s1.*n)./h));
e2=2.*s4.*(s1./h);
e3=(2.*s3.*s4.*s1)./h;
e4=s4.*(s2+((s1.*n)./h));
e11=e1(Node);
e21=e2(Node);
e31=e3(Node);
e41=e4(Node);
b1(1)=0;
for j=2:Node
    b10=(-2./(D.*h)).*f_zeta_disturbance.*exp((n./2)*(z(j)-z)).*...
        sinh((h./2)*(z(j)-z));
    b1(j)=trapz(z(1:j),b10(1:j));

end

s33=(-2./(D.*h)).*f_zeta_disturbance.*exp((n./2)*(1-z)).*...
sinh((h./2)*(1-z));
b11=trapz(z(1:end),s33(1:end));

```

```

b2(1)=0;
for j=2:Node
    b20=(-1./(D)).*f_zeta_disturbance.*exp((n./2)*(z(j)-z)).*...
        (cosh((h./2)*(z(j)-z))+((sinh((h./2)*(z(j)-z))).*n)./h));
    b2(j)=trapz(z(1:j),b20(1:j));
end
s44=(-1./(D)).*f_zeta_disturbance.*exp((n./2)*(1-z)).*...
(cosh((h./2)*(1-z))+((sinh((h./2)*(1-z))).*n)./h));
b21=trapz(z(1:end),s44(1:end));

R_FI_fzeta=(((-(e21.*b21)./e41)+b11)./(((Δ-a1)/R)-e11+...
((e21.*e31)./e41)));
R_II_fzeta=(((e1-(e2.*e31)./e41)).*...
(((e21.*b21)./e41)+b11)./(((Δ-a1)/R)-e11+(e21.*e31)./e41)))+...
b1-(e2.*b21)./e41);
Md=sqrt(2*Δ).*[R_FI_fzeta,R_II_fzeta];
end
%Constructing discrete observer gain (Ld)
function Ld=discrete_L(x,v,psi,Δ,z,Node)
global R D a1
llf=x(1);
llI=x(2:end);
n=v/D;
h=sqrt(n.^2+4.*((Δ-psi)./D));
s1=sinh((h./2).*z);
s2=cosh((h./2).*z);
s3=(Δ-psi)./D;
s4=exp((n./2).*z);
e1=s4.*(s2-((s1.*n)./h));
e2=2.*s4.*(s1./h);
e3=(2.*s3.*s4.*s1)./h;
e4=s4.*(s2+((s1.*n)./h));
e11=e1(Node);
e21=e2(Node);
e31=e3(Node);
e41=e4(Node);
b1(1)=0;
for j=2:Node
    b10=(-2./(D.*h)).*llI.*exp((n./2)*(z(j)-z)).*sinh((h./2)*(z(j)-z));
    b1(j)=trapz(z(1:j),b10(1:j));
end

s33=(-2./(D.*h)).*llI.*exp((n./2)*(1-z)).*sinh((h./2)*(1-z));
b11=trapz(z(1:end),s33(1:end));
b2(1)=0;
for j=2:Node
    b20=(-1./(D)).*llI.*exp((n./2)*(z(j)-z)).*(cosh((h./2)*(z(j)-z))+...
        ((sinh((h./2)*(z(j)-z))).*n)./h));
    b2(j)=trapz(z(1:j),b20(1:j));
end
s44=(-1./(D)).*llI.*exp((n./2)*(1-z)).*(cosh((h./2)*(1-z))+...
        ((sinh((h./2)*(1-z))).*n)./h));
b21=trapz(z(1:end),s44(1:end));
R_FF=(((llf/R))./(((Δ-a1)/R)-e11+(e21.*e31)./e41)));

```

```

R_FI=((( (- ( (e21.*b21) ./e41)+b11) ./((Δ-a1)/R)-e11+...
(e21.*e31) ./e41)))));
R_IF=(((e1-((e2.*e31) ./e41)) .*((1lf/R)) ./((Δ-a1)/R)-...
e11+(e21.*e31) ./e41)))));
R_II=(((e1-((e2.*e31) ./e41)) .*...
((- ( (e21.*b21) ./e41)+b11) ./((Δ-a1)/R)-...
e11+(e21.*e31) ./e41)))+b1-((e2.*b21) ./e41));
Ld=sqrt(2.*Δ) .*[R_FF+R_FI,R_IF+R_II];
end
%Terminal state penalty operator
function Qbar=operator_Qbar(x,z,N,Q,lambda,Phi,Phi_s)
global a1
Q_finite=Q(1,1);
Q_I=Q(1,2:end);
xf=x(1);
xx=x(2:end);
Qbar=0;
for i=1:N
    for j=1:N
        q=Phi(i,:).*Q_I.*Phi_s(j,:);
        b=xx.*Phi_s(j,:);
        Qbar=Qbar-1/(lambda(i)+lambda(j))*...
        trapz(z(1:end),q(1:end))*trapz(z(1:end),b(1:end))*Phi(i,:);
    end
end
Qbar_finite=Q_finite./2.*a1;
Qbar=[Qbar_finite.*xf,Qbar];
end

```

Appendix C

Adjoint operator and boundary conditions

One can find the adjoint operator A^* and its corresponding boundary conditions based on the below definition:

$$\langle A\Phi, \Psi \rangle = \langle \Phi, A^*\Psi \rangle \quad (\text{C.1})$$

which leads to:

$$\begin{aligned} \left\langle \begin{bmatrix} A_{11} & A_{12} \\ A_{21} & A_{22} \end{bmatrix} \begin{bmatrix} \Phi_1 \\ \Phi_2 \end{bmatrix}, \begin{bmatrix} \Psi_1 \\ \Psi_2 \end{bmatrix} \right\rangle &= \langle A_{11}\Phi_1, \Psi_1 \rangle + \langle A_{12}\Phi_2, \Psi_1 \rangle \\ &+ \langle A_{21}\Phi_1, \Psi_2 \rangle + \langle A_{22}\Phi_2, \Psi_2 \rangle \end{aligned} \quad (\text{C.2})$$

with

$$\begin{aligned} A_{11} &= \frac{1}{Pe_m} \frac{\partial^2}{\partial \zeta^2} - \frac{\partial}{\partial \zeta} + \bar{R}_1, \quad A_{12} = \bar{R}_2 \\ A_{21} &= \delta \bar{R}_1, \quad A_{22} = \frac{1}{Pe_T} \frac{\partial^2}{\partial \zeta^2} - \frac{\partial}{\partial \zeta} + (\delta \bar{R}_2 - \sigma) \end{aligned} \quad (\text{C.3})$$

By employing integration by parts and some simple manipulations, one can get the

following:

$$\begin{aligned}
 & \langle A_{11}\Phi_1, \Psi_1 \rangle + \langle A_{12}\Phi_2, \Psi_1 \rangle + \langle A_{21}\Phi_1, \Psi_2 \rangle + \langle A_{22}\Phi_2, \Psi_2 \rangle \\
 &= \frac{1}{Pe_m}\Psi_1(1)\frac{\partial\Phi_1}{\partial\zeta}\Big|_{\zeta=1} - \frac{1}{Pe_m}\Psi_1(0)\frac{\partial\Phi_1}{\partial\zeta}\Big|_{\zeta=0} - \frac{1}{Pe_m}\Phi_1(1)\frac{\partial\Psi_1}{\partial\zeta}\Big|_{\zeta=1} \\
 &+ \frac{1}{Pe_m}\Phi_1(0)\frac{\partial\Psi_1}{\partial\zeta}\Big|_{\zeta=0} - \Phi_1(1)\Psi_1(1) + \Phi_1(0)\Psi_1(0) + \frac{1}{Pe_T}\Psi_2(1)\frac{\partial\Phi_2}{\partial\zeta}\Big|_{\zeta=1} \\
 &- \frac{1}{Pe_T}\Psi_2(0)\frac{\partial\Phi_2}{\partial\zeta}\Big|_{\zeta=0} - \frac{1}{Pe_T}\Phi_2(1)\frac{\partial\Psi_2}{\partial\zeta}\Big|_{\zeta=1} + \frac{1}{Pe_T}\Phi_2(0)\frac{\partial\Psi_2}{\partial\zeta}\Big|_{\zeta=0} - \Phi_2(1) \\
 &\Psi_2(1) + \Phi_2(0)\Psi_2(0) + \int_0^1 \left(\frac{1}{Pe_m}\Phi_1\frac{\partial^2\Psi_1}{\partial\zeta^2} + \Phi_1\frac{\partial\Psi_1}{\partial\zeta} + \bar{R}_1\Phi_1\Psi_1 \right) d\zeta \\
 &+ \int_0^1 \bar{R}_2\Phi_1\Psi_1 d\zeta + \int_0^1 \left(\frac{1}{Pe_T}\Phi_2\frac{\partial^2\Psi_2}{\partial\zeta^2} + \Phi_2\frac{\partial\Psi_2}{\partial\zeta} + (\delta\bar{R}_2 - \sigma)\Phi_2\Psi_2 \right) d\zeta \\
 &+ \int_0^1 \delta\bar{R}_1\Phi_1\Psi_2 d\zeta = \langle \Phi, A^*\Psi \rangle
 \end{aligned} \tag{C.4}$$

Then, injecting the boundary conditions given in (3.11), leads to the following new boundary conditions which describes the adjoint operator:

$$\begin{aligned}
 \frac{\partial\Psi_1(\zeta, t)}{\partial\zeta}\Big|_{\zeta=1} &= -Pe_m(\Psi_1(\zeta=1) - r\Psi_1(\zeta=0)) \\
 \frac{\partial\Psi_2(\zeta, t)}{\partial\zeta}\Big|_{\zeta=1} &= -Pe_T(\Psi_2(\zeta=1) - r\Psi_2(\zeta=0)) \\
 \frac{\partial\Psi_1(\zeta, t)}{\partial\zeta}\Big|_{\zeta=0} &= \frac{\partial\Psi_2(\zeta, t)}{\partial\zeta}\Big|_{\zeta=0} = 0
 \end{aligned} \tag{C.5}$$

where the operators are:

$$\begin{aligned}
 A_{11}^* &= \frac{1}{Pe_m}\frac{\partial^2}{\partial\zeta^2} + \frac{\partial}{\partial\zeta} + \bar{R}_1, \quad A_{12}^* = \delta\bar{R}_1 \\
 A_{21}^* &= \bar{R}_2, \quad A_{22}^* = \frac{1}{Pe_T}\frac{\partial^2}{\partial\zeta^2} + \frac{\partial}{\partial\zeta} + (\delta\bar{R}_2 - \sigma)
 \end{aligned} \tag{C.6}$$

Appendix D

Resolvent operators

D.1 Resolvent of the tubular reactor with recycle

The resolvent operator can be written as below:

$$\mathfrak{R}(s, A)(\cdot) = \begin{bmatrix} \mathfrak{R}_{11} & \mathfrak{R}_{12} \\ \mathfrak{R}_{21} & \mathfrak{R}_{22} \end{bmatrix} \begin{bmatrix} (\cdot)_1 \\ (\cdot)_2 \end{bmatrix} \quad (\text{D.1.1})$$

Considering $u(s) = 0$ and utilizing boundary conditions, one can find the followings:

$$\begin{aligned} \mathfrak{R}_{11} &= T_{1j}^{(\zeta)}(M_{ij}\gamma_i) - \int_0^\zeta \left(F_{12}^{(\zeta,\eta)} Pe_m(\cdot)_1 \right) d\eta \\ \mathfrak{R}_{12} &= T_{1j}^{(\zeta)}(M_{ij}\Gamma_i) - \int_0^\zeta \left(F_{14}^{(\zeta,\eta)} Pe_T(\cdot)_2 \right) d\eta \\ \mathfrak{R}_{21} &= T_{3j}^{(\zeta)}(M_{ij}\gamma_i) - \int_0^\zeta \left(F_{32}^{(\zeta,\eta)} Pe_m(\cdot)_1 \right) d\eta \\ \mathfrak{R}_{22} &= T_{3j}^{(\zeta)}(M_{ij}\Gamma_i) - \int_0^\zeta \left(F_{34}^{(\zeta,\eta)} Pe_T(\cdot)_2 \right) d\eta \end{aligned} \quad (\text{D.1.2})$$

with

$$M_{ij} = \begin{bmatrix} T_{21}^{(\zeta=1)} & T_{22}^{(\zeta=1)} & T_{23}^{(\zeta=1)} & T_{24}^{(\zeta=1)} \\ T_{41}^{(\zeta=1)} & T_{42}^{(\zeta=1)} & T_{43}^{(\zeta=1)} & T_{44}^{(\zeta=1)} \\ Pe_m(rT_{11}^{(\zeta=1)} - 1) & 1 + Pe_m r T_{12}^{(\zeta=1)} & Pe_m r T_{13}^{(\zeta=1)} & Pe_m r T_{14}^{(\zeta=1)} \\ Pe_T r T_{31}^{(\zeta=1)} & Pe_T r T_{32}^{(\zeta=1)} & Pe_T(rT_{33}^{(\zeta=1)} - 1) & 1 + Pe_T r T_{34}^{(\zeta=1)} \end{bmatrix}^{-1},$$

$$\begin{aligned}
 \gamma_i &= \begin{bmatrix} \int_0^{\zeta=1} (F_{22}^{(\zeta=1,\eta)} P e_m(\cdot)_1) d\eta \\ \int_0^{\zeta=1} (F_{42}^{(\zeta=1,\eta)} P e_m(\cdot)_1) d\eta \\ P e_{mr} \int_0^{\zeta=1} (F_{12}^{(\zeta=1,\eta)} P e_m(\cdot)_1) d\eta \\ P e_{Tr} \int_0^{\zeta=1} (F_{32}^{(\zeta=1,\eta)} P e_m(\cdot)_1) d\eta \end{bmatrix}, \\
 \Gamma_i &= \begin{bmatrix} \int_0^{\zeta=1} (F_{24}^{(\zeta=1,\eta)} P e_T(\cdot)_2) d\eta \\ \int_0^{\zeta=1} (F_{44}^{(\zeta=1,\eta)} P e_T(\cdot)_2) d\eta \\ P e_{mr} \int_0^{\zeta=1} (F_{14}^{(\zeta=1,\eta)} P e_T(\cdot)_2) d\eta \\ P e_{Tr} \int_0^{\zeta=1} (F_{34}^{(\zeta=1,\eta)} P e_T(\cdot)_2) d\eta \end{bmatrix}
 \end{aligned} \tag{D.1.3}$$

for B_d , zero initial condition should be taken into account. This leads to the following resolvent:

$$(sI - A)^{-1} B = \mathfrak{R}(s, A) B = \begin{bmatrix} \mathfrak{R}_1 B \\ \mathfrak{R}_2 B \end{bmatrix} \tag{D.1.4}$$

where

$$\mathfrak{R}_1 B = T_{1j}^{(\zeta)} (M_{ij} \Omega_i) - \int_0^{\zeta} (F_{14}^{(\zeta,\eta)} P e_T \sigma) d\eta \tag{D.1.5}$$

$$\mathfrak{R}_2 B = T_{3j}^{(\zeta)} (M_{ij} \Omega_i) - \int_0^{\zeta} (F_{34}^{(\zeta,\eta)} P e_T \sigma) d\eta \tag{D.1.6}$$

and Ω_i is defined as below:

$$\Omega_i = \begin{bmatrix} \int_0^{\zeta=1} (F_{24}^{(\zeta=1,\eta)} P e_T \sigma) d\eta \\ \int_0^{\zeta=1} (F_{44}^{(\zeta=1,\eta)} P e_T \sigma) d\eta \\ P e_{mr} \int_0^{\zeta=1} (F_{14}^{(\zeta=1,\eta)} P e_T \sigma) d\eta \\ P e_{Tr} \int_0^{\zeta=1} (F_{34}^{(\zeta=1,\eta)} P e_T \sigma) d\eta \end{bmatrix} \tag{D.1.7}$$

D.2 Resolvent of adjoint operators

By the same procedure described in Section 3.5.2 for the operator A , consider T^* and F^* as the exponential matrices, $e^{P^* \zeta}$ and $e^{P^* (\zeta - \eta)}$, for the adjoint operator (A^*).

This leads to the following resolvent by imposing the corresponding adjoint boundary conditions:

$$\mathfrak{R}(s, A^*)(\cdot) = \begin{bmatrix} \mathfrak{R}_{11}^* & \mathfrak{R}_{12}^* \\ \mathfrak{R}_{21}^* & \mathfrak{R}_{22}^* \end{bmatrix} \begin{bmatrix} (\cdot)_1 \\ (\cdot)_2 \end{bmatrix} \quad (\text{D.2.1})$$

where

$$\begin{aligned} \mathfrak{R}_{11}^* &= T_{11}^{*(\zeta)}(M_{1j}^* \gamma_j^*) + T_{13}^{*(\zeta)}(M_{2j}^* \gamma_j^*) - \int_0^\zeta \left(F_{12}^{*(\zeta, \eta)} Pe_m(\cdot)_1 \right) d\eta \\ \mathfrak{R}_{12}^* &= T_{11}^{*(\zeta)}(M_{1j}^* \Gamma_j^*) + T_{13}^{*(\zeta)}(M_{2j}^* \Gamma_j^*) - \int_0^\zeta \left(F_{14}^{*(\zeta, \eta)} Pe_T(\cdot)_2 \right) d\eta \\ \mathfrak{R}_{21}^* &= T_{31}^{*(\zeta)}(M_{1j}^* \gamma_j^*) + T_{33}^{*(\zeta)}(M_{2j}^* \gamma_j^*) - \int_0^\zeta \left(F_{32}^{*(\zeta, \eta)} Pe_m(\cdot)_1 \right) d\eta \\ \mathfrak{R}_{22}^* &= T_{31}^{*(\zeta)}(M_{1j}^* \Gamma_j^*) + T_{33}^{*(\zeta)}(M_{2j}^* \Gamma_j^*) - \int_0^\zeta \left(F_{34}^{*(\zeta, \eta)} Pe_T(\cdot)_2 \right) d\eta \end{aligned} \quad (\text{D.2.2})$$

and $(\gamma_i^*, \Gamma_i^*, M_{ij}^*)$ are expressed as below:

$$\begin{aligned} \gamma_i^* &= \begin{bmatrix} \int_0^{\zeta=1} \left(F_{22}^{*(\zeta=1, \eta)} Pe_m(\cdot)_1 + F_{12}^{*(\zeta=1, \eta)} Pe_m^2(\cdot)_1 \right) d\eta \\ \int_0^{\zeta=1} \left(F_{42}^{*(\zeta=1, \eta)} Pe_m(\cdot)_1 d\eta + F_{32}^{*(\zeta=1, \eta)} Pe_m Pe_T(\cdot)_1 \right) d\eta \end{bmatrix}, \\ \Gamma_i^* &= \begin{bmatrix} \int_0^{\zeta=1} \left(F_{24}^{*(\zeta=1, \eta)} Pe_T(\cdot)_2 + F_{14}^{*(\zeta=1, \eta)} Pe_m Pe_T(\cdot)_2 \right) d\eta \\ \int_0^{\zeta=1} \left(F_{44}^{*(\zeta=1, \eta)} Pe_T(\cdot)_2 d\eta + F_{34}^{*(\zeta=1, \eta)} Pe_T^2(\cdot)_2 \right) d\eta \end{bmatrix}, \\ M_{ij}^* &= \begin{bmatrix} T_{21}^{*(\zeta=1)} - Pe_m R + Pe_m T_{11}^{*(\zeta=1)} & T_{23}^{*(\zeta=1)} + Pe_m T_{13}^{*(\zeta=1)} \\ T_{41}^{*(\zeta=1)} + Pe_T T_{31}^{*(\zeta=1)} & T_{43}^{*(\zeta=1)} - Pe_T R + Pe_T T_{33}^{*(\zeta=1)} \end{bmatrix}^{-1} \end{aligned} \quad (\text{D.2.3})$$

Finally, for B_d^* it is possible to define it as follows:

$$(\mathfrak{R}_1 B)^*(\cdot)_1 = \int_0^1 (\mathfrak{R}_1 B)(\cdot)_1 d\zeta \quad (\text{D.2.4})$$

$$(\mathfrak{R}_2 B)^*(\cdot)_2 = \int_0^1 (\mathfrak{R}_2 B)(\cdot)_2 d\zeta \quad (\text{D.2.5})$$

Appendix E

Terminal cost operator

In this appendix, the algorithm for calculating the the operator $\bar{Q} = [\bar{Q}_1 \quad \bar{Q}_2]^T$ is demonstrated. Let us consider the following discrete Lyapunov equation:

$$A_d^* \bar{Q} A_d - \bar{Q} = -Q \quad (\text{E.1})$$

It should be emphasized based on the Cayley-Tustin method, the solution of the above equation leads to the same unique solution in the continuous time setting ($A^* \bar{Q} + \bar{Q} A = -Q$). The continuous Lyapunov equations can be formulated by the inner product as (Curtain and Zwart, 1995b):

$$\langle Ax_1, \bar{Q}x_2 \rangle + \langle \bar{Q}x_1, Ax_2 \rangle = - \langle x_1, Qx_2 \rangle \quad (\text{E.2})$$

Based on the operator A , let us consider $x_1 = \hat{\Phi}_m$ $x_2 = \hat{\Phi}_n^*$ as the normalized eigenfunctions and corresponding adjoint eigenfunctions, respectively. The eigenvalue problem directly denotes that $A\hat{\Phi}_m = \lambda_m \hat{\Phi}_m$ and $A\hat{\Phi}_n^* = \lambda_n \hat{\Phi}_n^*$. Thus, the above equation leads to:

$$\begin{aligned} \langle \lambda_m \hat{\Phi}_m, \bar{Q} \hat{\Phi}_n^* \rangle + \langle \bar{Q} \hat{\Phi}_m, \lambda_n \hat{\Phi}_n^* \rangle &= \lambda_m \langle \hat{\Phi}_m, \bar{Q} \hat{\Phi}_n^* \rangle \\ + \lambda_n \langle \bar{Q} \hat{\Phi}_m, \hat{\Phi}_n^* \rangle &= - \langle \hat{\Phi}_m, Q \hat{\Phi}_n^* \rangle \end{aligned} \quad (\text{E.3})$$

where \bar{Q} is a bounded symmetric operator ($D(A^*) = D(A)$) and it is self-adjoint, see Curtain and Zwart (1995b). Therefore, $\langle \hat{\Phi}_m, \bar{Q} \hat{\Phi}_n^* \rangle = \langle \bar{Q} \hat{\Phi}_m, \hat{\Phi}_n^* \rangle = \bar{Q}_{mn}$ and it is possible to write the following simplified equation:

$$\bar{Q}_{mn} = \frac{- \langle \hat{\Phi}_m, Q \hat{\Phi}_n^* \rangle}{\lambda_m + \lambda_n} \quad (\text{E.4})$$

Finally, based on the solution of the continuous Lyapunov equation, the terminal cost operator can be computed by

$$\bar{Q}(\cdot) = \sum_{m=0}^{\infty} \sum_{n=0}^{\infty} \frac{- \langle \hat{\Phi}_m, Q \hat{\Phi}_n^* \rangle}{\lambda_m + \lambda_n} \langle (\cdot), \hat{\Phi}_n^* \rangle \hat{\Phi}_m \quad (\text{E.5})$$

Appendix F

Stability of the discrete observer error

First, we need to show that the discrete observer error can be written as the following equation:

$$\hat{e}_d(\zeta, k) = x(\zeta, k) - \hat{x}(\zeta, k) = (A_d - L_d C_d) \hat{e}_d(\zeta, k - 1) \quad (\text{F.1})$$

Let us recall that the discrete operators of the observer dynamics are given by:

$$\begin{aligned} A_d(\cdot) &= -I(\cdot) + 2\alpha [\alpha I - A]^{-1}(\cdot) \\ B_d &= \sqrt{2\alpha} [\alpha I - A]^{-1} B \\ C_{d_o}(\cdot) &= \sqrt{2\alpha} [I + C(\alpha I - A)L_T]^{-1} C [\alpha I - A]^{-1}(\cdot) \\ D_{d_o} &= [I + C(\alpha I - A)L_T]^{-1} C [\alpha I - A]^{-1} B \\ M_{d_o} &= (I + C(\alpha I - A)^{-1} L_T)^{-1} C(\alpha I - A)^{-1} L_T \\ L_d &= \sqrt{2\alpha} [\alpha I - A]^{-1} L_T \end{aligned} \quad (\text{F.2})$$

Notice that in above equations M_{d_o} is defined based on L_T , such that the discrete observer error is stable. The relations between (C_{d_o}, D_{d_o}) and (C_d, D_d) are written as:

$$\begin{aligned} C_d &= (I + C(\alpha I - A)^{-1} L_T) C_{d_o} \\ D_d &= (I + C(\alpha I - A)^{-1} L_T) D_{d_o} \end{aligned} \quad (\text{F.3})$$

By the operators defined earlier, it is possible to find:

$$y(k) - \hat{y}(k) = (I - M_{d_o}) (C_d x(\zeta, k - 1) + D_d u(k)) - C_{d_o} \hat{x}(\zeta, k - 1) - D_{d_o} u(k) \quad (\text{F.4})$$

Then, from Eq.(F.3) and Eq.(F.4), one can get the following:

$$\begin{aligned} y(k) - \hat{y}(k) &= (I - M_d) (I + C(\alpha I - A)^{-1} L_T) (C_{d_o} x(\zeta, k - 1) + D_{d_o} u(k)) \\ &\quad - C_{d_o} \hat{x}(\zeta, k - 1) - D_{d_o} u(k) \rightarrow \\ I - M_{d_o} &= I - \left(I + C(\alpha I - A)^{-1} L_T \right)^{-1} C(\alpha I - A)^{-1} L_T \\ &= (I + C(\alpha I - A)^{-1} L_T)^{-1} \left(I + C(\alpha I - A)^{-1} L_T - C(\alpha I - A)^{-1} L_T \right) \\ &= (I + C(\alpha I - A)^{-1} L_T)^{-1} \rightarrow y(k) - \hat{y}(k) = - (C_{d_o} x(\zeta, k - 1) + D_{d_o} u(k)) \\ &\quad + \left(I + C(\alpha I - A)^{-1} L_T \right)^{-1} \left(I + C(\alpha I - A)^{-1} L_T \right) (C_{d_o} x(\zeta, k - 1) + D_{d_o} u(k)) \\ &= C_{d_o} (x(\zeta, k - 1) - \hat{x}(\zeta, k - 1)) \end{aligned} \quad (\text{F.5})$$

Hence, the discrete observer error takes the following form:

$$\begin{aligned} \hat{e}_d(\zeta, k) &= x(\zeta, k) - \hat{x}(\zeta, k) = A_d (x(\zeta, k - 1) - \hat{x}(\zeta, k - 1)) - L_d (y(k) - \hat{y}(k)) \\ &= (A_d - L_d C_{d_o}) \hat{e}_d(\zeta, k - 1) \end{aligned} \quad (\text{F.6})$$

The above equation can be linked to the continuous time setting as below:

$$\begin{aligned}
 (A_d - L_d C_{d_o}) &= -I + 2\alpha(\alpha - A)^{-1} - 2\alpha \left[I - (I + (\alpha I + A)^{-1} L_T C)^{-1} \right] (\alpha I - A)^{-1} \\
 &= -I + 2[\alpha I - A + L_T C]^{-1} = -I + 2[\alpha I - A_o]^{-1}
 \end{aligned} \tag{F.7}$$

which would be the discrete version of $(A_o = A - L_T C)$. Therefore, if the selected continuous observer gain (L_T) ensures that the operator (A_o) is stable, then the discrete version of the observer is stable as well.